

Submitted to *Manufacturing & Service Operations Management*

# Two-Sided Flexibility in Platforms

(Authors' names blinded for peer review)

Authors are encouraged to submit new papers to INFORMS journals by means of a style file template, which includes the journal title. However, use of a template does not certify that the paper has been accepted for publication in the named journal. INFORMS journal templates are for the exclusive purpose of submitting to an INFORMS journal and are not intended to be a true representation of the article's final published form. Use of this template to distribute papers in print or online or to submit papers to another non-INFORM publication is prohibited.

**Abstract.** **Problem definition:** Flexibility is a crucial tool in operations research and computer systems to hedge against stochasticity in product demands, service requirements, or supply availability. In two-sided platforms, flexibility is also two-sided and can be viewed as the compatibility of agents on one side with agents on the other side. Platform actions often influence the flexibility on either the demand side or the supply side. But how should flexibility be jointly allocated to both sides? Whereas the literature has traditionally focused on only one side at a time, our work initiates the study of two-sided flexibility in matching platforms. **Methodology/results:** We propose a parsimonious matching model in random graphs and identify the allocation of flexibility across both sides that yields the largest maximum matching. Our findings reveal that the flexibility allocation problem is a first-order issue: for a given flexibility budget, the resulting matching size can vary greatly depending on how the flexibility budget is allocated. Moreover, even in the simple and symmetric settings we study, the quest for the optimal allocation is complicated. In particular, costly mistakes can be made if the flexibility decisions on the demand and supply side are optimized independently (e.g., by two different teams in the company), rather than jointly. To guide the search for optimal flexibility allocation, we uncover two effects, *flexibility cannibalization* and *flexibility abundance*, that govern when placing a flexibility budget only on one side or equally on both sides is the optimal design. **Managerial implications:** Our work identifies the study of two-sided flexibility as a significant aspect of platform efficiency. The interplay of different flexibility levers deserves significant attention from platform managers to guide the optimal flexibility design.

**Key words:** Flexibility, Two-sided Platforms, Bipartite Matching, Incentive Designs

## 1. Introduction

Flexibility is arguably one of the fundamental topics in operations research and computer systems. As an operational concept, it classically applies to a range of settings including for example (1) the ability of a plant to process multiple types of products in a manufacturing system (Fine and Freund 1990), (2) the ability of servers, due to cross-training, to handle multiple types of requests (Wallace and Whitt 2005), or (3) the pooling of resources in a network of newsvendors (Bassamboo et al. 2010). All of these classical applications target the supply side of an operating system. More recently, flexibility has also been used for the

demand side: its value has been demonstrated in opaque selling for retail inventory management (Elmachtoub and Hamilton 2021), in online grocery shopping delivery (Zhou 2021), and in car-sharing (Ströhle et al. 2019). In both the traditional, supply-focused, and the more recent, demand-focused, applications, the literature identifies the necessary investment in one lever of flexibility to gain operational value.

However, contemporary markets feature flexibility on both sides. In online retail markets, for instance, Amazon provides a spectrum of delivery time options, ranging from a few hours to several weeks. Price differentiation across these options exploits different levels of flexibility among the customers, which leads to lower (higher) revenue from more (less) flexible customers. On the supply side, Amazon operates both local storage hubs and larger regional warehouses to fulfill demand. Storage at local hubs is more expensive but yields the necessary inventory flexibility to fulfill customer demand with short delivery windows. Two-sided flexibility is also prevalent in platforms that connect buyers and service providers. In Table 1 we provide examples that illustrate how flexibility levers, on both sides of a platform, increase the likelihood of connections between demand and supply being feasible. Despite the significant role that flexibility plays on both the demand and the supply side, due to their organizational structure, flexibility is usually optimized independently on each side. Moreover, we also know of no prior work that examines how different kinds of flexibility on two market sides interact with each other.

Industry	Platform(s)	Demand side lever	Supply side lever
Retail	Amazon	Wider delivery windows	Heterogeneous inventory storage
Trucking	Uber Freight	Flexible load types (e.g., LTL)	Load bundles
Hospitality	Airbnb	Flexible duration/location of stay	Professional residence photos
Ride-hailing	Lyft	Wait and save	Car seat mode

**Table 1 Examples of two-sided platforms with flexibility incentives on both the supply and the demand sides. These levers typically encourage flexibility on the demand side on how/when the service is fulfilled and increase compatibility on the supply side to cater to diverse customer needs.**

Motivated by this gap in the literature, we study how a given budget of flexibility should be allocated across the two sides of a platform. This allocation question differs from traditional studies of flexibility in that it examines the interplay between different flexibility levers. Since most of our examples in Table 1 (i.e., trucking, hospitality, ride-hailing) originate in different types of matching platforms, we consider a parsimonious matching model to identify a platform's optimal flexibility investment on both market sides. Our matching problem is modeled as a bipartite random graph, where flexibility is captured through *flexible nodes* (on either side) with an increased probability of forming edges with the other side of the graph. We optimize over the fraction of flexible nodes on each market side to maximize the expected size of a maximum matching, i.e., the expected fraction of nodes that are part of a maximum matching.

Our results show that flexibility allocation significantly impacts the performance of a two-sided matching platform. Even with a constant flexibility budget, the matching probability (and consequently the profit of a

matching platform) can vary significantly depending on how the budget is allocated between the two sides of the platform. As illustrated in Fig. 4, the profit gap between different allocations of the same flexibility budget for every model we consider can be as large as 20%. Specifically, optimality occurs at one of two natural flexibility allocation strategies: (1) the one-sided allocation, which places flexibility only on one side, and (2) the balanced allocation, which evenly distributes half of the flexibility budget to both sides. As shown in Fig. 3, either of these allocations can improve the matching size by more than 8% compared to the other. Hence, matching platforms with flexibility levers on both sides may pay a high price if they only optimize their flexibility budget but not its allocation.

Despite the impact of flexibility allocation, optimizing it poses nontrivial difficulties. Even in a simple and symmetric matching model, our analysis of the geometry of the matching size (as a function of the flexibility allocation) reveals saddle points in which a platform might get stuck. In particular, the current practice of many platforms, wherein separate teams optimize separate flexibility levers on different market sides, might converge to such saddle points. Near these saddle points, both teams mistakenly perceive themselves to be at an optimum, as flexibility should neither be increased nor decreased on either market side; however, the platform would benefit from jointly reducing flexibility on one side while increasing it on the other. These structural insights are unique to our study of two-sided flexibility, and our numerical results show that they generalize beyond our particular models. We show that these geometries and the dominance of different flexibility allocations are driven by an interplay of two opposing effects: *flexibility cannibalization* and *flexibility abundancy*. These effects lend strength to the one-sided and the balanced allocations respectively, and they allow us to outline the parameter regimes where each effect and the corresponding flexibility allocation dominate. In identifying these different behaviors, and their first-order impact on performance, our results underscore the need to understand the interactions of different flexibility levers to enable more efficient market designs.

### 1.1. Contributions

Our work initiates the study of two-sided flexibility. It characterizes the interactions between different flexibility levers through a parsimonious matching model and allows us to study different questions regarding the optimal allocation of flexibility.

**Flexibility structures and their driving effects.** We examine three graph models within the framework of Section 2: the  $2 \times 2$  model, the local model, and the global model. The  $2 \times 2$  model is a small setting that can be fully characterized, and the local model is an asymptotic generalization that shares the same local edge structure and leads to similar results. A surprising result is that the one-sided allocation of flexibility is optimal, whereas following the usual guidance to add just a little flexibility incrementally<sup>1</sup> likely leads to a suboptimal saddle point. In particular, we show that the matching probability is concave with respect

<sup>1</sup>A little flexibility is all you need, see Jordan and Graves (1995), Bassamboo et al. (2012)

to flexibility on either the demand or supply side but is jointly convex as one moves between the one-sided allocation on the supply side and that on the demand side. In other words, our setting reveals that it may be better to focus a lot of flexibility on one side instead of a little flexibility on each side. We present these results in Section 3 and highlight the need for joint experimentation to avoid the suboptimal saddle points.

The global model does not have a local edge structure, introducing new complex effects. In particular, we show that the one-sided allocation can be suboptimal. In Section 4 we present the *flexibility cannibalization* effect, which results from the fact that flexible nodes have a higher expected degree in the balanced allocation. Since each node can only be matched through one edge, the balanced allocation cannibalizes many of the edges incident to high-degree nodes, which degrades its performance. Such cannibalization drives the dominance of the one-sided allocation in particularly sparse graphs (roughly, average degree less than  $e$ ). When flexible nodes have a much higher average degree, and there is an abundant number of incident edges, we highlight a countering effect, which we term *flexibility abundance*. In Section 5 we show that flexibility cannibalization becomes a second-order effect in that regime and the balanced allocation becomes optimal. Section 7 numerically demonstrates the robustness of these effects in various modeling extensions.

**Analyses of sparse bipartite random graphs.** Our main technical contributions aim to characterize and compare the matching probability in bipartite random graphs with heterogeneous node types, a task that is especially challenging for the global model. In comparing different flexibility designs for that model, we develop three very different techniques. In Section 4 we design a careful coupling between realizations under the balanced and the one-sided flexibility allocations and show, for certain parameters, that flexibility cannibalization leads to a smaller matching size for the balanced allocation. Then, in Section 5 we apply concentration bounds for parameters where flexible nodes have high average degree. In such settings, both allocations match almost all flexible nodes, but the balanced allocation is better at matching non-flexible ones. Finally, in Section 6 we analyze the Karp-Sipser (KS) algorithm (Karp and Sipser 1981) to explicitly characterize the asymptotic matching probability in the so-called subcritical regime (see Section 3). Our KS-style analysis innovates upon prior works in that we (i) analyze a graph with heterogeneous node types, and (ii) explicitly compute the asymptotic matching probability with a provable level of precision, which allows us to compare different flexibility allocations in computer-aided proofs.

## 1.2. Related Work

**Flexibility in operations.** Flexibility has a long history in operations with early works, dating back to Buzacott and Yao (1986) and Fine and Freund (1990), focusing on the ability of a manufacturing system to produce multiple types of products. Most early works in this literature have focused on determining the optimal amount of flexible manufacturing capacity (Fine and Freund 1990, Van Mieghem 1998, Netessine et al. 2002, Chod and Rudi 2005), thus optimizing over a single dimension on the supply side. In contrast, our decision also involves the demand side. More importantly, we identify not just the optimal flexibility

investment, but also structural properties that arise from the interplay of flexibility on both sides and can cause potential pitfalls in practice.

In our focus on structural insights, our study relates more closely to those works in process flexibility that aim to identify the optimal flexibility design rather than the optimal amount of flexibility. The seminal work of (Jordan and Graves 1995) first introduced the “long chain”, which enables a small amount of flexibility ( $2n$  carefully placed edges in a manufacturing system with  $n$  plants and  $n$  types of products) to yield almost all the benefits of a perfectly flexible system (one with all  $n^2$  edges). Since then, a vast literature has studied process flexible designs and the value thereof for manufacturing and service systems (Iravani et al. 2005, Akşin and Karaesmen 2007, Chou et al. 2011, Simchi-Levi and Wei 2012, Chen et al. 2015, Désir et al. 2016). Effective flexibility designs have also been investigated in staffing (Wallace and Whitt 2005) and queuing (Tsitsiklis and Xu 2017), among other settings.

A key distinction between our work and this stream of work lies in the structure of our flexibility levers: as most contemporary matching platforms involve stochastically formed edges that connect the supply and demand sides, we cannot model flexibility as a fixed compatibility design. Instead, platforms use various incentive levers to increase the likelihood of compatibility between the supply and demand sides of the market. As such, our approach optimizes over the fraction of flexible nodes on each side, rather than optimizing over specific edges, and requires a fundamentally different toolkit.

Our work also relates to papers that study flexibility on online marketplaces, though they focus on flexibility on a single side. In ride-hailing services, prior works study supply-side levers such as driver repositioning incentives (Ong et al. 2021) or a priority mode (Krishnan et al. 2022), and demand-side levers such as waiting mechanisms (Freund and van Ryzin 2021) or subscriptions Berger et al. (2023). More explicitly focused on demand-side flexibility, some works study opaque selling Elmachtoub et al. (2019) and flexible time windows (Zhou 2021) in online retail. Our work differs from all of these in that we focus on the interplay of two different flexibility levers.

**In-organization Incentives.** A reasonable interpretation of our structural results is that modern platforms are unlikely to find the optimal flexibility allocation if they optimize over two sides independently. Nonetheless, given the organizational structure of many platforms, with separate verticals working on the supply and the demand side, jointly experimenting and thus optimizing over levers on different market sides is uncommon. This misalignment relates to a stream of literature that identifies conflicting organizational incentives, e.g., the so-called marketing-operations alignment. There, organizations may face inefficiencies due to opposing incentives of two departments (marketing and operations) (Shapiro 1977). Solutions for marketing-operations conflicts focus on aligning incentives, including through internal integration of different teams within an organization (Weir et al. 2000), increasing the interface between manufacturing and marketing management (Hausman et al. 2002), and achieving a strategic alignment between external positioning and internal arrangement (Henderson and Venkatraman 1999). In our work, the separate verticals

do not have misaligned incentives; instead, the inefficiency arises from a lack of visibility, i.e., without joint experimentation, both teams lack visibility over the interplay between the two flexibility decisions.

**Random graphs.** The core technical component of our work relies on an asymptotic analysis of random graphs. Classical related works include characterizations of the asymptotic threshold for connectivity (Erdős et al. 1960) or the existence of perfect matchings (Erdős and Rényi 1966, Walkup 1980). As we focus on sparse random graphs, where the asymptotic probability that a node is matched is strictly between 0 and 1, our work falls into an area in which the Karp-Sipser (KS) algorithm is commonly applied (Karp and Sipser 1981). This algorithm is asymptotically optimal for the canonical maximum matching problem in a sparse random graph with  $n$  nodes and a uniform edge probability  $c/n$  between any two nodes (for constant  $c$  as  $n \rightarrow \infty$ ). Karp and Sipser prove this by characterizing the asymptotic matching probability as a solution to a system of nonlinear equations, using convergence results (Kurtz 1970). Some of our results (Theorems 3 and 7) resemble a class of papers that adapt the KS algorithm (Aronson et al. 1998, Bohman and Frieze 2011, Zdeborová and Mézard 2006) to different classes of random graphs. Most closely related is the work of Balister and Gerke (2015), who proved that the KS algorithm yields the asymptotically optimal matching probability in a class of bipartite random graphs based on a “configuration model.” Though similar, their model does not capture our setting with flexible and non-flexible nodes.<sup>2</sup> Nonetheless, we extend a similar analysis to our setting. Finally, a significant distinction between our work and the above is that we leverage our KS-style derivation in computer-aided proofs. Despite computer-aided proofs having a proud tradition in combinatorics, including proofs of the four-color theorem (Appel and Haken 1977, Robertson et al. 1996), we know of no other papers with provable comparisons of the limiting behavior of different random graphs that combine a KS-style analysis, continuity arguments, and a computer-aided grid search. In that regard, Gamarnik et al. (2006) may be closest to our approach, though they only compute a single explicit solution to a nonlinear equation (to compute the size of a largest independent set), whereas our grid search requires us to solve, within provable tolerance, approximately  $\approx 6 \times 10^6$  systems of nonlinear equations.

## 2. Model

Our two-sided platform flexibility models all share the same structure: maximum matching in a random bipartite graph. We first present this framework before introducing each specific model.

**Random Graph Formation.** We consider a bipartite graph  $G$  containing  $n \in \mathbb{N}^+$  nodes on each side<sup>3</sup>. The set of nodes on the left-hand side and right-hand side of  $G$  are denoted by  $V_l$  and  $V_r$ , respectively, and  $V = V_l \cup V_r$  is the set of all nodes. Nodes are indexed from  $1, \dots, n$  on each side, so that  $V_l = \{v_1^l, \dots, v_n^l\}$  and  $V_r = \{v_1^r, \dots, v_n^r\}$ . We denote the set  $\{1, \dots, n\}$  by  $[n]$ .

<sup>2</sup>E.g., our model, but not theirs, allows two nodes with positive expected degree to have 0 probability of being adjacent.

<sup>3</sup>While we focus on balanced bipartite graphs in the main body of the paper, we also conduct simulations to explore imbalanced markets in Section 7.

The sole decision variable in our model is  $\mathbf{b} = (b_l, b_r) \in [0, 1]^2$ , where  $b_l$  and  $b_r$  respectively specify probabilities that a node on the left-hand side and right-hand side is *flexible*. For each node in  $V_k$ ,  $k \in \{l, r\}$ , we independently sample Bernoulli random variables  $F_i^k \sim \text{Bernoulli}(b_k)$ ,  $\forall i \in [n]$ . Then, a node  $v_i^k \in V_k$  is *flexible* if  $F_i^k = 1$ ; otherwise, it is *non-flexible*. The flexibility decision  $(b_l, b_r)$  incurs a linear cost of  $c \cdot (b_l + b_r)$  for some constant  $c > 0$ .

The decision  $\mathbf{b}$  impacts the edge probabilities in our random bipartite graph. The presence of each edge is controlled by a Bernoulli random variable  $R_{ij}$ ,  $\forall i, j \in [n]$ . The edge that connects node  $v_i^l$  and  $v_j^r$  realizes if and only if  $R_{ij} = 1$ . If a node is flexible, we assume that the probability of any potential incident edges increases in a stochastic dominance sense:

$$\begin{aligned} \forall i, j \in [n] : \mathbb{P} \left[ R_{ij} = 1 | F_i^l = 1, F_j^r = 1 \right] &\geq \mathbb{P} \left[ R_{ij} = 1 | F_i^l = 1, F_j^r = 0 \right] = \mathbb{P} \left[ R_{ij} = 1 | F_i^l = 0, F_j^r = 1 \right] \\ &\geq \mathbb{P} \left[ R_{ij} = 1 | F_i^l = 0, F_j^r = 0 \right]. \end{aligned}$$

This implicitly assumes that we are in a symmetric setting where flexibility on either side contributes equally to the formation of an edge. In Section 2.1-2.3, we explore three models with specific edge distributions. In all of them,  $R_{ij}$  is sampled independently (but not necessarily identically) conditional on  $F_i^l$  and  $F_j^r$ .

**Maximum Matching.** In the resulting  $n \times n$  random bipartite graph  $G$ , we use the random variable  $\mathcal{M}_n(b_l, b_r)$  to denote the size of a *maximum matching*—that is, a matching that contains the largest possible number of edges. We define the *matching probability*  $\mu_n(b_l, b_r)$  as the expected fraction of nodes that are part of a maximum matching, i.e.,  $\mu_n(b_l, b_r) = \mathbb{E} [\mathcal{M}_n(b_l, b_r)/n]$ . We drop the dependency on  $n$  whenever it is clear from context.

**Objective.** We choose the flexibility parameters  $(b_l, b_r)$  to maximize the matching probability while accounting for the cost of flexibility. That is, we focus on the optimization problem

$$\max_{\mathbf{b} \in [0, 1]^2} \mu(b_l, b_r) - c \cdot (b_l + b_r) \quad (1)$$

We will use the notation  $g(b_l, b_r) := \mu(b_l, b_r) - c \cdot (b_l + b_r)$  to refer to this objective function. The optimization problem in (1) can be decomposed into two stages:

- (i) For a given budget  $B \geq 0$ , we optimize the allocation  $(b_l, b_r)$  subject to  $b_l + b_r = B$ .
- (ii) Knowing the optimal allocation for every given budget  $B \geq 0$ , we find  $B$  that maximizes (1).

Stage (ii) represents the trade-off between the benefit and the cost of flexibility, and the optimal flexibility budget  $B$  depends on the exogenous cost parameter  $c$ . Stage (i), the main focus of our work, optimizes the flexibility allocation  $(b_l, b_r)$  given a budget  $B$ . For instance, if  $(b_l^*, b_r^*)$  is an optimal solution to Eq. (1), does setting  $b_l^* = B$  and  $b_r^* = 0$  maximize  $\mu(b_l, b_r)$  for fixed  $B$ ? If so, then this suggests that two-sided marketplaces should only invest in flexibility on one side of their market; on the other hand, if  $b_l^* = b_r^*$ , then

teams responsible for flexibility levers on different market sides should jointly identify the optimal level of flexibility to invest in. To characterize this optimal solution structure, we aim to understand the geometric properties of  $\mu(b_l, b_r)$ .

We explore three versions of the matching model that capture different aspects of matching applications. In our simplest model with non-trivial effects, the  $2 \times 2$  model, there are only two nodes on each side. Then, we move on to a *local* model that takes the number of nodes to infinity, but nodes can only be matched if they are physically or spatially close to each other. This assumption holds true in ride-hailing dispatch systems, for instance. Finally, we consider the most complex model, the *global* model, which also takes the number of nodes to infinity but allows edges to form between any two nodes on both sides of the market (with equal probability conditioned on whether neither, one, or both of the nodes are flexible). We formally define these three models in the remainder of this section and state our results in Section 3. In the formalism we defined above, our results are of the following flavor: we show that  $\mu(B, 0) > \mu(b_l, B - b_l)$  for any  $B \in (0, 1]$ ,  $b_l \in [0, B]$  for the  $2 \times 2$  and the local model, whereas for the global model, depending on the value of  $B$  and the probability of edges occurring, we can have either  $\mu(B, 0) > \mu(B/2, B/2)$  or  $\mu(B, 0) < \mu(B/2, B/2)$ .

## 2.1. The $2 \times 2$ Model

Our  $2 \times 2$  model helps illustrate the set-up. We introduce two exogenous parameters  $p^f, p$ , and take

$$\mathbb{P} \left[ R_{ij} = 1 | F_i^l, F_j^r \right] = 2p + (F_i^l + F_j^r) \cdot (p^f - p), \forall i, j \in [2].$$

As illustrated in Fig. 1, this means that for every pair of nodes  $v_i^l$  and  $v_j^r$ , having a flexible node increases the probability of incident edges realizing by  $p^f - p$ . This additive edge probability ensures that the expected number of edges is affine in  $B = b_l + b_r$ , and in particular that it is invariant to  $(b_l, b_r)$  for fixed  $B$ . To ensure that flexibility increases the probability of edges forming and that the edge probability remains in  $[0, 1]$ , we make the following assumption:

**ASSUMPTION 1.**  $0 \leq p < p^f \leq 1/2$ .

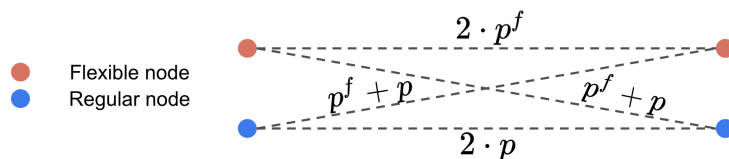


**Figure 1** Illustration of the edge probability in the  $2 \times 2$  model, for a given realization of the node types.

In line with notations defined in the general model, we denote the size of a maximum matching in the  $2 \times 2$  model by  $\mathcal{M}_2^{2 \times 2}(b_l, b_r)$  and the matching probability by  $\mu_2^{2 \times 2}(b_l, b_r) = \mathbb{E} \left[ \frac{\mathcal{M}_2^{2 \times 2}(b_l, b_r)}{2} \right]$ . Then,  $g_2^{2 \times 2}(b_l, b_r) := \mu_2^{2 \times 2}(b_l, b_r) - c \cdot (b_l + b_r)$ . Our goal is to characterize the optimal solution to

$$\max_{\mathbf{b} \in [0,1]^2} g_2^{2 \times 2}(b_l, b_r) = \max_{\mathbf{b} \in [0,1]^2} \mu_2^{2 \times 2}(b_l, b_r) - c \cdot (b_l + b_r).$$

We omit the super- and subscripts for the  $2 \times 2$  model whenever it is clear from the context.

An advantage of the  $2 \times 2$  model is that we can fully characterize the  $\mu(b_l, b_r)$  as a polynomial function with respect to  $b_l, b_r, p^f$  and  $p$ . The  $2 \times 2$  model has two features that will inspire our more complex models. First, each node only connects to a limited number of nodes. Second, conditioned on whether the nodes are flexible/non-flexible, all edges in the  $2 \times 2$  model have the same distribution. When scaling to larger networks, the *local* model maintains the first property, whereas the *global* model maintains the second, as illustrated in Fig. 2.

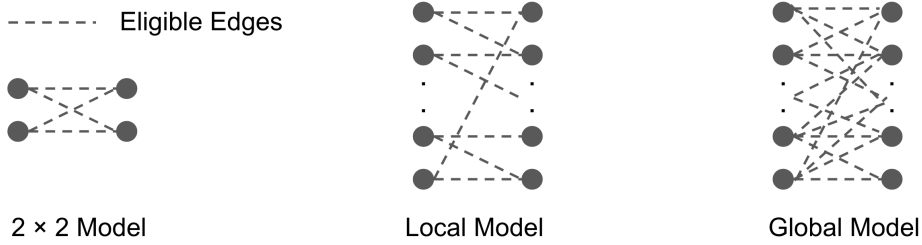


**Figure 2 Illustration of the graph models.**

## 2.2. The Local Model

In the local model, for any  $i < n$ ,  $v_i^l \in V_l$  is only eligible to connect to  $v_i^r$  and  $v_{i+1}^r$  in  $V_r$ , and  $v_n^l \in V_l$  is only eligible to connect to  $v_n^r$  and  $v_1^r$ . Therefore,  $v_j^r \in V_r$  can only connect to its previous two neighbors in  $V_l$ . As with the  $2 \times 2$  model, we take exogenous parameters  $p^f$  and  $p$  subject to Assumption 1. Edges then realize with the following conditional probabilities:

$$\mathbb{P} \left[ R_{ij} = 1 \mid F_i^l, F_j^r \right] = \begin{cases} 2p + (F_i^l + F_j^r) \cdot (p^f - p) & \text{if } ((j - i) \bmod n) \leq 1 \\ 0 & \text{otherwise} \end{cases}$$

Notice that these conditional probabilities follow the same additive properties as in the  $2 \times 2$  model.

In line with notations for the general model, for the local model the size of a maximum matching is denoted by  $\mathcal{M}_n^{loc}(b_l, b_r)$  and the matching probability by  $\mu_n^{loc}(b_l, b_r) := \mathbb{E} \left[ \frac{\mathcal{M}_n^{loc}(b_l, b_r)}{n} \right]$ . We are interested in the asymptotic behavior of  $\mu_n^{loc}(b_l, b_r)$  with respect to  $(b_l, b_r)$  as  $n \rightarrow \infty$ , a conventional scale of interest

in the study of random graphs. We denote this asymptotic quantity<sup>4</sup> by  $\mu^{loc}(b_l, b_r)$ , and with  $g^{loc}(b_l, b_r) := \mu^{loc}(b_l, b_r) - c \cdot (b_l + b_r)$ , our goal will be to characterize the optimum of

$$\max_{\mathbf{b} \in [0,1]^2} g^{loc}(b_l, b_r) = \max_{\mathbf{b} \in [0,1]^2} \mu^{loc}(b_l, b_r) - c \cdot (b_l + b_r) = \max_{\mathbf{b} \in [0,1]^2} \lim_{n \rightarrow \infty} \mu_n^{loc}(b_l, b_r) - c \cdot (b_l + b_r).$$

We omit the superscript for the local model whenever it is clear from the context.

### 2.3. The Global Model

An orthogonal extension of the  $2 \times 2$  model scales the number of nodes on each side to  $n$  and allows nodes to connect with any node on the opposite side of the graph. This gives rise to our global model, illustrated in Fig. 2. We focus on the *sparse* random graph regime, where the expected degree of each node remains constant as the size of the graph  $n$  scales large.<sup>5</sup> Specifically, we take constants  $\alpha^f$  and  $\alpha$  such that  $0 \leq \alpha < \alpha^f$  and define  $p_n^f = \alpha^f/n$ ,  $p_n = \alpha/n$ , respectively. Then,

$$\mathbb{P}\left[R_{ij} = 1 | F_i^l, F_j^r\right] = 2p_n + (F_i^l + F_j^r) \cdot (p_n^f - p_n), \forall i, j \in [n].$$

As in the  $2 \times 2$  model, the conditional probabilities are additive and independent of  $i$  and  $j$ .

In the global model, we denote the size of a maximum matching realization by  $\mathcal{M}_n^{glb}(b_l, b_r)$  and the matching probability by  $\mu_n^{glb}(b_l, b_r) := \mathbb{E}\left[\frac{\mathcal{M}_n^{glb}(b_l, b_r)}{n}\right]$ . As in the local model, we are interested in the asymptotic matching probability  $\mu^{glb}(b_l, b_r) := \limsup_{n \rightarrow \infty} \mu_n^{glb}(b_l, b_r)$ , which is equal to  $\lim_{n \rightarrow \infty} \mu_n^{glb}(b_l, b_r)$  when the latter exists. Then, with  $g^{glb}(b_l, b_r) = \mu^{glb}(b_l, b_r) - c \cdot (b_l + b_r)$ , our goal is to characterize  $\arg \max_{\mathbf{b} \in [0,1]^2} g^{glb}(b_l, b_r)$ . We drop the superscript when clear from context.

Due to the difficulties of analyzing this model, we complement our theoretical results for a subset of instances with numerical results. Specifically, we resort to simulations to compute the empirical mean for given  $(b_l, b_r)$ . Provided with  $s$  random graph samples yielding maximum matching sizes  $\mathcal{M}_n^1(b_l, b_r), \mathcal{M}_n^2(b_l, b_r), \dots, \mathcal{M}_n^s(b_l, b_r)$ , the empirical mean is computed as

$$\mu_{n,s}^{\text{EMP}}(b_l, b_r) := \frac{\sum_{s'} \mathcal{M}_n^{s'}(b_l, b_r)}{s \cdot n}.$$

Since the samples are independently and identically distributed (i.i.d.), the Law of Large Numbers (LLN) implies that  $\mu_{n,s}^{\text{EMP}}(b_l, b_r) \rightarrow \mu_n(b_l, b_r)$  almost surely as  $s \rightarrow \infty$ . In our experiments, unless stated otherwise, we use  $s = 1000$  and omit the dependency of  $\mu_{n,s}^{\text{EMP}}(b_l, b_r)$  on  $s$  for brevity.

<sup>4</sup>We prove the existence of the limit in Theorem 2.

<sup>5</sup>Erdős and Rényi (1966) proved for  $c > 1$  that a random graph with  $n$  nodes and i.i.d. edge probability  $c \cdot \log(n)/n$  almost surely possesses a perfect matching as  $n \rightarrow \infty$ . Thus, subsequent studies (Karp and Sipser 1981, Balister and Gerke 2015) often focus on the case where the edge probability is in  $\mathcal{O}(1/n)$  and each node's expected degree is  $\mathcal{O}(1)$ .

**Plans for the subsequent sections.** Recall that our main interest lies in the second stage described after Eq. (1), i.e., identifying the optimal allocation  $(b_l, b_r)$  given budget  $B \geq 0$ . For all our models,  $B$  determines the expected number of edges; thus, differences in the maximum matching size are due to the distribution of edges within the graph rather than their expected quantity. In the next section, we aim to characterize the geometry of  $\mu(b_l, b_r)$  by answering the following questions:

- I. For given budget  $B$ , what does the optimal flexibility allocation look like in these models?
- II. More broadly, does the surface of  $g(b_l, b_r)$  exhibit convexity, concavity, both or neither?

Then, in Section 4 and 5, we characterize intuitive effects driving the results in the global model.

### 3. Main Results

This section presents the main results to address questions I and II for each of our models.

#### 3.1. Comparison of Different Flexibility Allocations

We start by defining two intuitive flexibility allocation strategies: one-sided and balanced.

**DEFINITION 1.** For given budget  $B \in (0, 1]$ , the flexibility allocation  $\mathbf{b} = (B, 0)$  or  $\mathbf{b} = (0, B)$  is called the *one-sided allocation*, whereas  $\mathbf{b} = (B/2, B/2)$  is called the *balanced allocation*.

We have strong evidence that in all three models, given fixed  $B \in (0, 1]$ , either the one-sided allocation<sup>6</sup>  $(B, 0)$  or the balanced allocation  $(B/2, B/2)$  is optimal for  $\mu(b_l, b_r)$ : in the  $2 \times 2$  model, we find that  $(B, 0)$  is the optimal flexibility profile for any given  $B > 0$ . In the local model, we prove that  $(1, 0)$  dominates any other flexibility design when  $b_l + b_r = B = 1$ , and our simulations indicate that the same holds true for  $B < 1$ . In the global model, numerical evidence strongly suggests that optimality occurs at either  $(B, 0)$  or  $(B/2, B/2)$  for any given  $B > 0$ .<sup>7</sup>

Motivated by these findings, we compare the performance of the one-sided and the balanced allocation. Table 2 summarizes the results: in the  $2 \times 2$  and the local model, the one-sided allocation consistently dominates. However, in the global model either one can dominate, depending on the edge density and the budget. In our model  $\alpha^f + \alpha$  measures the edge density, and for a range of sparse random graphs  $e$ , the Euler's number, is known as a critical value that demarcates a transition from tree-like graph analyses to more complex structures (Karp and Sipser 1981, Aronson et al. 1998). In our analysis as well, the *subcritical*, where  $\alpha^f + \alpha < e$ , and the *supercritical* regime, where  $\alpha^f + \alpha \geq e$ , show stark differences. In the subcritical regime, or when  $B = 1$ , we recover the result from the other models that the one-sided flexibility allocation performs best. However, when  $B < 1$ , balanced allocation may be a better flexibility design in the supercritical regime. We formalize these in the following theorems.

<sup>6</sup>We omit allocation  $(0, B)$  in the subsequent discussions since it is trivially equivalent to  $(B, 0)$  by symmetry.

<sup>7</sup>The finding in the global model is supported by a combination of simulation results and a grid search over  $\mu^{\text{KS}}(b_l, b_r)$ , an analytical expression adapted from the literature (Section 6). Whereas we prove  $\mu(b_l, b_r) = \mu^{\text{KS}}(b_l, b_r)$  for some parameters, simulations suggest that the two quantities are always close.

Model	Quantity	Comparison
$2 \times 2$ model	$\mu^{2 \times 2}(b_l, b_r)$	$\forall B \in (0, 1] : \mu^{2 \times 2}(B, 0) > \mu^{2 \times 2}(B/2, B/2)$
Local model	$\mu^{loc}(b_l, b_r)$	$\forall B \in (0, 1] : \mu^{loc}(B, 0) > \mu^{loc}(B/2, B/2)$
Global model (most of subcritical regime, and whenever $\alpha = 0$ )	$\mu^{glb}(b_l, b_r)$	$\mu^{glb}(1, 0) \geq \mu^{glb}(1/2, 1/2)$
Global model (subset of supercritical regime)	$\mu^{glb}(b_l, b_r)$	$\forall B \in [0.4, 0.8] : \mu^{glb}(B, 0) < \mu^{glb}(B/2, B/2)$

**Table 2 Comparison of the one-sided and the balanced allocations. We prove the results for the subcritical regime for  $10^{-4} < \alpha < 0.77\alpha^f - 0.16$ , and those for the supercritical regime for  $\alpha^f \geq 22, \alpha \in [0.01, 0.05]$ .**

**THEOREM 1.**  $\mu^{2 \times 2}(B, 0) > \mu^{2 \times 2}(B/2, B/2)$  for any  $B \in (0, 1]$ .

In the  $2 \times 2$  model we derive a closed-form solution to the matching probabilities by computing the probability of each subset of the edges realizing (see Appendix B). A similar analysis yields the results for the local model (Appendix C).

**THEOREM 2.**  $\mu^{loc}(B, 0) > \mu^{loc}(B/2, B/2)$  for any  $B \in (0, 1]$ .

These properties also hold, for parameters as specified in Theorem 3, in the global model. We prove Theorem 3 (i) through a careful coupling technique (Section 4); in the proof of Theorem 3 (ii) we use the KS algorithm to exactly characterize the matching probability (see Section 6).

**THEOREM 3.**  $\mu^{glb}(1, 0) \geq \mu^{glb}(1/2, 1/2)$  if either (i)  $\alpha = 0$ , or (ii)  $10^{-4} < \alpha < 0.77\alpha^f - 0.16$  and  $\alpha^f + \alpha < e$ .<sup>8</sup>

However, in the global model the balanced allocation may be better than the one-sided one. The next result states that this occurs in a parameter regime with large  $\alpha^f$ , small positive  $\alpha$  and  $B < 1$ .

**THEOREM 4.** For any  $B \in [0, 4, 0.8]$ ,  $\alpha \in [0.01, 0.05]$ , and  $\alpha^f \geq 22$ ,  $\mu^{glb}(B/2, B/2) > \mu^{glb}(B, 0)$ .

In Section 4 and 5 we describe two key effects –*flexibility cannibalization* and *flexibility abundancy* – that drive the diverging behaviors in Theorem 3 and 4. Intuitively, flexibility cannibalization is a problem of the balanced allocation, where flexible nodes can make edges with flexible nodes. This increases the degree of flexible nodes, which already have the highest degree, and may lead to wasted edges as each flexible node can only be matched once: the flexible edges cannibalize each other. Flexibility abundancy arises when  $\alpha^f$  is so large that such cannibalization becomes insignificant; instead, the primary driver of the matching probability shifts towards matching the regular nodes among themselves, a task that is more effectively achieved by the balanced allocation.

<sup>8</sup>This boundary arises from the ability for a computer-aided proof to verify the inequality within a reasonable runtime: for  $\delta > 0$ , we construct and compute a lower bound the value of  $\mu(1, 0) - \mu(1/2, 1/2)$  within each set of  $[\alpha^f, \alpha^f + \delta] \times [\alpha, \alpha + \delta]$  within the subcritical regime. Taking  $\delta = 0.001$  yields the boundary in Theorem 3 (ii) and runs in approximately 20 hours.

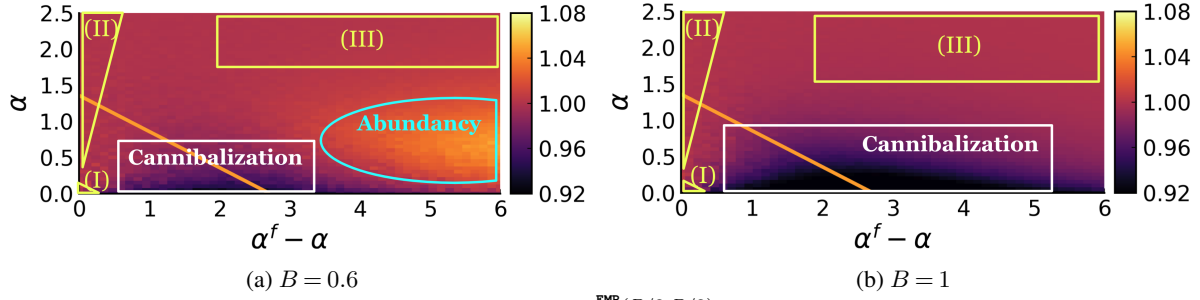


**Figure 3** The plots present heat-map values of  $\frac{\mu_n^{\text{EMP}}(B/2, B/2)}{\mu_n^{\text{EMP}}(B, 0)}$  across varying  $\alpha$  and  $\alpha^f - \alpha$  values when  $n = 100$ . The orange line highlights the boundary of the subcritical and supercritical regimes.

Our theoretical results suggest that flexibility cannibalization is most prominent for moderate values of  $\alpha^f$  and  $\alpha$ , whereas flexibility abundance arises when  $\alpha^f$  is large,  $\alpha$  is small and  $B < 1$ . Fig. 3 displays simulation results for  $\mu_n^{\text{EMP}}(b_l, b_r)$  when  $n = 100$ , and confirms that insight. It also displays that both allocations perform equally well in the regions labeled I-III. In region (I),  $\alpha^f + \alpha$  is extremely small, creating a very sparse graph in which almost all edges appear in a maximum matching. When the number of matches approximates the number of edges, we know that  $\mu(B/2, B/2) \approx \mu(B, 0)$  as both flexibility allocations yield the same number of edges in expectation. In region (II) flexibility does not notably increase the edge probability as  $((\alpha^f - \alpha)/\alpha) \approx 0$ ; thus, it matters little how flexibility is allocated. Finally, in region (III), with large  $\alpha^f$  and  $\alpha$ , almost all nodes are matched irrespective of the flexibility allocation. In contrast to these patterns, which are easily understood, Section 4 and 5 characterize where flexibility cannibalization and abundance arise.

### 3.2. Geometric Properties of $g(b_l, b_r)$

Beyond characterizing the optimal flexibility allocation, we also identify other geometric properties of  $g(b_l, b_r)$ . In particular, we explore the existence of local optima or saddle points. Such points provide insights for the experimental design of a platform that applies different flexibility levers, e.g., they may indicate that one should run experiments in which  $b_l$  and  $b_r$  are varied jointly. To derive such results for  $g(b_l, b_r)$ , we first define directional concavity and convexity.

**DEFINITION 2 (DIRECTIONAL CONCAVITY AND CONVEXITY).** Consider a function  $g : [0, 1]^2 \mapsto \mathbb{R}$  and a vector  $\mathbf{d} = (d_l, d_r) \in \mathbb{R}^2$ . The directional derivative of  $g$  at  $(b_l, b_r)$  in the direction  $(d_l, d_r)$  is, provided this limit exists,  $\nabla_{\mathbf{d}} g(b_l, b_r) = \lim_{h \rightarrow 0} \frac{g(b_l + h \cdot d_l, b_r + h \cdot d_r) - g(b_l, b_r)}{h}$ . Similarly, the second directional derivative of  $g$  at  $(b_l, b_r)$  in the direction  $(d_l, d_r)$  is, provided this limit exists,

$$\nabla_{\mathbf{d}}^2 g(b_l, b_r) = \lim_{h \rightarrow 0} \frac{g(b_l + h \cdot d_l, b_r + h \cdot d_r) - 2g(b_l, b_r) + g(b_l - h \cdot d_l, b_r - h \cdot d_r)}{h^2}.$$

Then,  $g$  is concave (resp. convex) in the direction of  $(d_l, d_r)$  at  $(b_l, b_r)$  if  $\nabla_{\mathbf{d}}^2 g(b_l, b_r) \leq 0$  (resp.  $\geq 0$ ). The convexity or concavity is strict if the corresponding inequality is strict.

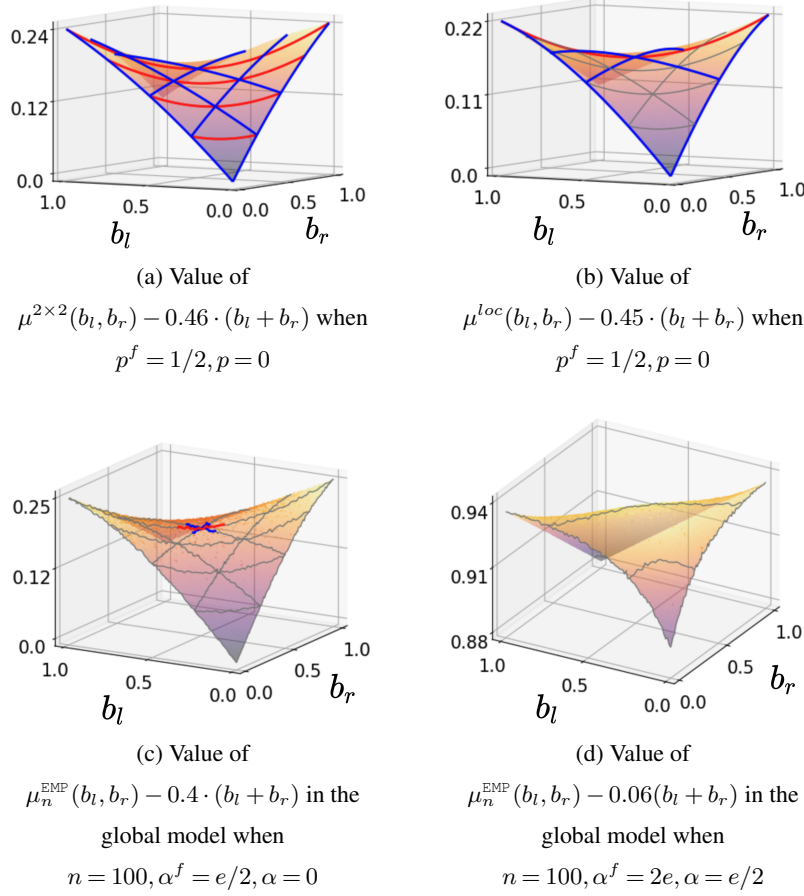


**Figure 4** In instances (a) and (b) we highlight provable concavity in blue and provable convexity in red; in instance (c) we show local convexity and concavity for  $\mu^{KS}(b_l, b_r)$  at  $(1/2, 1/2)$ ; in instance (d) we illustrate that convexity can break down in the supercritical regime of the global model.

We investigate the concavity and convexity properties of the function  $g(b_l, b_r)$  (or, equivalently, the function  $\mu(b_l, b_r)$ ) in the directions  $(1, 0), (0, 1)$  and  $(1, -1)$ . Fig. 4 illustrates our results: in the  $2 \times 2$  model we establish that  $g(b_l, b_r)$  is concave in the directions  $(1, 0), (0, 1)$  and convex in the direction  $(1, -1)$  for any  $(b_l, b_r) \in (0, 1)^2$ . In the local model, we obtain the same results, but only along specific axes of interest. As we do not, in general, have a closed form solution for the global model, we resort to a surrogate function  $\mu^{KS}(b_l, b_r)$ , later explained in Section 6 and Appendix A.3, which is provably equal to  $\mu^{KS}(b_l, b_r)$  at  $(b_l, b_r) = (1/2, 1/2)$  and numerically indistinguishable otherwise. We prove for most of the subcritical regime that  $\mu^{KS}(b_l, b_r)$  exhibits local convexity and concavity at  $(1/2, 1/2)$ . We formalize these results in the statements below.<sup>9</sup>

**THEOREM 5.** At any  $\mathbf{b} \in (0, 1)^2$ ,  $\mu^{2 \times 2}(b_l, b_r)$  is (i) strictly concave in the directions  $(0, 1), (1, 0)$  and  $(1, 1)$ , and (ii) strictly convex in the direction  $(1, -1)$ .

<sup>9</sup>Since the cost of flexibility is linear, the structural properties of  $\mu(b_l, b_r)$  extend directly to the function  $g(b_l, b_r)$ .

For the local model we find similar geometric properties along three specific diagonals.

**THEOREM 6.**  $\mu^{loc}(b_l, b_r)$  is strictly concave in the direction  $(0, 1)$  when  $b_l \in \{0, \frac{1}{2}\}$  and in the direction  $(1, 0)$  when  $b_r \in \{0, \frac{1}{2}\}$ .  $\mu^{loc}(b_l, b_r)$  is strictly convex in the direction  $(1, -1)$  when  $b_l + b_r = 1$ .

In most of the subcritical regime, the surrogate function  $\mu^{KS}(1/2, 1/2)$  for the global model exhibits similar geometric properties.

**THEOREM 7.** When  $10^{-4} < \alpha < 0.64\alpha^f - 0.03$  and  $0.62\alpha^f + \alpha < 1.68$ ,  $\mu^{KS}(1/2, 1/2)$  is (i) strictly concave in the directions  $(0, 1)$  and  $(1, 0)$ , and (ii) strictly convex in the direction  $(1, -1)$ .

Beyond the subcritical regime, the geometries of the global model can be more nuanced (see Fig. 4 (d)).

**REMARK 1.** The concavity results in the directions  $(1, 0)$  and  $(0, 1)$  highlight the decreasing marginal return of flexibility, which aligns with previous works that study the trade-off between the cost and the benefit of flexibility in different contexts of revenue management (E.g., Fine and Freund (1990)). However, the convexity results in the direction  $(1, -1)$  uncovers a novel and surprising interplay of two flexibility levers. As formalized in Appendix D, these geometric properties imply that the balanced allocation can be a saddle point and a sub-optimal (local) Nash Equilibrium in the respective models.

#### 4. Flexibility Cannibalization

The intuition for when flexibility cannibalization occurs in the global model comes from the simple insight that a feasible matching includes at most one of the edges incident to any given node. As such, flexibility designs should strive to avoid having many edges incident to the same node, as many of these end up wasted. In a balanced allocation, each flexible node has an expected degree of  $\alpha^f(1 + B/2) + \alpha(1 - B/2)$ . This is greater than the expected degree of any node in the one-sided flexibility design, which can be at most  $\alpha^f + \alpha$ . Intuitively, the edges that create this higher (expected) degree cannibalize each other in the balanced flexibility design. Fig. 5 provides an example to illustrate how flexible nodes tend to have higher average degrees in balanced allocations; moreover, it shows that edges end up being cannibalized in the concentrated subgraph of flexible nodes, which leaves more regular nodes unmatched than in the one-sided allocation. In this section we leverage flexibility cannibalization in the proof of Theorem 3 (i).

*Proof of Theorem 3 (i)* We prove that the one-sided allocation dominates the balanced one when  $B = 1$  and  $\alpha = 0$ . We first state two lemmas and prove they imply the theorem, deferring the proofs and constructions for the lemmas to Section 4.1-4.2 and the corresponding appendices.

We first introduce a new bipartite random graph distribution, denoted  $G_n^b$ , which is easier to analyze than the balanced allocation random graph (denoted  $G_n(1/2, 1/2)$ ) but has the same asymptotic matching probability. In  $G_n^b$ , exactly  $n/2$  nodes are flexible on each side (represented in the top sub-graph in the figures below). Each flexible node generates edges to the nodes on the other side (flexible or not), independently and with a probability  $p_n^f$  for each edge. This means that an edge between two flexible nodes can be generated

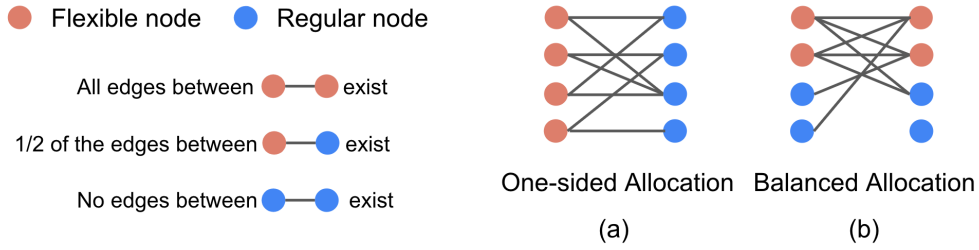


**Figure 5** Intuition for flexibility cannibalization. Plot (a) and (b) present realizations of one-sided and balanced allocations, assuming that all edges between two flexible nodes exist, half of those between flexible and regular node exist, and no edges between two regular nodes exist. In particular, plot (a) and (b) contain the same number of edges, but plot (b) has fewer matches due to a concentration of edges on the top subgraph.

twice (in that case, it's equivalent to one edge for matching purposes), and we distinguish them by using directed edges that start from the flexible node that generated them. This construction will enable a coupling between the generated edges of the balanced allocation with the ones of the one-sided allocation. Denoting the size of a realized maximum matching in  $G_n^b$  by the random variable  $\mathcal{M}_n^b$  and that of  $G_n(1/2, 1/2)$  by  $\mathcal{M}_n(1/2, 1/2)$ , we show nodes in  $G_n^b$  and  $G_n(1/2, 1/2)$  have the same asymptotic matching probability.

**LEMMA 1.** When  $\alpha = 0$ ,  $\limsup_{n \rightarrow \infty} \mathbb{E} [\mathcal{M}_n(1/2, 1/2) - \mathcal{M}_n^b] / n = 0$ .

Now, we compare  $G_n^b$  to the random graph with one-sided allocation. We denote the latter by  $G_n^o$  and its maximum matching size by  $\mathcal{M}_n(1, 0)$ . The next lemma compares  $\mathcal{M}_n^b$  and  $\mathcal{M}_n(1, 0)$ .

**LEMMA 2.** When  $\alpha = 0$ ,  $\mathbb{E} [\mathcal{M}_n^b] \leq \mathbb{E} [\mathcal{M}_n(1, 0)] \forall n$ .

For  $\alpha = 0$ , Lemma 1 gives us the second equality and Lemma 2 the inequality in the derivation

$$\mu(1/2, 1/2) = \limsup_{n \rightarrow \infty} \mathbb{E} \left[ \frac{\mathcal{M}_n(1/2, 1/2)}{n} \right] = \limsup_{n \rightarrow \infty} \mathbb{E} \left[ \frac{\mathcal{M}_n^b}{n} \right] \leq \limsup_{n \rightarrow \infty} \mathbb{E} \left[ \frac{\mathcal{M}_n(1, 0)}{n} \right] = \mu(1, 0),$$

which completes the proof of Theorem 3 (i).  $\square$

#### 4.1. Proof sketch of Lemma 1

The graph  $G_n^b$  is a directed random graph that contains edges generated from left to right (denoted  $R_{ij}^l$ ) and edges generated from right to left ( $R_{ij}^r$ ). The edge probabilities are given by:

$$\mathbb{P} [R_{ij}^l = 1] = p_n^f, \forall i \in [n/2], j \in [n] \text{ and } \mathbb{P} [R_{ij}^r = 1] = p_n^f, \forall j \in [n/2], i \in [n]. \quad (2)$$

$G_n^b$  differs from  $G_n(1/2, 1/2)$  in two ways: (i)  $G_n^b$  contains  $n/2$  nodes on each side of the bipartite graph that may generate edges towards the other side, whereas every node in  $G_n(1/2, 1/2)$  is flexible with probability  $1/2$ ; (ii) in  $G_n^b$  an edge between  $v_i^l$  and  $v_j^r$ ,  $i, j \in [n/2]$ , is generated from each side with probability  $p_n^f$ , instead of being generated only once with probability  $2p_n^f$ . It is intuitive that neither (i) or (ii) significantly

change the asymptotic matching size: standard concentration bounds guarantee that (i) affects  $o(n)$  nodes, and (ii) affects  $\sum_{i,j \in [n/2]} (p_n^f)^2 = \sum_{i,j \in [n/2]} (\alpha^f/n)^2 \in \mathcal{O}(1)$  possible edges in expectation. In Appendix A.1.1 we formalize this intuition.

#### 4.2. Proof sketch of Lemma 2

In our proof we construct a coupling between pairs of realizations of  $G_n^b$  and of  $G_n^o$  to compare the maximum matching sizes therein. First, we show that this coupling is valid in the sense that the coupled realizations occur with the same probability in their respective graphs. Second, we show that the average maximum matching size in the pair of realizations in  $G_n^b$  is smaller-equal to that in  $G_n^o$ . We present the key steps of our proof here and defer the complete proof to Appendix A.1.2.

**Coupling the Realizations of Graphs.** We partition the directed edges in a realization of  $G_n^b$  into sets  $X_1, X_2, X_3$  and  $X_4$ , depending on whether they are from left/right to top/bottom (see Fig. 6 (A)).

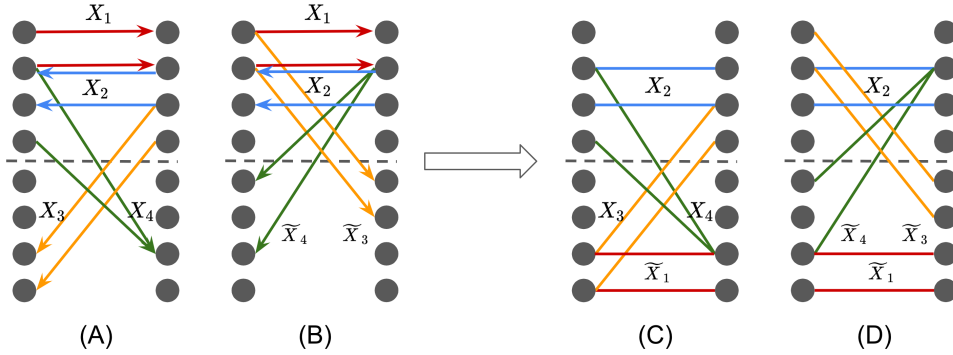
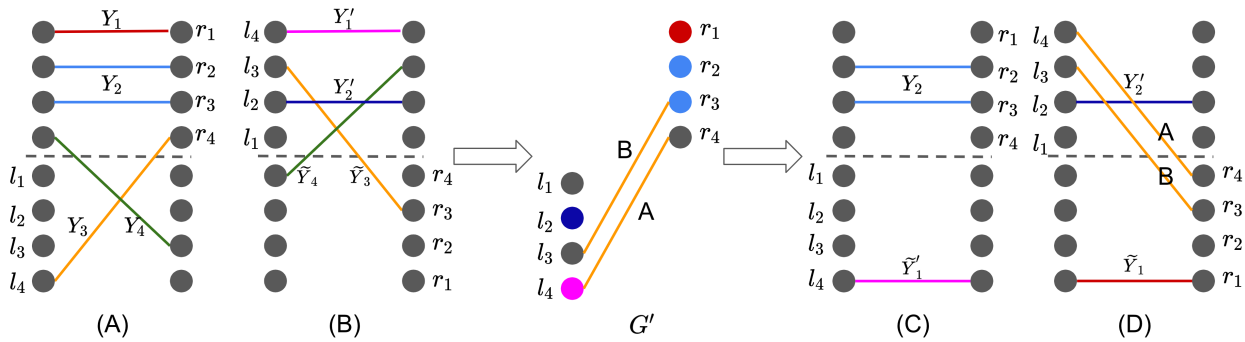


Figure 6 Illustration of the edges in graph (A) - (D)

We couple each such realization of edges, i.e., of sets  $X_1, X_2, X_3$  and  $X_4$ , with a second realization (B), also from  $G_n^b$ , that occurs with the same probability (Fig. 6 (B)). Essentially, we “flip” the edges in  $X_3$  and  $X_4$  across the vertical axis to obtain the sets  $\tilde{X}_3$  and  $\tilde{X}_4$ . Then, we couple (A) and (B) with two realizations, (C) and (D) (see Fig. 6 (C) and (D)). There, we “flip” the edges in  $X_1$  from the upper sub-graph in (A) and (B) to the lower sub-graph in (C) and (D). Denoting by  $M_A, M_B, M_C, M_D$  the maximum matching sizes in the respective graphs, we then show that  $M_A + M_B \leq M_C + M_D$  holding for all  $X_1, X_2, X_3$ , and  $X_4$  guarantees that  $\mathbb{E} [\mathcal{M}_n^b] \leq \mathbb{E} [\mathcal{M}_n(1, 0)]$ . We include the formal coupling and proof in Appendix A.1.2.

**Proving the Dominance of One-sided Allocation.** We still need to show that the required property  $M_A + M_B \leq M_C + M_D$  holds for arbitrary  $X_1, X_2, X_3$  and  $X_4$ . Denote by sets  $Y_i \subset X_i$  the edges that are part of a maximum matching, with  $Y'_i, \tilde{Y}_i$  defined accordingly. We start by copying all matches formed by edges in  $X_1$  and  $X_2$  in graph (A) and (B) into (C) and (D) as shown in Fig. 7. As the nodes in (C) and (D) that are matched through these edges can no longer be matched to any other node in the graphs, we denote the remaining nodes in (C) and (D) by  $\bar{C}$  and  $\bar{D}$  and the set of edges among these nodes by  $E(\bar{C})$



**Figure 7** The plot illustrates an example of  $G'$  constructed based on graphs (A) and (B). The labels indicate the correspondence between nodes/edges in  $G'$  and those in graphs (A)-(D).

and  $E(\bar{D})$ . Then, it suffices to show that we can injectively map all other matches (that we have not copied already) in (A) and (B) to  $M(\bar{C}) \cup M(\bar{D})$ , where  $M(\bar{C})$  and  $M(\bar{D})$  are respectively matchings in  $E(\bar{C})$  and  $E(\bar{D})$ . We construct such a mapping for edges in  $Y_3$  and  $\tilde{Y}_3$  based on a  $\frac{n}{2} \times \frac{n}{2}$  colored bipartite graph  $G'$ .  $G'$  includes all edges from  $Y_3$  and  $\tilde{Y}_3$  that occur in graph (A) and (B); we label edges in  $G'$  that come from  $Y_3$  as type A edges and edges from  $\tilde{Y}_3$  as type B edges (edges may be both type A and type B). Analogous to  $G'$ , we create a second graph  $G''$  that contains all the edges from  $X_4$  that are part of maximum matchings in (A) and (B). We show that edges in  $G', G''$  can be mapped into graphs (C) and/or (D) in such a way that combining the range of the map with the already copied edges produces feasible matchings in (C) and (D). As a result, each edge from  $M_A$  and  $M_B$  can be found in a matching in either (C) or (D), implying that  $M_A + M_B \leq M_C + M_D$ . Thus,  $\mathbb{E} [\mathcal{M}_n^b] \leq \mathbb{E} [\mathcal{M}_n(1, 0)]$ ,  $\forall n$  when  $\alpha = 0$ . We formalize these constructions in Appendix A.1.2.

**REMARK 2.** Flexibility cannibalization arises in  $G_B^n$  due to an over-concentration of edges in the upper subgraph (see Fig. 6 (A) and (B)). Our coupling method shows that this yields fewer matches than would be possible when some edges are moved to the lower subgraph (see (C) and (D)).

## 5. Flexibility Abundance

A second effect, that counters flexibility cannibalization, occurs in regions where  $\alpha^f$  is very large. In that case, flexible nodes have so many incident edges, that their cannibalization ceases to be a primary concern; we call this the flexibility abundance effect. In order to understand the flexibility abundance effect, consider a setting where  $\alpha^f$  is very large. Indeed, to gain intuition suppose flexibility is so abundant that each flexible node is adjacent to every node on the other side of the graph (see Fig. 8 (a) and (b)).

In this case, an optimal matching procedure is to (i) identify a maximum matching among the regular nodes, (ii) match as many flexible nodes as possible to remaining regular nodes.<sup>10</sup> When this procedure

<sup>10</sup>If flexible nodes remained thereafter, these could be matched to each other, but this does not occur in the regime with small  $\alpha$  that we focus on.

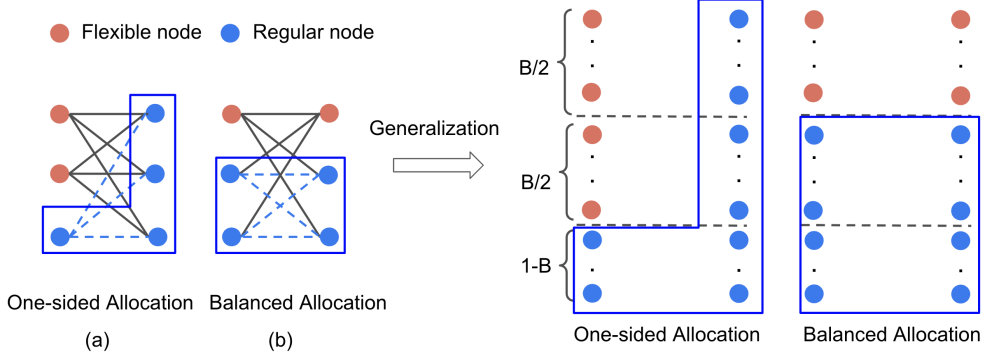


**Figure 8** Intuition for flexibility abundance. Plot (a) and (b) assume that each flexible node is connected to all nodes on the other side of the graph. We find that a perfect matching in plot (a) requires the realization of one the three dashed edges, whereas one in plot (b) requires the realization of one of the four dashed edges.

assigns all flexible nodes to remaining nonflexible ones, a balanced allocation of flexibility is more effective, as illustrated in Fig. 8. In Fig. 8 (c) and (d) we see that the balanced allocation leads to a higher number of expected edges among regular nodes. Concretely, observe in (a) and (b) that with all flexible nodes on one side, a perfect matching requires the realization of one of *three* potential blue edges among the regular nodes, whereas an even distribution of flexible nodes means that any one *four* potential blue edges realizing guarantees a perfect matching.

As we have observed in Fig. 3 (a), flexibility abundance arises for a wide range of parameters. Intuitively, it requires three ingredients: a high value of  $\alpha^f$  to ensure that flexible nodes have abundant incident edges (and that wasting such edges is not a primary concern), (ii)  $B < 1$  to ensure that one-sided flexibility cannot just match all flexible nodes to all regular nodes, and (iii) small (but positive)  $\alpha$  to ensure that there exists a non-trivial matching among the regular nodes while avoiding an outcome that is so dense that all nodes can trivially be matched<sup>11</sup> Thus, we expect flexibility abundance to be most pronounced in a parameter regime with high  $\alpha^f$ ,  $B < 1$ , and low  $\alpha$ . Theorem 4 exemplifies such a regime, requiring  $B \in [0, 4, 0.8]$ ,  $\alpha \in [0.01, 0.05]$  and  $\alpha^f \geq 22$  to assert that  $\mu(B/2, B/2) > \mu(B, 0)$ .

**Proof sketch of Theorem 4.** We now provide a proof sketch for Theorem 4 that generalizes the insights from Fig. 8 (a) and (b). Our proof derives an upper bound on the number of matched nodes under one-sided flexibility, and a lower bound on the number of matched nodes under balanced flexibility. For one-sided flexibility, we rely on the number of isolated (regular) nodes on the side on which we have flexibility. As there are about  $(1 - B)n$  regular nodes on this side, out of which about  $(1 - B)n e^{-2\alpha}$  are isolated, at most  $(1 - B)(1 - e^{-2\alpha})n$  of these regular nodes can be matched. For balanced flexibility, we

<sup>11</sup>Recalling the example in Fig. 8, it should be significantly more likely for one of four edges to realize than for one of three edges to realize: with large  $\alpha$ , the latter is too likely for this to be the case, when  $\alpha = 0$ , both are impossible.

analyze what happens when we first match the regular nodes among themselves (stage 1), and then show that sufficiently many flexible nodes can be matched afterwards (stage 2). For stage 1, we prove (Appendix A.2.1) the following bound on the maximum matching size in a  $(1 - B/2)n \times (1 - B/2)n$  graph of regular nodes,<sup>12</sup> denoted by random variable  $m_1$ :

**LEMMA 3.**  $\mathbb{E}[m_1] \geq 2 \cdot (1 - B/2)n [1 - (1 - B/2)\alpha - e^{-2\alpha(1-B/2)}]$  as  $n \rightarrow \infty$ .

Intuitively, for small  $\alpha$  the expected maximum matching size should be close to the expected number of edges because very few nodes have degree more than 1. Our proof explicitly characterizes this, and lower bounds  $m_1$  by subtracting the “extra edges” (those incident to nodes with degree  $> 1$ ) from all edges. This allows us to derive the lower bound for  $\mathbb{E}[m_1]$  in Lemma 3.

Assuming that all flexible nodes are matched to an unmatched regular node in stage 2, it suffices to compare the number of matches between regular nodes. By verifying that

$$(1 - B)(1 - e^{-2\alpha})n < 2 \cdot (1 - B/2)n [1 - (1 - B/2)\alpha - e^{-2\alpha(1-B/2)}]$$

for  $\alpha \in [0.01, 0.05]$  and  $B \in [0.4, 0.8]$ , the balanced allocation creates more matches in the sub-graph of regular nodes. In the proof of Theorem 4 (Appendix A.2.2) we show that the gap in the above inequality is sufficiently large to account for the fact that, in the balanced allocation, some flexible nodes may not be matched in stage 2.

## 6. Analyses Based on the Karp-Sipser Algorithm

In this section we devise a less intuitive, but more powerful tool, to better understand the properties of  $\mu(b_l, b_r)$  in the global model. In particular, this will allow us to overcome a limitation of the intuitive coupling proof presented in Section 4 for Theorem 3 (i) which is that the method is specific to  $\alpha = 0$ . To some extent this is unavoidable: the proof applies to arbitrarily large  $\alpha^f$  and, as we saw in the previous section, with large  $\alpha^f$ ,  $B < 1$  and  $\alpha > 0$ , the one-sided allocation does not yield a larger matching. In contrast, in this section, we predominantly target the subcritical regime. A classical approach to analyzing the maximum matching size in sparse random graphs is the Karp-Sipser (KS) algorithm, which is known to be asymptotically optimal for a range of sparse random graphs (Karp and Sipser 1981, Balister and Gerke 2015). As formalized in Algorithm 1 in Appendix A.3, the KS algorithm iteratively matches and prunes nodes with degree 1 until no such nodes remain; thereafter it randomly selects edges to match. In this section we generalize the known analyses of the KS algorithm to the bipartite random graphs in our model.

Our analysis is based on the quantity  $\mu^{KS}(b_l, b_r)$ , which is constructed from a set of 8 nonlinear equations provided in (9) and Theorem 9. Known analyses of the KS algorithm characterize the matching probability

<sup>12</sup>While the number of regular nodes on each side of the graph is not deterministically  $(1 - B/2)n$ , it concentrates around this value as  $n$  scales large and we assume this deterministic number for the purpose of this proof sketch.

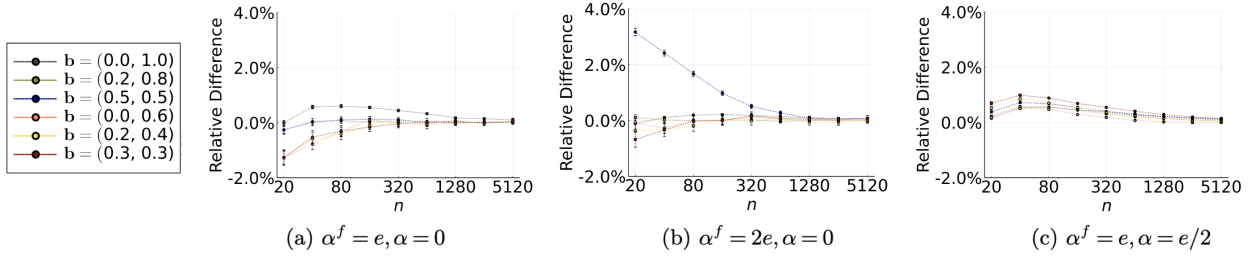


**Figure 9 The plots present  $(\mu_n^{KS}(b_l, b_r) - \mu_n^{EMP}(b_l, b_r)) / \mu_n^{EMP}(b_l, b_r)$  across varying  $(b_l, b_r)$  as  $n$  scales large.**

based on the fraction of nodes that are “target” or “loser” (Karp and Sipser 1981). In our case, we require 8 equations to determine the probability for flexible or regular nodes on either side to be either target or loser. The next result demonstrates the equivalence of  $\mu(b_l, b_r)$  and  $\mu^{KS}(b_l, b_r)$  for the one-sided and balanced allocations in almost all of the subcritical regime:

**THEOREM 8.** *When  $10^{-4} < \alpha < \alpha^f, \alpha^f + \alpha < e$ , and  $\mathbf{b} = (1, 0)$  or  $(1/2, 1/2)$ ,  $\mu(b_l, b_r) = \mu^{KS}(b_l, b_r)$ .*

Though Theorem 8 characterizes regions where  $\mu(\cdot, \cdot) = \mu^{KS}(\cdot, \cdot)$ , this in itself is not sufficient to make formal comparisons between  $\mu(1, 0)$  and  $\mu(1/2, 1/2)$ ; we also need to show that we can solve the nonlinear equations that  $\mu^{KS}(b_l, b_r)$  depends on to provable precision in these regions (see (21) in Appendix A.3.4). This then allows us to compare  $\mu(1, 0)$  and  $\mu(1/2, 1/2)$  for these  $\alpha^f$  and  $\alpha$  values. Moreover, by deriving a continuity property of  $\mu^{KS}$  in  $\alpha^f$  and  $\alpha$ , we can construct local lower bounds for  $\mu(1, 0) - \mu(1/2, 1/2)$  (see (19) and (20)), and conclude by verifying in a computer-aided proof that this lower bound exceeds 0 across the parameters specified by Theorem 3 (ii).<sup>13</sup>

Though Theorem 8 only applies to particular parameters, our numerical results (Fig. 9) suggest that  $\mu_n^{EMP}(b_l, b_r)$  approaches  $\mu^{KS}(b_l, b_r)$  for any parameters as  $n$  scales large. We thus use  $\mu^{KS}(b_l, b_r)$  to evaluate different flexibility allocations, not just the balanced and one-sided ones. Specifically, we conduct a grid search over  $B, \alpha^f, \alpha, b_l, b_r$  with the set of parameters denoted  $S$  (details in Appendix A.3.2); we trust this to give a better estimate of the true asymptotic matching probability while also being computationally more efficient. We illustrate the results in Fig. 10 and highlight the following observations.

**Either the one-sided or the balanced allocation is optimal.** This finding supports our focus on a comparison between the one-sided and the balanced allocations. Intuitively, one-sided flexibility (i) minimizes the cannibalization effect (no flexible node can be a neighbor of another) and (ii) maximizes the abundance effect (least number of potential edges between the regular nodes). For the balanced allocation, these two are exactly reversed. Our numerical findings suggest that across all parameters, one always wants to minimize the effect of one of these two in order to have an optimal allocation. In particular, this suggests

<sup>13</sup>The geometric properties stated in Theorem 7 follows from a similar computer-aided proof. For concavity, we construct local upper bounds to show that the second-order derivative (SOD) of  $\mu^{KS}(1/2, 1/2)$  is negative in the direction  $(0, 1)$ ; for convexity, we use local lower bounds to show that the SOD is positive in the direction  $(1, -1)$ .

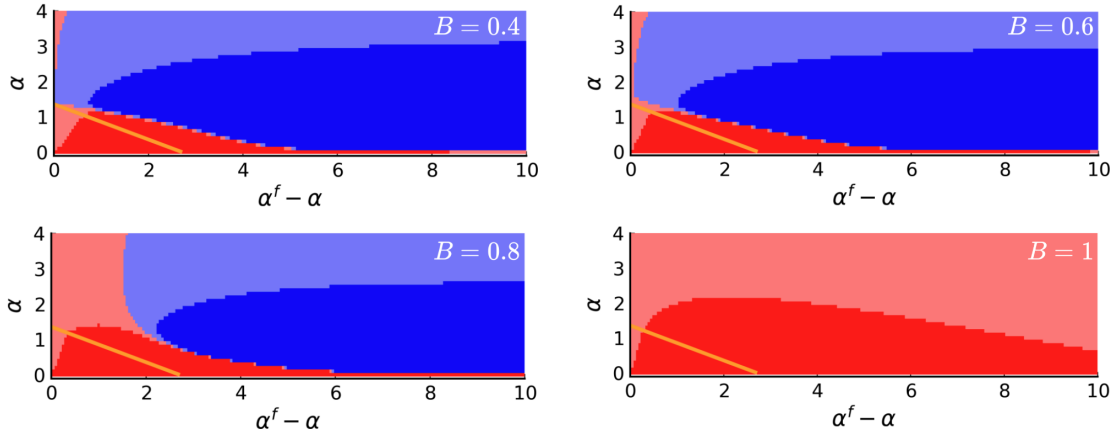


**Figure 10** The plots present the values of  $\frac{\mu^{\text{KS}}(B/2, B/2)}{\mu^{\text{KS}}(B, 0)}$  across varying  $\alpha^f$  and  $\alpha - \alpha^f$ : the ratio is smaller than 1 in the red region (light red if between 0.999 and 1) and greater than 1 in blue region (light blue if between 1 and 1.001). The orange line highlights the boundary of the subcritical and supercritical regimes.

that the (negative) impact of these effects is concave in the allocation, the optimum always occurs at one of the two endpoints (either one-sided or balanced) rather than at any point in between. This finding also matches our convexity results for the objective in the  $2 \times 2$  and local models.

**In the subcritical regime the one-sided allocation is better.** In Theorem 3 (ii) we proved this result for most of the sub-critical regime when  $B = 1$ . For  $B < 1$  we do not know how to prove Theorem 8, and as a result we cannot provably generalize our computer-aided proof to this regime. However, we still find numerically that the one-sided allocation is better within the sub-critical regime for all tested values of  $B$ . This also matches our theoretical findings in that  $\alpha^f$  cannot be too large in the subcritical regime, and thus the impact of flexibility abundance is also limited.

**When  $B = 1$  or  $\alpha = 0$  the one-sided allocation is better.** We find that  $B = 1$  and  $\alpha = 0$  are the special cases where the one-sided allocation always dominates,<sup>14</sup> regardless of the value of  $\alpha^f$ . Comparing this with our reasoning in Section 5, we find that these are exactly the cases where the flexibility abundance effect dissipates. This also explains why the coupling technique presented in Section 4 is specific to  $B = 1$  and  $\alpha = 0$ : for large  $\alpha^f$  Fig. 10 shows that the dominance of the one-sided allocation breaks down very close to the regime where  $B = 1$  and  $\alpha = 0$ .

Finally, these results confirm the characterization of Fig. 3 that we gave in Section 3.1: when  $\alpha^f$  and  $\alpha$  are very small (region (I) of Fig. 3), when  $\alpha^f/\alpha \approx 1$  (region (II)), and when  $\alpha^f$  and  $\alpha$  are very large (region (III)). In the remaining regions, it is either flexibility abundance or flexibility cannibalization that drives the optimality of a particular flexibility design.

<sup>14</sup>For  $\alpha = 0$ , though hard to see in the plots, there is always a thin red line just above the x-axis.

## 7. Simulation Results for Extended Models

Beyond the matching models considered thus far, we find numerically in two modeling extensions that both the flexibility cannibalization and abundance effects translate into these extended models. We start by introducing a spatial matching model in Section 7.1 to capture abstracted features of the matching problem faced by ride-hailing platforms. Then, on top of the spatial model, we further allow an unequal number of supply and demand nodes in Section 7.2 to model an imbalanced market.

We evaluate these models numerically by computing the empirical average matching probability  $\mu_{n,s}^{\text{EMP}}(b_l, b_r)$ . For these experiments, we set  $n = 100, s = 1000$  and drop the dependency of  $\mu_{n,s}^{\text{EMP}}(b_l, b_r)$  on these two parameters. Our findings reveal that even when we relax assumptions - such as conditional independence in edge generation, linearity in expected edge count, and symmetry of the two sides of the graph - flexibility cannibalization and abundance effects are still largely present in the relevant parameter regimes. However, due to the additional complexities introduced by these extended models, the results are further influenced by effects from non-linear expected edge counts and market imbalances.

### 7.1. Spatial Matching

In the spatial matching model, we consider a two-dimensional grid  $[0, 1]^2$  containing  $n$  drivers and  $n$  riders, uniformly distributed. Driver locations are denoted by vectors  $\mathbf{d}_1, \mathbf{d}_2, \dots, \mathbf{d}_n$ , and rider locations by  $\mathbf{r}_1, \mathbf{r}_2, \dots, \mathbf{r}_n$ . For a given flexibility allocation  $\mathbf{b} = (b_l, b_r)$ , driver  $i$  is flexible if random variable  $F_i^l \sim \text{Bernoulli}(b_l)$  takes the value of 1, otherwise the driver is regular. Similarly, each rider  $j$  is associated with  $F_j^r \sim \text{Bernoulli}(b_r)$ , and the rider is flexible if and only if  $F_j^r = 1$ . We take constants  $\alpha^f$  and  $\alpha$  such that  $0 \leq \alpha < \alpha^f$  and define  $p_n^f = \alpha^f / \sqrt{n}, p_n = \alpha / \sqrt{n}$ , respectively. We assume that an edge exists between a driver  $i$  and a rider  $j$  if their distance is within a threshold decided by their respective flexibility types:

$$\mathbb{P}[R_{ij} = 1 | F_i^l, F_j^r] = \begin{cases} 1 & \text{if } \|\mathbf{d}_i - \mathbf{r}_j\|_2 \leq 2p_n + (F_i^l + F_j^r) \cdot (p_n^f - p_n) \\ 0 & \text{otherwise} \end{cases}$$

In other words,  $\mathbf{r}_j$  has an edge with any  $\mathbf{d}_i$  within an area of  $\pi \cdot (2p_n + (F_i^l + F_j^r) \cdot (p_n^f - p_n))^2$ . The asymptotic set-up  $p_n^f, p_n \in \Theta(1/\sqrt{n})$  ensures that the expected number of edges in the spatial graph is in  $\Theta(1)$ , same as the asymptotic regime studied in the global model.

The spatial model relaxes (1) the conditional independence assumption on edge realization  $R_{ij}$  with respect to indices  $i$  and  $j$ , and (2) the equivalence of different flexibility allocations in expected edge counts. In particular, in one-sided allocation the expected number of riders that connects to a random driver is<sup>15</sup>  $(B(p_n^f + p_n)^2 + (1 - B)(2p_n)^2) \cdot \pi \cdot n^2$ . This is smaller than the expected number of riders that connects to a random driver in balanced allocation, which equals

$$\left( (B/2)^2 (2p_n^f)^2 + 2 \cdot B/2(1 - B/2) (p_n^f + p_n)^2 + (1 - B/2)^2 (2p_n)^2 \right) \cdot \pi \cdot n^2.$$

<sup>15</sup>We assume for simplicity that the driver is at least  $2p_n$  away from the boundary of the  $[0, 1]^2$  grid, an event that occurs with probability 1 as  $n \rightarrow \infty$ .

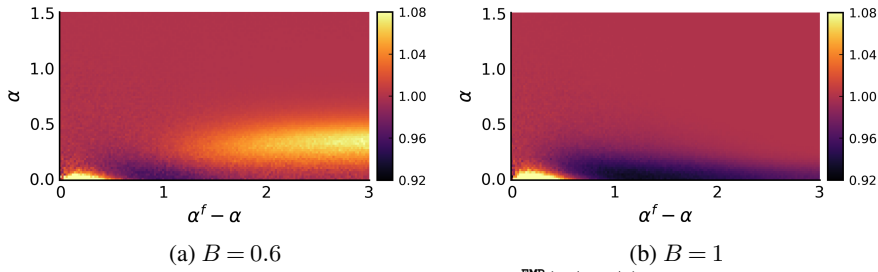


**Figure 11** The plots present heat-map values of  $\frac{\mu_{\text{EMP}}(B/2, B/2)}{\mu_{\text{EMP}}(B, 0)}$  across varying  $\alpha$  and  $\alpha^f - \alpha$ .

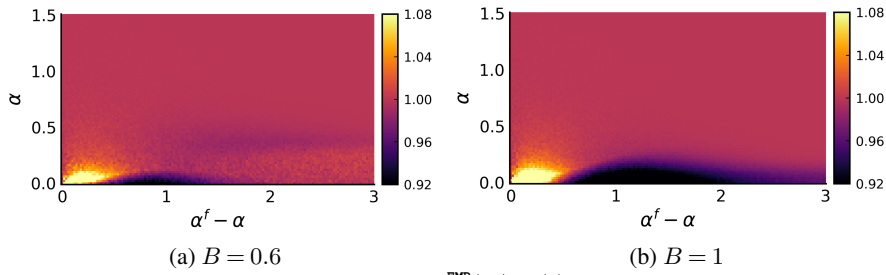


**Figure 12** The plots present heat-map values of  $\frac{\mu^{\text{EMP}}(B/2, B/2)}{\mu^{\text{EMP}}(B, 0)}$  across varying  $\alpha$  and  $\alpha^f - \alpha$  when  $\lambda = 0.8$ .

As such, we expect the balanced allocation to have an advantage over the one-sided allocation in the spatial setting. Indeed, in Fig. 11 we find that in a parameter regime with small  $\alpha^f$  and  $\alpha$ , balanced allocation now outperforms one-sided allocation. This is because in this very sparse regime the maximum matching size is close to the number of edges in the graph, and the later is higher in expectation in the balanced allocation. In other parts of the heatmap we find consistency with results in the global model: one-sided allocation can be over 8% better than the balanced allocation when  $B = 1$  or when  $\alpha^f$  is moderate; moreover, it can be over 8% worse than the balanced allocation when  $\alpha^f$  is very large,  $\alpha$  is a positive small number, and  $B < 1$ .

## 7.2. Imbalanced Market

Our theoretical analysis has focused on extremely symmetric markets to identify structural insights. Most real markets have less symmetry, which makes them more likely to favor one-sided flexibility. This subsection delves into numerically exploring flexibility allocations in imbalanced spatial matching markets and highlighting the complexity of this setting. Specifically, we extend the spatial model in the previous subsection, allowing  $\lambda \cdot n$  rather than  $n$  riders, where  $\lambda \in (0, 1]$ .<sup>16</sup> We assume that for a given flexibility allocation  $(b_l, b_r)$ , each driver is flexible with probability  $b_l \cdot \lambda$  and each rider is flexible with probability  $b_r$ . This ensures that the cost of incentivizing an equal number of riders and drivers remains the same. Notice that due to market imbalances the one-sided flexibility allocation  $(B, 0)$  shall no longer be equivalent to  $(0, B)$ , with the latter generating more edges in expectation. Intuitively, allocating flexibility to the side with fewer nodes (riders, in this case) more effectively maximizes the chances of these nodes being matched, which are the bottlenecks in an imbalanced market. As we observe in Fig. 12 (a) and (b), such market imbalance

<sup>16</sup>We ignore for symmetry the setting where the market has more demand than supply.

creates an advantage for one-sided allocation, partially counteracting the flexibility abundance effect that previously occurred when  $B < 1$ . Yet, the regions where flexibility cannibalization dominates align with observations in the global model and the symmetric spatial matching model.

## 8. Conclusion

Our work initiates the study of two-sided flexibility. We characterize the space of outcomes of different flexibility allocations, which results from the interplay of flexibility levers on different sides. We identify two effects, flexibility cannibalization and flexibility abundance, that respectively lend strength to the one-sided and balanced allocations. In doing so, we devise a coupling construction, employ concentration bounds, and generalize analyses based on the KS algorithm. Nonetheless, our work leaves many questions open: (1) whereas our model intentionally focuses on a particular type of edge probabilities, which keeps the expected number of edges invariant for a given budget  $B$ , different constructions (e.g., based on random geometric graphs) may be of practical interest; (2) though our effects seem to be robust under some such different constructions (see Section 7), all of our results are based on a central decision maker maximizing an unweighted matching whereas many platforms in practice involve choice among agents on both sides; we know of no results in this direction and believe it to likely yield many interesting findings; (3) finally, our work focuses on a matching model, but two-sided flexibility can also appear in queueing and manufacturing settings. All of these directions may yield ample interesting results in the years to come.

## References

- O Zeynep Akşin and Fikri Karaesmen. Characterizing the performance of process flexibility structures. *Operations Research Letters*, 35(4):477–484, 2007.
- Kenneth Appel and Wolfgang Haken. The solution of the four-color-map problem. *Scientific American*, 237(4):108–121, 1977.
- Jonathan Aronson, Alan Frieze, and Boris G Pittel. Maximum matchings in sparse random graphs: Karp–sipser revisited. *Random Structures & Algorithms*, 12(2):111–177, 1998.
- Paul N Balister and Stefanie Gerke. Controllability and matchings in random bipartite graphs. *Surveys in combinatorics*, 424:119, 2015.
- Achal Bassamboo, Ramandeep S Randhawa, and Jan A Van Mieghem. Optimal flexibility configurations in newsvendor networks: Going beyond chaining and pairing. *Management Science*, 56(8):1285–1303, 2010.
- Achal Bassamboo, Ramandeep S Randhawa, and Jan A Van Mieghem. A little flexibility is all you need: on the asymptotic value of flexible capacity in parallel queuing systems. *Operations Research*, 60(6):1423–1435, 2012.
- Ben Berger, Hongyao Ma, David Parkes, and Shreyas Sekar. Optimal subscription pricing design for ridesharing platforms. 2023.
- Tom Bohman and Alan Frieze. Karp–sipser on random graphs with a fixed degree sequence. *Combinatorics, Probability and Computing*, 20(5):721–741, 2011.

- John A Buzacott and David D Yao. Flexible manufacturing systems: a review of analytical models. *Management science*, 32(7):890–905, 1986.
- Xi Chen, Jiawei Zhang, and Yuan Zhou. Optimal sparse designs for process flexibility via probabilistic expanders. *Operations Research*, 63(5):1159–1176, 2015.
- Jiri Chod and Nils Rudi. Resource flexibility with responsive pricing. *Operations Research*, 53(3):532–548, 2005.
- Mabel C Chou, Geoffrey A Chua, Chung-Piaw Teo, and Huan Zheng. Process flexibility revisited: The graph expander and its applications. *Operations research*, 59(5):1090–1105, 2011.
- Antoine Désir, Vineet Goyal, Yehua Wei, and Jiawei Zhang. Sparse process flexibility designs: Is the long chain really optimal? *Operations Research*, 64(2):416–431, 2016.
- Adam N Elmachtoub and Michael L Hamilton. The power of opaque products in pricing. *Management Science*, 67(8):4686–4702, 2021.
- Adam N Elmachtoub, David Yao, and Yeqing Zhou. The value of flexibility from opaque selling. *Available at SSRN* 3483872, 2019.
- Pál Erdős and Alfréd Rényi. On the existence of a factor of degree one of a connected random graph. *Acta Math. Acad. Sci. Hungar.*, 17:359–368, 1966.
- Paul Erdős, Alfréd Rényi, et al. On the evolution of random graphs. *Publ. math. inst. hung. acad. sci.*, 5(1):17–60, 1960.
- Charles H Fine and Robert M Freund. Optimal investment in product-flexible manufacturing capacity. *Management science*, 36(4):449–466, 1990.
- Daniel Freund and Garrett van Ryzin. Pricing fast and slow: Limitations of dynamic pricing mechanisms in ride-hailing. *Available at SSRN* 3931844, 2021.
- David Gamarnik, Tomasz Nowicki, and Grzegorz Swirszczy. Maximum weight independent sets and matchings in sparse random graphs. exact results using the local weak convergence method. *Random Structures & Algorithms*, 28(1):76–106, 2006.
- Warren H Hausman, David B Montgomery, and Aleda V Roth. Why should marketing and manufacturing work together?: Some exploratory empirical results. *Journal of operations management*, 20(3):241–257, 2002.
- John C Henderson and Harihara Venkatraman. Strategic alignment: Leveraging information technology for transforming organizations. *IBM systems journal*, 38(2.3):472–484, 1999.
- Seyed M Iravani, Mark P Van Oyen, and Katharine T Sims. Structural flexibility: A new perspective on the design of manufacturing and service operations. *Management Science*, 51(2):151–166, 2005.
- William C Jordan and Stephen C Graves. Principles on the benefits of manufacturing process flexibility. *Management science*, 41(4):577–594, 1995.
- Richard M Karp and Michael Sipser. Maximum matching in sparse random graphs. In *22nd Annual Symposium on Foundations of Computer Science (sfcs 1981)*, pages 364–375. IEEE, 1981.

- Varun Krishnan, Ramon Iglesias, Sebastien Martin, Su Wang, Varun Pattabhiraman, and Garrett Van Ryzin. Solving the ride-sharing productivity paradox: Priority dispatch and optimal priority sets. *INFORMS Journal on Applied Analytics*, 52(5):433–445, 2022.
- Thomas G Kurtz. Solutions of ordinary differential equations as limits of pure jump markov processes. *Journal of applied Probability*, 7(1):49–58, 1970.
- Serguei Netessine, Gregory Dobson, and Robert A Shumsky. Flexible service capacity: Optimal investment and the impact of demand correlation. *Operations Research*, 50(2):375–388, 2002.
- NLsolve. NLsolve.jl: A Julia package for solving nonlinear equations. <https://github.com/JuliaNLsolvers/NLsolve.jl>, 2017. Version v4.5.1, MIT License.
- Hao Yi Ong, Daniel Freund, and Davide Crapis. Driver positioning and incentive budgeting with an escrow mechanism for ride-sharing platforms. *INFORMS Journal on Applied Analytics*, 51(5):373–390, 2021.
- Neil Robertson, Daniel Sanders, Paul Seymour, and Robin Thomas. A new proof of the four-colour theorem. *Electronic research announcements of the American Mathematical Society*, 2(1):17–25, 1996.
- Benson P Shapiro. Can marketing and manufacturing co-exist. *Harvard Business Review*, 55(5):104, 1977.
- David Simchi-Levi and Yehua Wei. Understanding the performance of the long chain and sparse designs in process flexibility. *Operations research*, 60(5):1125–1141, 2012.
- Philipp Ströhle, Christoph M Flath, and Johannes Gärttner. Leveraging customer flexibility for car-sharing fleet optimization. *Transportation Science*, 53(1):42–61, 2019.
- John N Tsitsiklis and Kuang Xu. Flexible queueing architectures. *Operations Research*, 65(5):1398–1413, 2017.
- Jan A Van Mieghem. Investment strategies for flexible resources. *Management Science*, 44(8):1071–1078, 1998.
- David W Walkup. Matchings in random regular bipartite digraphs. *Discrete mathematics*, 31(1):59–64, 1980.
- Rodney B Wallace and Ward Whitt. A staffing algorithm for call centers with skill-based routing. *Manufacturing & Service Operations Management*, 7(4):276–294, 2005.
- KA Weir, AK Kochhar, SA LeBeau, and DG Edgeley. An empirical study of the alignment between manufacturing and marketing strategies. *Long Range Planning*, 33(6):831–848, 2000.
- Douglas Brent West et al. *Introduction to graph theory*, volume 2. Prentice hall Upper Saddle River, 2001.
- Nicholas C Wormald et al. The differential equation method for random graph processes and greedy algorithms. *Lectures on approximation and randomized algorithms*, 73(155):0943–05073, 1999.
- Lenka Zdeborová and Marc Mézard. The number of matchings in random graphs. *Journal of Statistical Mechanics: Theory and Experiment*, 2006(05):P05003, 2006.
- Yeqing Zhou. *Supply Chain and Service Operations with Demand-Side Flexibility*. Columbia University, 2021.

## Appendix A: Proofs of the Global Model

### A.1. Proofs of the Global Model through the Coupling Argument

In this section, we prove Lemma 1 and Lemma 2, which are the key auxiliary results for Theorem 3 (i).

#### A.1.1. Proof of Lemma 1

*Proof.* Recall that we have constructed a random graph  $G_n^b$  in (2) that decomposes the  $2p_n^f$  edges as two groups of directed edges, in each of which an edge exists with probability  $p_n^f$ . Notice that when constructing a maximum matching in  $G_n^b$  we do not differentiate between edges of different directions but we maintain the requirement that no two edges (of either direction) can share a node in the matching.

We assume without loss of generality that  $n$  is an even number (else we can ignore nodes  $v_n^l$  and  $v_n^r$  without changing the asymptotic matching probability). We start by observing that in  $G_n(1/2, 1/2)$  the event

$$E_1 := \left\{ \left| \sum_i F_i^l - n/2 \right| \leq n^{5/8} \text{ and } \left| \sum_j F_j^r - n/2 \right| \leq n^{5/8} \right\}$$

occurs with high probability. Specifically, letting  $E_1^c$  be the complement of event  $E_1$ , we have

$$\begin{aligned} \mathbb{E} [\mathcal{M}_n(1/2, 1/2) - \mathcal{M}_n^b] &= \mathbb{E} [\mathcal{M}_n(1/2, 1/2) | E_1^c] \mathbb{P}[E_1^c] + \mathbb{E} [\mathcal{M}_n(1/2, 1/2) | E_1] \mathbb{P}[E_1] - \mathbb{E} [\mathcal{M}_n^b] \\ &\leq n \cdot e^{-\Omega(n^{1/4})} + \mathbb{E} [\mathcal{M}_n(1/2, 1/2) | E_1] - \mathbb{E} [\mathcal{M}_n^b] \\ &\leq \mathbb{E} [\mathcal{M}_n(1/2, 1/2) | E_1] - \mathbb{E} [\mathcal{M}_n^b] + \mathcal{O}(1) \\ &\leq \mathbb{E} [\mathcal{M}_n(1/2, 1/2) \left| \sum_i F_i^l = \sum_j F_j^r = n/2 \right.] + o(n) - \mathbb{E} [\mathcal{M}_n^b] + \mathcal{O}(1) \\ &= \mathbb{E} [\mathcal{M}_n(1/2, 1/2) - \mathcal{M}_n^b \left| \sum_i F_i^l = \sum_j F_j^r = n/2 \right.] + o(n). \end{aligned}$$

Notice that the first inequality above is a concentration result that follows from the Chernoff bound, and the third inequality above follows from the fact that having  $n^{5/8}$  additional flexible nodes on each side of  $G_n(1/2, 1/2)$  creates at most  $o(n)$  additional matches.

Conditional on  $\sum_i F_i^l = \sum_j F_j^r = n/2$ , we may assume without loss of generality that the first  $n/2$  nodes on each side of  $G_n(1/2, 1/2)$  are flexible, and thus  $\mathbb{P}[R_{ij} = 1] = 2p_n^f, \forall i, j \in [n/2]$  in such a graph. On the other hand, in  $G_n^b$  we have

$$\mathbb{P}[R_{ij} = 1] = \mathbb{P}[R_{ij}^l + R_{ij}^r \geq 1] = 2p_n^f - (p_n^f)^2, \forall i, j \in [n/2].$$

The probabilities for all other edges are common in both graphs. Thus, we can draw  $\omega_{ij}$  from uniform distribution  $U(0, 1)$  for every  $i, j \in [n]$  and use it to couple  $G_n^b$  and a balanced graph with  $\sum_i F_i^l = \sum_j F_j^r = n/2$ . For any  $i, j \in [n]$ , in each graph we have  $R_{ij} = 1$  if and only if  $\omega_{ij} \leq \mathbb{P}[R_{ij} = 1]$  in the respective graph. Then,

$$\begin{aligned} \mathbb{E} [\mathcal{M}_n(1/2, 1/2) - \mathcal{M}_n^b] &\leq \mathbb{E} [\mathcal{M}_n(1/2, 1/2) - \mathcal{M}_n^b \left| \sum_i F_i^l = \sum_j F_j^r = n/2 \right.] + o(n) \\ &= \mathbb{E} [\mathbb{E} [\mathcal{M}_n(1/2, 1/2) - \mathcal{M}_n^b | \omega] \left| \sum_i F_i^l = \sum_j F_j^r = n/2 \right.] + o(n) \end{aligned}$$

$$\begin{aligned}
&\leq \mathbb{E} \left[ \mathbb{E} \left[ \sum_{i,j \in [n/2]} \mathbb{1}_{\omega_{ij} \in [2p_n^f - (p_n^f)^2, 2p_n^f]} \middle| \boldsymbol{\omega} \right] \middle| \sum_i F_i^l = \sum_j F_j^r = n/2 \right] + o(n) \\
&= \sum_{i,j \in [n/2]} \mathbb{P} \left[ \omega_{ij} \in [2p_n^f - (p_n^f)^2, 2p_n^f] \right] + o(n) = \sum_{i,j \in [n/2]} (p_n^f)^2 + o(n) = o(n),
\end{aligned}$$

where the last inequality comes from the fact that in the additional matches in  $\mathcal{M}_n(1/2, 1/2)$  is upper bounded by the additional edges in the graph. Thus, when  $\alpha = 0$  we have  $\limsup_{n \rightarrow \infty} \mathbb{E} [\mathcal{M}_n(1/2, 1/2) - \mathcal{M}_n^b] / n = 0$ .  $\square$

### A.1.2. Proof of Lemma 2

*Proof.* Recall from Section 4.2 that we will start by constructing a valid coupling of realizations of  $G_n^b$  and  $G_n^o$ , and then compare the matching sizes among the coupled graphs. In  $G_n^b$ , we denote an edge from  $v_i^l$  to  $v_j^r$  by  $(v_i^l, v_j^r)$  and an edge from  $v_j^r$  to  $v_i^l$  by  $(v_j^r, v_i^l)$ . Then, we categorize the realized edges in  $G_n^b$  into four groups:

$$\begin{aligned}
X_1 &:= \left\{ (v_i^l, v_j^r) \mid i, j \in [n/2], R_{ij}^l = 1 \right\}, \quad X_2 := \left\{ (v_j^r, v_i^l) \mid i, j \in [n/2], R_{ij}^r = 1 \right\}, \\
X_3 &:= \left\{ (v_j^r, v_i^l) \mid j \in [n/2], i \in \{n/2+1, \dots, n\}, R_{ij}^r = 1 \right\}, \quad X_4 := \left\{ (v_i^l, v_j^r) \mid i \in [n/2], j \in \{n/2+1, \dots, n\}, R_{ij}^l = 1 \right\}.
\end{aligned}$$

In Fig. 6 (A) we illustrate the set of edges  $X_1, X_2, X_3, X_4$  by red, blue, yellow, and green, respectively.

In  $G_n^b$ , fix a realization of  $X_1, X_2, X_3$  and  $X_4$ . We start by flipping  $X_1, X_3$  and  $X_4$  vertically around the middle of the bipartite graph and swapping the directions accordingly, defining

$$\begin{aligned}
\tilde{X}_1 &:= \left\{ (v_{n+1-i}^l, v_{n+1-j}^r) \text{ for each } (v_i^l, v_j^r) \in X_1 \right\}, \quad \tilde{X}_3 := \left\{ (v_{n+1-i}^l, v_{n+1-j}^r) \text{ for each } (v_j^r, v_i^l) \in X_3 \right\}, \\
\text{and } \tilde{X}_4 &:= \left\{ (v_{n+1-j}^r, v_{n+1-i}^l) \text{ for each } (v_i^l, v_j^r) \in X_4 \right\}.
\end{aligned}$$

Then, we construct the following graphs: graph (A) contains edges in  $X_1, X_2, X_3$  and  $X_4$ ; graph (B) contains edges in  $X_1, X_2, \tilde{X}_3$  and  $\tilde{X}_4$ ; graph (C) contains edges in  $\tilde{X}_1, X_2, X_3, X_4$ , (and drop their directions); and graph (D) contains edges in  $\tilde{X}_1, X_2, \tilde{X}_3, \tilde{X}_4$ , (and drop their directions). Fig. 6 provides an illustration of the constructed graph (A)-(D) that colors the edges in  $X_1, X_2, X_3, X_4$  as red, blue, yellow, and green, respectively. We use the same color for the flipped edges to highlight that they mirror the original edges. Essentially, we flip  $X_3$  and  $X_4$  to construct graph (B), and then we flip  $X_1$  in (A) and (B) to construct (C) and (D).

We couple two realizations rather than a single realization to control for the differences in matching sizes that arise from the asymmetry between the top and bottom of  $X_3$  and  $X_4$ . Dropping for notational convenience the dependency of (A)-(D) on  $X_1, X_2, X_3$  and  $X_4$ , we denote the sizes of a maximum matching in the four graphs by  $M_A, M_B, M_C$  and  $M_D$ . We now argue that graph (A) and (B) are possible realizations of  $G_n^b$ , while graph (C) and (D) are possible realizations of  $G_n^o$ , all of which occur with the same probability in the respective random graphs. With  $p_n = \alpha/n = 0$ , in  $G_n^o$  we have  $\mathbb{P}[R_{ij} = 1] = p_n^f, \forall i, j \in [n]$ . Combined with (2), we thus know that, given  $X_1, X_2, X_3$  and  $X_4$ ,

$$\begin{aligned}
\mathbb{P}[G_n^b \text{ realizes as (A)}] &= \mathbb{P}[G_n^b \text{ realizes as (B)}] = \mathbb{P}[G_n^o \text{ realizes as (C)}] = \mathbb{P}[G_n^o \text{ realizes as (D)}] \\
&= (p_n^f)^{|X_1|+|X_2|+|X_3|+|X_4|} (1-p_n^f)^{n^2-(|X_1|+|X_2|+|X_3|+|X_4|)}.
\end{aligned}$$

We then couple the realization of  $G_n^b$  as graph (A) and (B) with the realization of  $G_n^o$  as graph (C) and (D). When  $X_3 = \tilde{X}_3$  and  $X_4 = \tilde{X}_4$ , i.e., (A) and (B) are identical, we trivially have  $M_A = M_B$ , and the maximum matching size in (A) can be written as  $(M_A + M_B)/2$ . On the other hand, when  $X_3 \neq \tilde{X}_3$  or  $X_4 \neq \tilde{X}_4$ , since  $G_n^b$  realize as (A) and

(B) with the same probability the weighted average maximum matching size in (A) and (B) is also  $(M_A + M_B)/2$ . Thus, for any  $n$ ,

$$\mathbb{E} [\mathcal{M}_n^b] = \sum_{\substack{\text{all realizations of} \\ X_1, X_2, X_3, X_4 \text{ in } G_n^b}} (p_n^f)^{|X_1|+|X_2|+|X_3|+|X_4|} (1-p_n^f)^{n^2 - (|X_1|+|X_2|+|X_3|+|X_4|)} \cdot \frac{M_A + M_B}{2}.$$

Similarly, we find that

$$\mathbb{E} [\mathcal{M}_n(1,0)] = \sum_{\substack{\text{all realizations of} \\ X_1, X_2, X_3, X_4 \text{ in } G_n^o}} (p_n^f)^{|X_1|+|X_2|+|X_3|+|X_4|} (1-p_n^f)^{n^2 - (|X_1|+|X_2|+|X_3|+|X_4|)} \cdot \frac{M_C + M_D}{2}.$$

Thus, as long as we can show that, for any  $X_1, X_2, X_3$  and  $X_4$ ,  $M_A + M_B \leq M_C + M_D$ , we can conclude that  $\mathbb{E} [\mathcal{M}_n^b] \leq \mathbb{E} [\mathcal{M}_n(1,0)] \forall n$  when  $\alpha = 0$ .

In the rest of the proof, we verify this inequality for arbitrary  $X_1, X_2, X_3$  and  $X_4$ . We pick an arbitrary maximum matching in (A) and denote the edges in  $X_1, X_2, X_3$  and  $X_4$  that are involved in the maximum matching by  $Y_1, Y_2, Y_3$  and  $Y_4$ . Similarly, we pick any maximum matching in (B) and denote the edges in  $X_1, X_2, \tilde{X}_3$  and  $\tilde{X}_4$  that are involved in the maximum matching by  $Y'_1, Y'_2, \tilde{Y}_3$  and  $\tilde{Y}_4$ .<sup>17</sup> We drop the direction of the edges as  $(v_i^l, v_j^r)$  and  $(v_j^r, v_i^l)$  cannot appear in the same matching,  $\forall i, j$ , and with a slight abuse of notation we denote an undirected edge between  $v_i^l$  and  $v_j^r$  by  $(v_i^l, v_j^r)$ . Fig. 13 (A) and (B) illustrate  $Y_1, Y'_1, Y_2, Y'_2, Y_3, Y_4$  as red, pink, blue, navy, yellow and green, respectively.

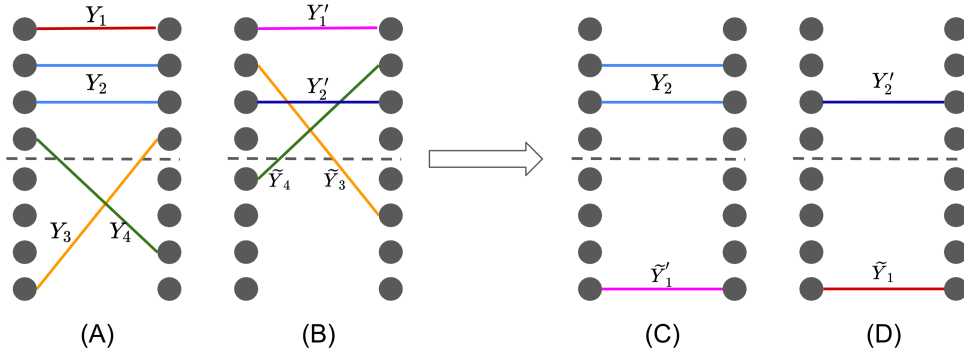


**Figure 13 Illustration of the matches in graph (A) - (D)**

To construct matchings in (C) and (D), we flip  $Y_1, Y'_1$  vertically and define

$$\tilde{Y}_1 := \left\{ (v_{n+1-i}^l, v_{n+1-j}^r) \text{ for each } (v_i^l, v_j^r) \in Y_1 \right\} \quad \text{and} \quad \tilde{Y}'_1 := \left\{ (v_{n+1-i}^l, v_{n+1-j}^r) \text{ for each } (v_i^l, v_j^r) \in Y'_1 \right\}.$$

Since graph (C) contains all edges in  $\tilde{X}_1$  and  $X_2$ ,  $\tilde{Y}'_1$  and  $Y_2$  are part of a feasible matching in (C). Similarly, since graph (D) also contains all edges in  $\tilde{X}_1$  and  $X_2$ ,  $Y'_2$  and  $\tilde{Y}_1$  are part of a feasible matching in (D). As illustrated in Fig. 13 (C) and (D), we copy  $\tilde{Y}'_1$  and  $Y_2$  into the construction of a matching in (C), and copy  $Y'_2$  and  $\tilde{Y}_1$  into a matching in (D). As before, we use the same color for the flipped edges.

Recall that  $\bar{C}$  and  $\bar{D}$  denote the remaining nodes in (C) and (D) that are not incident to the copied matches, and that  $E(\bar{C})$  and  $E(\bar{D})$  denote the edges among  $\bar{C}$  and  $\bar{D}$ . We construct a mapping  $\phi$  that injectively maps all other matches

<sup>17</sup>Notice that the distinction between  $Y_1, Y_2$  and  $Y'_1, Y'_2$  arises from the fact that the edges in  $X_1$  and  $X_2$  that are involved in a maximum matching for (A) may be different from those for (B).

in (A) and (B) (those in  $Y_3, \tilde{Y}_3, Y_4$  and  $\tilde{Y}_4$ ) to a matching  $M(\bar{C}) \cup M(\bar{D}) \subseteq E(\bar{C}) \cup E(\bar{D})$ . This then immediately implies that  $M_A + M_B \leq M_C + M_D$ .

Since the edges in  $X_3 (\tilde{X}_3)$  are not incident to those in  $X_4 (\tilde{X}_4)$ , the resulting matches  $Y_3, \tilde{Y}_3$  and  $Y_4, \tilde{Y}_4$  can be analyzed separately. Through a constructed graph  $G'$  we next show that the matches in  $Y_3$  and  $\tilde{Y}_3$  can be injectively mapped to  $(M(\bar{C}) \cap X_3) \cup (M(\bar{D}) \cap \tilde{X}_3)$  in graph (C) and (D); the injective mapping from  $Y_4$  and  $\tilde{Y}_4$  to  $(M(\bar{C}) \cap X_4) \cup (M(\bar{D}) \cap \tilde{X}_4)$  through  $G''$  follows from symmetry. Specifically, we construct  $G'$  as a bipartite graph with  $n/2$  nodes on each side. The edges in  $G'$  include *type A edges*:  $\{(v_i^l, v_j^r) \text{ for each } (v_i^l, v_j^r) \in Y_3\}$  and *type B edges*:  $\{(v_{n/2+1-i}^l, v_{n+1-j}^r) \text{ for each } (v_i^l, v_j^r) \in \tilde{Y}_3\}$ . Based on this construction an edge in  $G'$  can be both type A and B. Finally, we color the nodes in  $G'$ :

- We color  $v_j^r$  in  $G'$  by red (blue) if in graph (A)  $v_j^r$  is involved in  $Y_1 (Y_2)$ ;
- We color  $v_i^l$  in  $G'$  by pink (navy) if in graph (B)  $v_{n/2+1-i}^l$  is involved in  $Y'_1 (Y'_2)$ .

Fig. 7 provides an illustration of  $G'$  that is constructed based on Fig. 13 (A) and (B).

We begin by analyzing the degree of nodes in  $G'$ . If an uncolored node in  $G'$  has degree more than 2, then at least two of the edges come from the same matching. This would lead to a contradiction because in a matching no edges should share the same node. Thus, each uncolored node in  $G'$  has a degree of at most 2. Similarly, we find that each colored node in  $G'$  has a degree of at most 1 because, if the colored node is already involved in the matching of graph (A), then it cannot connect to any type A edges; if it is involved in the matching of graph (B), then it cannot connect to any type B edges. Thus, in  $G'$  each colored node can connect to at most one edge from either type A or type B.

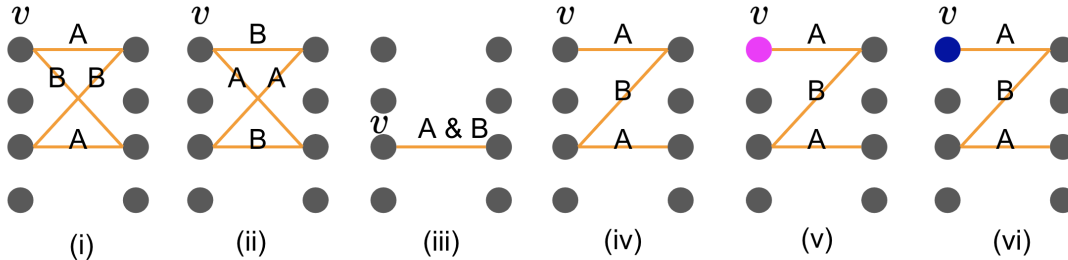


**Figure 14 Illustrations of possible connected components in  $G'$ .**

Since nodes in  $G'$  have a degree of at most 2, any connected component in  $G'$  is either a path or a cycle (page 109 of West et al. (2001)). Fig. 14 illustrates examples of connected components in  $G'$ . We next construct matching  $M(\bar{C})$  and  $M(\bar{D})$  based on the structure of paths and cycles in  $G'$ . The mappings ensure that (i) all edges in  $G'$  of either type A or B are mapped to either  $M(\bar{C}) \cap X_3$  or  $M(\bar{D}) \cap \tilde{X}_3$ , and (ii) all edges of both type A and B are mapped to both  $M(\bar{C}) \cap X_3$  and  $M(\bar{D}) \cap \tilde{X}_3$ . This then immediately completes the proof. In doing so, we use the following bijective mappings from edges in  $G'$  to  $M(\bar{C}) \cap X_3$  and  $M(\bar{D}) \cap \tilde{X}_3$ , which we denote by  $f_C$  and  $f_D$ , respectively:

$$f_C : (v_i^l, v_j^r) \rightarrow (v_{i+n/2}^l, v_j^r), f_D : (v_i^l, v_j^r) \rightarrow (v_{n/2+1-i}^l, v_{n+1-j}^r), \forall i, j \in [n/2]. \quad (3)$$

To find appropriate mappings for edges in  $G'$ , we begin by considering the case of cycles. Since all nodes in a cycle have a degree of 2, no node involved in the cycle can be colored. Moreover, in a bipartite graph, all cycles are of even length. Since no two type A edges or two type B edges may share the same node, the edges in the cycle must be alternating in type A and B. That is, the edges must either be of (1) type A, B, A, B,..., or (2) type B, A, B, A,..., as

illustrated in Fig. 14 (assuming that we start from the node  $v$  on the top left and move to the top right). For structure (1), we can simply allocate any type A edge to graph (C) by  $f_C$  to become part of  $M(\bar{C})$ , and type B edge to graph (D) by  $f_D$  to become part of  $M(\bar{D})$ . Such allocation always leads to a feasible matching because the allocated edges are not incident to any colored nodes, and thus not incident to any matches already copied from  $Y_1, Y_2, Y'_1$ , and  $Y'_2$ . The allocation based on structure (2) is symmetric.

Now we consider the case of paths. Since all but the endpoints of a path have a degree of 2, only the two endpoints of a path may be colored. Thus, it suffices to consider the following three sub-cases: (1) the two endpoints of the path are both uncolored, (2) one of the endpoints is colored, and (3) both of the endpoints of the path are colored.

- In sub-case (1), if the path has a length of one, as illustrated in Fig. 14 (iii), the edge may be of both type A and B. In this case, it is included into both  $M(\bar{C})$  and  $M(\bar{D})$  using  $f_C$  and  $f_D$ . In all other situations, as illustrated in Fig. 14 (iv), the path must alternate between edges of type A and B. Thus, we can iteratively include all edges in the path into  $M(\bar{C})$  or  $M(\bar{D})$ , as we did in the case of cycles.
- In sub-case (2), if an end-point  $v$  is colored pink, as illustrated in Fig. 14 (v), then the edge that connects to the endpoint must be of type A. Any subsequent edge to  $v$  must then alternate between type B, A, B, .... To avoid the first edge sharing a node with  $\tilde{Y}'_1$  in graph (C), we include all type A edges into  $M(\bar{D})$  by  $f_D$ , and all type B edges into  $M(\bar{C})$  by  $f_C$ . In contrast, if an end-point  $v$  is navy, as illustrated in Fig. 14 (vi), then the edge that connects to the endpoint must be of type A. Thus, the subsequent edges follow type B,A,B, .... To avoid the first edge sharing a node with  $Y'_2$  in graph (D), we then include all type A edges into  $M(\bar{C})$  by  $f_C$  and type B edges into  $M(\bar{D})$  by  $f_D$ . The cases with one of the endpoints being red or blue are symmetric. Fig. 7 provides an illustration of how type A and type B edges are mapped to graph (C) and (D) based on colors in  $G'$ .
- Finally, we observe that it is not possible for both endpoints of a path to be colored. If the path is of odd length, one of the endpoints is colored pink/navy, and the other is colored red/blue. Since the edges, starting from the endpoint colored pink/navy, must alternate between type A and B, with an odd number of edges the last edge must be of type A. This contradicts the feasibility of the matching in graph (A) because the colored node is already occupied by  $Y_1$  or  $Y_2$  in graph (A). On the other hand, if the path is of even length, both of the endpoints will be on the same side of the bipartite graph. Assume for simplicity that both endpoints are colored pink/navy, we find that alternating between type A and B edges is guaranteed to lead to a contradiction in one of the endpoints. Thus, sub-case (3) is not possible.

Therefore, in all possible sub-cases the matches in  $Y_3$  and  $\tilde{Y}_3$  can be injectively mapped to  $(M(\bar{C}) \cap X_3) \cup (M(\bar{D}) \cap \tilde{X}_3)$  in graph (C) and (D). This shows that  $M_A + M_B \leq M_C + M_D$  for any  $X_1, X_2, X_3$  and  $X_4$ , and thus  $\mathbb{E}[\mathcal{M}_n^b] \leq \mathbb{E}[\mathcal{M}_n(1,0)] \ \forall n$  when  $\alpha = 0$ .  $\square$

## A.2. Proofs of the Global Model through Probability Bounds

### A.2.1. Proof of Lemma 3

*Proof.* Denote the number the nodes in  $V_l$  and  $V_r$  that have a degree of  $d$  by  $q_d^l$  and  $q_d^r$ , respectively. We start by showing that, in any realization of the  $(1 - B/2)n \times (1 - B/2)n$  bipartite graph,

$$m_1 \geq \sum_d q_d^l \cdot d - \sum_{d=2}^{(1-B/2)n} q_d^l \cdot (d-1) - \sum_{d=2}^{(1-B/2)n} q_d^r \cdot (d-1). \quad (4)$$

Notice that  $\sum_d q_d^l \cdot d = \sum_d q_d^r \cdot d$  is the number of edges in the graph, and the second and third term in (4) respectively capture the extra edges, i.e., those incident to nodes with degree  $> 1$ , on the left and right-hand side of the graph. This lower bound holds because, after deleting  $d-1$  edges from all nodes with degree  $d > 1$  in  $V_l$  and  $V_r$ , all remaining edges in the graph would have degree 1 on both ends. In other words, the remaining edges are not incident to each other and is trivially a (not necessarily maximum) matching.

Notice that the probability for a node  $v$  on the left or right-hand side of the graph to have degree  $d$  is the same in this symmetric bipartite graph. Taking expectation over the lower bound in (4), we find that

$$\begin{aligned} \mathbb{E}[m_1] &\geq (1 - B/2)n \sum_{d=1}^{(1-B/2)n} \mathbb{P}[\deg(v) = d] \cdot d - 2(1 - B/2)n \sum_{d=2}^{(1-B/2)n} \mathbb{P}[\deg(v) = d] \cdot (d-1) \\ &= (1 - B/2)n \mathbb{E}[\deg(v)] - 2(1 - B/2)n \sum_{d=2}^{(1-B/2)n} \mathbb{P}[\deg(v) = d] \cdot (d-1) \\ &= (1 - B/2)^2 n 2\alpha - 2(1 - B/2)n \sum_{d=2}^{(1-B/2)n} \mathbb{P}[\deg(v) = d] \cdot (d-1). \end{aligned} \quad (5)$$

We simplify the second term by observing that

$$\begin{aligned} \sum_{d=2}^{(1-B/2)n} \mathbb{P}[\deg(v) = d] \cdot (d-1) &= \sum_{d=2}^{(1-B/2)n} \binom{(1-B/2)n}{d} (2\alpha/n)^d \cdot (1-2\alpha/n)^{(1-B/2)n-d} \cdot (d-1) \\ &= \sum_{d=2}^n \binom{n}{d} (2\alpha(1-B/2)/n)^d \cdot (1-2\alpha(1-B/2)/n)^{n-d} \cdot (d-1) \\ &= 2\alpha(1-B/2) + e^{-2\alpha(1-B/2)} - 1 \text{ as } n \rightarrow \infty. \end{aligned}$$

Plugging this into (5), we find that

$$\begin{aligned} \mathbb{E}[m_1] &\geq (1 - B/2)^2 n 2\alpha - 2(1 - B/2)n \left( 2\alpha(1 - B/2) + e^{-2\alpha(1 - B/2)} - 1 \right) \\ &= 2 \cdot (1 - B/2) n \left[ 1 - (1 - B/2)\alpha - e^{-2\alpha(1 - B/2)} \right] \text{ as } n \rightarrow \infty. \end{aligned}$$

□

### A.2.2. Proof of Theorem 4

*Proof.* We first provide an upper bound on  $\mu(B, 0)$  and then derive a lower bound on  $\mu(B/2, B/2)$ . When  $\mathbf{b} = (B, 0)$ , a node  $v \in V_l$  is regular with probability  $1 - B$  and all nodes in  $V_r$  are regular nodes. Thus, regular node  $v$  forms an edge with a node  $u \in V_r$  with probability  $2\alpha/n$ . Then,

$$\begin{aligned} \mu(B, 0) &\leq 1 - \lim_{n \rightarrow \infty} \mathbb{P}[\text{regular node } v \in V_l \text{ has degree 0}] \\ &= 1 - \lim_{n \rightarrow \infty} (1 - B) (1 - 2\alpha/n)^n = 1 - (1 - B) \cdot e^{-2\alpha}. \end{aligned} \quad (6)$$

Then, to lower bound  $\mu(B/2, B/2)$ , we adopt a greedy matching scheme: in the first stage we only match the regular nodes in  $V_l$  with the regular nodes in  $V_r$ , and in the second stage we greedily match the rest of the flexible nodes. Denote the number of matches formed in stage 1 and 2 by  $n_1$  and  $n_2$ , respectively. Since each node  $v \in V_l$  is regular with probability  $1 - B/2$ , by Chernoff bound we find that there are  $(1 - B/2)n + \Omega(n^{5/8})$  regular nodes in  $V_l$  with a probability of at most  $2e^{-\Omega(n^{1/4})}$ . That is, there are  $(1 - B/2)n + o(n)$  regular nodes on each side with high probability (w.h.p)  $1 - e^{-\Omega(n^{1/4})}$ . Since each edge in this regular sub-graph realizes with probability  $2\alpha/n$ , we apply Lemma 3 and find that w.h.p.

$$\mathbb{E}[n_1] = \mathbb{E}[m_1] + o(n) \geq 2 \cdot (1 - B/2) n \left[ 1 - (1 - B/2)\alpha - e^{-2\alpha(1-B/2)} \right] + o(n) \text{ as } n \rightarrow \infty.$$

Since for any  $\alpha \leq 0.05$  we have

$$\begin{aligned} & \lim_{n \rightarrow \infty} \mathbb{P}[\text{regular node } v \in V_l \text{ not connected to any regular node in } V_r] \\ & \geq \lim_{n \rightarrow \infty} (1 - 2\alpha/n)^{(1-B/2)n+o(n)} \geq \lim_{n \rightarrow \infty} (1 - 0.1/n)^{(1-B/2)\cdot n+o(n)} = e^{-0.1(1-B/2)}, \end{aligned}$$

w.h.p we also have

$$\mathbb{E}[n_1] \leq \left(1 - e^{-0.1(1-B/2)}\right) ((1 - B/2)n + o(n)) \leq \left(1 - e^{-0.1(1-B/2)}\right) (1 - B/2) \cdot n + o(n).$$

Now we examine the flexible nodes and argue that, even if we greedily match the flexible nodes to any unmatched regular nodes on the opposite side, almost all of the flexible nodes will be matched in the second stage. Given  $n'$  unmatched regular nodes in  $V_r$ , the number of edges between a flexible node  $v \in V_l$  and these  $n'$  nodes is governed by  $\text{Binom}\left(n', \frac{\alpha^f + \alpha}{n}\right)$ . For any  $n' \in \Theta(n)$ , by the Poisson Limit Theorem we find that  $\text{Binom}\left(n', \frac{\alpha^f + \alpha}{n}\right)$  converges in distribution to  $\text{Poisson}\left(\frac{n'}{n} (\alpha^f + \alpha)\right)$  as  $n \rightarrow \infty$ . Thus, as  $n \rightarrow \infty$

$$\mathbb{P}[v \text{ not connected to any unmatched regular node in } V_r | n'] = e^{-\frac{n'}{n} (\alpha^f + \alpha)}.$$

We now apply this bound to the flexible nodes in  $V_l$ . By applying the Chernoff bound we find that w.h.p.  $n_1 \leq 0.08(1 - B/2)n + o(n)$ , and there are  $B/2 \cdot n + o(n)$  flexible nodes and  $(1 - B/2) \cdot n + o(n)$  regular nodes on each side of the graph, an event that we denote by  $E_1$ . Under  $E_1$ , we greedily match each flexible node to any unmatched regular node in  $V_r$ . In particular, for the  $i$ th flexible node under consideration, even if all previous  $i - 1$  flexible nodes are already matched to regular nodes in  $V_r$ , there will still be at least

$$(1 - B/2) \cdot n - i - \left(1 - e^{-0.1(1-B/2)}\right) (1 - B/2) \cdot n + o(n)$$

unmatched regular nodes in  $V_r$ . This allows us to bound:

$$\begin{aligned} & \mathbb{P}[i\text{th flexible node not connected to any unmatched regular node in } V_r | E_1] \\ & \leq e^{-\frac{(1-B/2)\cdot n - i - (1 - e^{-0.1(1-B/2)}) (1 - B/2) \cdot n + o(n)}{n} (\alpha^f + \alpha)} \leq e^{-\frac{(1-B/2) - i/n - (1 - e^{-0.1(1-B/2)}) (1 - B/2)}{\alpha^f}} \text{ as } n \rightarrow \infty. \end{aligned}$$

Thus, as  $n \rightarrow \infty$ , through the greedy algorithm that iteratively matches each flexible to any unmatched regular node, the  $i$ th flexible node ends up unmatched with probability at most

$$1 - e^{-\frac{(1-B/2) - i/n - (1 - e^{-0.1(1-B/2)}) (1 - B/2)}{\alpha^f}}.$$

The argument for matching flexible nodes in  $V_r$  with regular nodes in  $V_l$  is symmetric. Since this is a lower bound on the matching probability for any  $i \in \{1, 2, \dots, B/2 \cdot n\}$ , we find that when  $\alpha \in [0.01, 0.05]$ ,

$$\begin{aligned} \lim_{n \rightarrow \infty} \mathbb{E} \left[ \frac{n_2}{n} | E_1 \right] &\geq 2 \cdot \lim_{n \rightarrow \infty} \left[ \sum_{i=1}^{B/2 \cdot n} \left( 1 - e^{-((1-B/2)-i/n - (1-e^{-0.1(1-B/2)})(1-B/2))\alpha^f} \right) / n \right] \\ &= 2 \cdot B/2 - 2 \cdot \lim_{n \rightarrow \infty} \left[ \sum_{i=1}^{B/2 \cdot n} e^{-((1-B/2)-i/n - (1-e^{-0.1(1-B/2)})(1-B/2))\alpha^f} \right] / n \\ &= B - \frac{2}{\alpha^f} \left[ \left( e^{\alpha^f \cdot B/2} - 1 \right) e^{-\alpha^f (1-B/2) e^{-0.1(1-B/2)}} \right]. \end{aligned}$$

Thus, when  $\alpha \in [0.01, 0.05]$ ,

$$\begin{aligned} \mu(B/2, B/2) &\geq \lim_{n \rightarrow \infty} \mathbb{E} \left[ \frac{n_1 + n_2}{n} \right] \\ &\geq \lim_{n \rightarrow \infty} \left( \mathbb{E} \left[ \frac{n_1 + n_2}{n} | E_1 \right] \cdot \mathbb{P}[E_1] \right) + 0 \cdot \lim_{n \rightarrow \infty} (1 - \mathbb{P}[E_1]) \\ &\geq 2 \cdot (1 - B/2) \left[ 1 - (1 - B/2)\alpha - e^{-2\alpha(1-B/2)} \right] \\ &\quad + B - \frac{2}{\alpha^f} \left[ \left( e^{\alpha^f \cdot B/2} - 1 \right) e^{-\alpha^f (1-B/2) e^{-0.1(1-B/2)}} \right]. \end{aligned} \tag{7}$$

Due to the non-linearity of the bounds in (6) and (7), it is difficult to make an analytical comparison of  $\mu(B, 0)$  and  $\mu(B/2, B/2)$  for a wide range of  $B, \alpha^f$  and  $\alpha$  values. Instead, we fix  $\alpha^f = 22$  and construct local upper and lower bounds for  $\mu(B, 0)$  and  $\mu(B/2, B/2)$  within a small interval of  $B$  and  $\alpha$  values to show that  $\mu(B, 0) < \mu(B/2, B/2)$  within this small interval. Then, we adopt a computer-aided proof to verify the inequality over all such intervals. Specifically, given  $\delta > 0$ , for any  $(B', \alpha') \in [B - \delta, B] \times [\alpha - \delta, \alpha] \subseteq [0.4, 0.8] \times [0.01, 0.05]$ , we can upper bound

$$\mu(B', 0) \leq 1 - (1 - B') \cdot e^{-2\alpha'} \leq 1 - (1 - B) \cdot e^{-2\alpha}$$

and lower bound

$$\begin{aligned} \mu(B'/2, B'/2) &\geq 2 \cdot (1 - B'/2) \left[ 1 - (1 - B'/2)\alpha' - e^{-2\alpha'(1-B'/2)} \right] \\ &\quad + B' - \frac{2}{\alpha^f} \left[ \left( e^{\alpha^f \cdot B'/2} - 1 \right) e^{-\alpha^f (1-B'/2) e^{-0.1(1-B'/2)}} \right] \\ &\geq 2 \cdot (1 - B/2) \left[ 1 - (1 - (B - \delta)/2)\alpha - e^{-2(\alpha - \delta)(1-B/2)} \right] \\ &\quad + (B - \delta) - \frac{2}{\alpha^f} \left[ \left( e^{\alpha^f \cdot B/2} - 1 \right) e^{-\alpha^f (1-B/2) e^{-0.1(1-(B-\delta)/2)}} \right]. \end{aligned}$$

Thus, by showing that

$$\begin{aligned} 1 - (1 - B) \cdot e^{-2\alpha} &\leq 2 \cdot (1 - B/2) \left[ 1 - (1 - (B - \delta)/2)\alpha - e^{-2(\alpha - \delta)(1-B/2)} \right] \\ &\quad + (B - \delta) - \frac{2}{\alpha^f} \left[ \left( e^{\alpha^f \cdot B/2} - 1 \right) e^{-\alpha^f (1-B/2) e^{-0.1(1-(B-\delta)/2)}} \right]. \end{aligned} \tag{8}$$

we verify that  $\mu(B', 0) < \mu(B'/2, B'/2)$  for any  $(B', \alpha') \in [B - \delta, B] \times [\alpha - \delta, \alpha]$ .

In Theorem4.ipynb,<sup>18</sup> we take  $\delta = 0.0001$  and verify that (8) holds for  $B \in \{0.4000, 0.4001, \dots, 0.7999, 0.8000\}$  and  $\alpha \in \{0.0100, 0.0101, \dots, 0.0499, 0.0500\}$ . Therefore,  $\mu(B/2, B/2) > \mu(B, 0)$  for any  $B \in [0.4, 0.8], \alpha \in [0.01, 0.05]$  and  $\alpha^f \geq 22$ .  $\square$

<sup>18</sup>The computer-aided proof can be found at <https://bit.ly/3HMJL13>.

### A.3. Proofs of the Global Model through the KS algorithm

This section proceeds as follows: We begin with the definition of the KS algorithm in Algorithm 1. We then derive the asymptotic matching probability  $\mu^{\text{KS}}(b_l, b_r)$  that results from the KS algorithm, as stated in Theorem 9, and Condition 1 under which the KS algorithm is provably optimal. Next, we verify Condition 1 for a subset of instances, leading to Theorem 8 that states the equivalence of  $\mu(b_l, b_r)$  and  $\mu^{\text{KS}}(b_l, b_r)$  for a range of parameters.

The KS-based analyses drive two of the results presented in Section 3. First of all, it allows us to analytically compare the one-sided and the balanced allocations in parameter regimes specified by Theorem 3 (ii). Secondly, it allows us to investigate  $\mu^{\text{KS}}(b_l, b_r)$  as a proxy measure of interest and establish its structural properties at  $\mathbf{b} = (1/2, 1/2)$  in Theorem 7.

**A.3.1. KS Derivations.** We start by defining the KS algorithm. We denote by  $G_n^{glb}(b_l, b_r)$  an  $n \times n$  random bipartite graph that follows the global model with allocation  $\mathbf{b}$ , and drop the superscript, the dependency on  $n$  and  $\mathbf{b}$  whenever it is clear from the context.

**DEFINITION 3.** In graph  $G$ ,

- (i) An edge  $e$  is said to be *incident* to a node  $v$  if  $v$  is one of the endpoints of  $e$ ;
- (ii) The *degree* of a node  $v$  is the number of edges that are incident to  $v$ , and we denote this number by  $\deg(v)$ ;
- (iii) A node  $v$  is said to be *isolated* if  $\deg(v) = 0$ .

---

#### Algorithm 1 Karp-Sipser's (KS) Algorithm

---

- 1: **Input:** Graph  $G$
  - 2: Initialize graph  $G'$  as an empty graph on the same set of nodes as  $G$
  - 3: **while**  $G$  has edges **do**
  - 4:     **if** there exist nodes of degree 1 in  $G$  **then**
  - 5:         Choose uniformly at random an edge  $e$  incident to a node of degree 1
  - 6:     **else**
  - 7:         Choose uniformly at random an edge  $e$  from all remaining edges
  - 8:     Add edge  $e$  to graph  $G'$
  - 9:     Delete edge  $e$  and all edges incident to  $e$  from graph  $G$
  - 10: **Output:** The number of edges in  $G'$
- 

When all edges incident to a node  $v$  are deleted from  $G$  and not included in  $G'$ , the node  $v$  is termed *isolated*. Such a node will not be part of the resulting matching. The key to finding the size of a maximum matching using the KS algorithm is to count the number of nodes that either become matched or isolated as edges are deleted from the graph. We denote the steps before the first occurrence where no nodes have a degree of 1 in  $G$  as *Phase 1* of the KS algorithm. The subsequent steps are referred to as *Phase 2* of the KS algorithm. Let  $M_1^l, M_1^r, M_2^l$  and  $M_2^r$  respectively represent the set of nodes in  $V_l$  and  $V_r$  that enter the matching during phase 1 and 2. By symmetry, we know that

$m_1 := |M_1^l| = |M_1^r|$  and  $m_2 := |M_2^l| = |M_2^r|$ . Similarly, let  $\Psi_1^l, \Psi_1^r, \Psi_2^l$  and  $\Psi_2^r$  respectively represent the set of nodes that become isolated in  $V_l$  and  $V_r$  during phase 1 and 2. We define  $\psi_1 := \max\{|\Psi_1^l|, |\Psi_1^r|\}$  and

$$\psi_2 := n - m_1 - m_2 - \psi_1 = \min\{n - |M_1^l| - |M_2^l| - |\Psi_1^l|, n - |M_1^r| - |M_2^r| - |\Psi_1^r|\} = \min\{|\Psi_2^l|, |\Psi_2^r|\}.$$

Intuitively,  $\psi_2$  represents the number of additional nodes that become isolated in Phase 2 of the KS algorithm, excluding those already accounted for in Phase 1. It has been demonstrated that, for a wide range of sparse random graph settings, the expected number of nodes becoming isolated in Phase 2 of the KS algorithm is  $o(n)$ , i.e.,  $\mathbb{E}[\psi_2] \in o(n)$ . The proof typically relies on showing the probability of isolation remains small along the trajectory of an evolving system of differential equations, and verifying such results along the trajectory can be tedious. Therefore, we establish the following condition and verify it for a subset of instances later in Theorem 8.

**Condition 1** When the KS algorithm is applied to a random graph  $G$  of the global model,  $\mathbb{E}[\psi_2] \in o(n)$ .

Under Condition 1, it suffices to analyze the probability of a node becoming isolated in Phase 1 of the KS algorithm. For  $\mathbf{b} = (b_l, b_r)$ , this probability is determined by the following set of equations:

$$\begin{aligned} w_1^f(\mathbf{b}) &= e^{-2b_r\alpha^f(1-\hat{w}_2^f(\mathbf{b}))-(1-b_r)\cdot(\alpha^f+\alpha)(1-\hat{w}_2^{nf}(\mathbf{b}))}, \\ w_1^{nf}(\mathbf{b}) &= e^{-b_r\cdot(\alpha^f+\alpha)(1-\hat{w}_2^f(\mathbf{b}))-2(1-b_r)\alpha(1-\hat{w}_2^{nf}(\mathbf{b}))}, \\ w_2^f(\mathbf{b}) &= 1 - e^{-2b_r\alpha^f\hat{w}_1^f(\mathbf{b})-(1-b_r)(\alpha^f+\alpha)\hat{w}_1^{nf}(\mathbf{b})}, \\ w_2^{nf}(\mathbf{b}) &= 1 - e^{-b_r(\alpha^f+\alpha)\hat{w}_1^f(\mathbf{b})-2(1-b_r)\alpha\hat{w}_1^{nf}(\mathbf{b})}, \\ \hat{w}_1^f(\mathbf{b}) &= e^{-2b_l\alpha^f(1-w_2^f(\mathbf{b}))-(1-b_l)(\alpha^f+\alpha)(1-w_2^{nf}(\mathbf{b}))}, \\ \hat{w}_1^{nf}(\mathbf{b}) &= e^{-b_l(\alpha^f+\alpha)(1-w_2^f(\mathbf{b}))-2(1-b_l)\alpha(1-w_2^{nf}(\mathbf{b}))}, \\ \hat{w}_2^f(\mathbf{b}) &= 1 - e^{-2b_l\alpha^f w_1^f(\mathbf{b})-(1-b_l)(\alpha^f+\alpha)w_1^{nf}(\mathbf{b})}, \\ \hat{w}_2^{nf}(\mathbf{b}) &= 1 - e^{-b_l(\alpha^f+\alpha)w_1^f(\mathbf{b})-2(1-b_l)\alpha w_1^{nf}(\mathbf{b})}. \end{aligned} \tag{9}$$

We denote the smallest set of solutions

$$\mathbf{w} = (w_1^f(\mathbf{b}), w_1^{nf}(\mathbf{b}), w_2^f(\mathbf{b}), w_2^{nf}(\mathbf{b}), \hat{w}_1^f(\mathbf{b}), \hat{w}_1^{nf}(\mathbf{b}), \hat{w}_2^f(\mathbf{b}), \hat{w}_2^{nf}(\mathbf{b}))$$

to (9) by  $\mathbf{y} = (y_1^f(\mathbf{b}), y_1^{nf}(\mathbf{b}), y_2^f(\mathbf{b}), y_2^{nf}(\mathbf{b}), \hat{y}_1^f(\mathbf{b}), \hat{y}_1^{nf}(\mathbf{b}), \hat{y}_2^f(\mathbf{b}), \hat{y}_2^{nf}(\mathbf{b}))$ . Since each of the variables increases as the other variables increase, the smallest set of solutions is well-defined.

**THEOREM 9.** Let

$$\begin{aligned} \xi(b_l, b_r) &= 2 - b_l y_1^f(\mathbf{b}) - b_r \left(1 - \hat{y}_2^f(\mathbf{b})\right) \\ &\quad - b_r \left(1 - \hat{y}_2^f(\mathbf{b})\right) \left(2b_l\alpha^f y_1^f(\mathbf{b}) + (1-b_l)(\alpha^f+\alpha)y_1^{nf}(\mathbf{b})\right) \\ &\quad - (1-b_l)y_1^{nf}(\mathbf{b}) - (1-b_r) \left(1 - \hat{y}_2^{nf}(\mathbf{b})\right) \\ &\quad - (1-b_r) \left(1 - \hat{y}_2^{nf}(\mathbf{b})\right) \left(b_l(\alpha^f+\alpha)y_1^f(\mathbf{b}) + 2(1-b_l)\alpha y_1^{nf}(\mathbf{b})\right), \end{aligned} \tag{10}$$

$$\begin{aligned}
\hat{\xi}(b_l, b_r) = & 2 - b_r \hat{y}_1^f(\mathbf{b}) - b_l \left(1 - y_2^f(\mathbf{b})\right) \\
& - b_l \left(1 - y_2^f(\mathbf{b})\right) \left(2b_r \alpha^f \hat{y}_1^f(\mathbf{b}) + (1 - b_r)(\alpha^f + \alpha) \hat{y}_1^{nf}(\mathbf{b})\right) \\
& - (1 - b_r) \hat{y}_1^{nf}(\mathbf{b}) - (1 - b_l) \left(1 - y_2^{nf}(\mathbf{b})\right) \\
& - (1 - b_l) \left(1 - y_2^{nf}(\mathbf{b})\right) \left(b_r (\alpha^f + \alpha) \hat{y}_1^f(\mathbf{b}) + 2(1 - b_r) \alpha \hat{y}_1^{nf}(\mathbf{b})\right).
\end{aligned} \tag{11}$$

Define  $\mu^{\text{KS}}(b_l, b_r) = \min(\xi(b_l, b_r), \hat{\xi}(b_l, b_r))$ . Then, under Condition 1,  $\mu(b_l, b_r) = \mu^{\text{KS}}(b_l, b_r)$ .

We now translate Condition 1 into a looser (i.e., sufficient but not necessary) condition that is much easier to verify.

**LEMMA 4.** *Condition 1 holds when the solution to (9) is unique.*

To prove Theorem 8, which states the equivalence of  $\mu(b_l, b_r)$  and  $\mu^{\text{KS}}(b_l, b_r)$  for a range of parameters, we employ Theorem 9 and Lemma 4: we verify the uniqueness of the solution to (9) when  $10^{-4} < \alpha < \alpha^f$  and  $\alpha^f + \alpha < e$ , in which case  $\mu(b_l, b_r) = \mu^{\text{KS}}(b_l, b_r)$  by Theorem 9.

**A.3.2. Computational results based on  $\mu^{\text{KS}}(b_l, b_r)$ .** To compute  $\mu^{\text{KS}}(b_l, b_r)$ , we resort to the `NLsolve` package available in the Julia Programming Language to solve (9) at a tolerance level  $ftol = 10^{-8}$ . Specifically, `NLsolve` iteratively refines candidate solutions using the Trust Region Method until the infinite norm of the residuals of the current solution falls below the threshold  $ftol = 10^{-8}$  (`NLsolve` 2017). When  $10^{-4} < \alpha < \alpha^f$  and  $\alpha^f + \alpha < e$ , at  $\mathbf{b} = (1/2, 1/2), (1, 0)$  and  $(0, 1)$  we find that (9) reduces to a single non-linear equation that exhibits strict monotonicity on both sides and can be solved to provable precision using this method (see the proof of Theorem 3 (ii) for details). In other cases where there are no theoretical guarantees for the closeness of  $\mu^{\text{KS}}(b_l, b_r)$  to  $\mu(b_l, b_r)$ , numerical studies indicate that  $\mu_n^{\text{EMP}}(b_l, b_r)$  still tends to converge to  $\mu^{\text{KS}}(b_l, b_r)$  as  $n$  scales large. We thus employ  $\mu^{\text{KS}}(b_l, b_r)$  to compare the one-sided and the balanced allocations for a wide range of parameters. Specifically, the findings presented in Section 6 are based on values of  $(B, b_l, \alpha^f, \alpha)$  in a set  $S$  that contains all  $B \in \{0.1, 0.2, \dots, 1\}, b_l \in \{0, 0.01, \dots, 1\}, \alpha^f \in \{0.05, 0.10, \dots, 7.45, 7.50\}$  and  $\alpha \in \{0, 0.05, 0.10, \dots, 2.95, 3.00\}$  such that  $B \geq b_l$  and  $\alpha^f > \alpha$ .

**A.3.3. Phase 1 of the KS Algorithm** In this section, we analyze phase 1 of the KS algorithm for  $G_n^{glb}(b_l, b_r)$ , hereafter referred to as  $G$  for notational simplicity. The set of edges in  $G$  is denoted by  $E$ , and the set of nodes is denoted by  $V := V_l \cup V_r$ . Our analysis applies the results for sparse random graphs presented in Karp and Sipser (1981) to random bipartite graphs. In doing so, we also generalize the probabilistic computations to handle nodes associated with heterogeneous edge probabilities. We next present all auxiliary results needed for Theorem 9, Lemma 4 and Theorem 8, the three main technical results based on KS-style analyses, and provide proofs of these results by the end of this section.

We begin by introducing the concept of a *derivation* and related concepts for node categorization. These concepts are essential for computing the asymptotic size of a maximum matching.

**DEFINITION 4.** A *derivation* is a sequence  $a_1, b_1, a_2, b_2, \dots$ , of distinct nodes such that, for  $u = 1, 2, \dots$ :

- (1)  $\{a_i, b_i\} \in E$ ;
- (2)  $\{a_i, b\} \in E$  implies  $b \in \{b_1, b_2, \dots, b_i\}$ .

Being in a derivation implies a subcritical edge structure. As we will demonstrate in the upcoming proofs, by following the KS algorithm, one can optimally match nodes that occur in a derivation by starting with nodes of degree

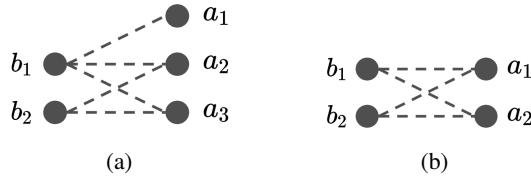


Figure 15 Example and counterexample of a derivation

1 and then iteratively resolve the rest of the nodes. As illustrated in Fig. 15, it can be verified that all nodes in Fig. 15 (a) appear in the derivation  $\{a_1, b_1, a_2, b_2, a_3\}$ , whereas none of the nodes in Fig. 15 (b) appear in any derivation.

Based on the concept of a derivation, we categorize nodes into *target* and *loser* based on the following definition:

**DEFINITION 5.** Define the relation  $\otimes \subseteq V \times V$  as  $v \otimes u$  if there exists a derivation  $a_1, b_1, a_2, b_2, \dots$  and an index  $i$  such that  $v = a_i$  and  $u = b_i$ . We call  $u$  a *target* if for some  $v, v \otimes u$ , and we call  $u$  a *loser* if for some  $v, u \otimes v$  or if  $u$  is the last element of an odd length derivation.

Based on Definition 5, all members of derivations are targets or losers or both. The next result characterizes the nodes that join the matching in phase 1 of KS algorithm, which is an immediate application of Theorem 8 in Karp and Sipser (1981) to bipartite graphs. We defer the proofs of Proposition 1 and all auxiliary results in this section to Appendix A.3.6.

**PROPOSITION 1 (Theorem 8 in Karp and Sipser (1981)).** Consider any execution of the KS algorithm on  $G$ . Denote by  $M_1$  the set of edges  $(v, u)$  that are added to  $G'$  in Phase 1. Then:

- (i) a node  $v$  is deleted from  $G$  during phase 1 iff  $v$  occurs in some derivation;
- (ii) if  $u$  is a target then  $M_1$  contains exactly one edge  $(v, u)$  such that  $v \otimes u$ ;
- (iii) if edge  $(v, u) \in M_1$  then  $v \otimes u$  or  $u \otimes v$ ;
- (iv) if  $v \otimes u$  and  $u \otimes v$  then edge  $(v, u) \in M_1$ ;

$$(v) \psi_1 = \max \left\{ \begin{array}{l} \left| \{v \in V_l \mid v \text{ is a loser}\} \right| - \left| \{v \in V_r \mid v \text{ is a target}\} \right|, \\ \left| \{v \in V_r \mid v \text{ is a loser}\} \right| - \left| \{v \in V_l \mid v \text{ is a target}\} \right| \end{array} \right\}.$$

Thus, the key to finding  $\psi_1$  lies in determining the probability of a node  $v$  being a target and/or a loser. We provide asymptotic answers to these questions by (1) conducting a probabilistic analysis of derivations in random trees and (2) demonstrating that a random tree is a good approximation to the structure obtained by selecting a vertex  $v$  in  $G$  and conducting a breadth-first search from  $v$ .

To approximate bipartite graphs using random trees, we alternate between sampling flexible nodes according to Bernoulli( $b_l$ ) and Bernoulli( $b_r$ ) throughout the sequential construction of different tree layers. Specifically, as illustrated in Fig. 16, we build the random tree  $\bar{G}_n(b_l, b_r)$  following a branching process: Let us assume, for simplicity, that the root node  $v$  follows a Bernoulli( $b_l$ ) distribution, which means  $v$  is a flexible node (i.e.,  $F_v = 1$ ) with probability  $b_l$  and a regular node with probability  $1 - b_l$ . Then,  $v$  has  $n$  potential children, each being a flexible node (i.e.,  $F_u = 1$ ) with probability  $b_r$  and a regular node with probability  $1 - b_r$ . A potential child becomes a realized child of  $v$  with probability  $2p_n + (F_v + F_u) \cdot (p_n^f - p_n)$ . Each realized child  $u$  then has  $n$  potential children, with flexible and regular probabilities of  $b_l$  and  $1 - b_l$ , respectively. This branching process continues until no further child exists for a tree

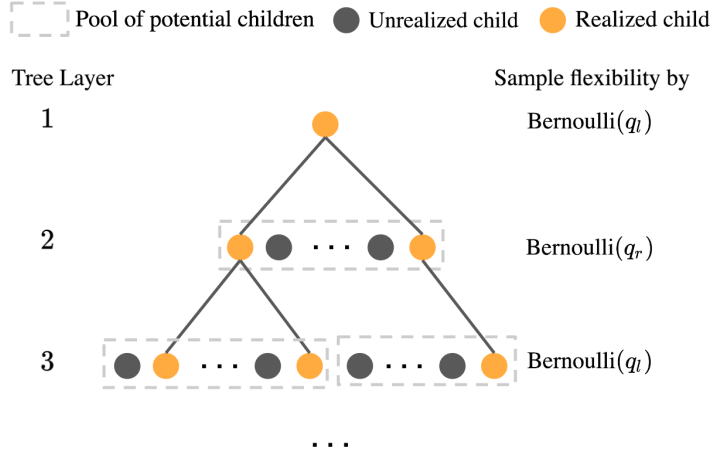


**Figure 16 Illustration of the branching process for  $\bar{G}$**

layer, a process that can be either finite or infinite. We omit the dependency on  $n$  and  $b$  in  $\bar{G}_n(b_l, b_r)$  whenever it is clear from the context.

For the probabilistic analysis of  $\bar{G}$ , we define two subsets of nodes: the *L-nodes* and the *H-nodes*, through the procedure outlined in Algorithm 2. A node is an  $L_d$ -node ( $H_d$ -node) if it becomes a *L-node* (*H-node*) within  $d$  steps of this procedure.

---

**Algorithm 2** Node Classification for  $\bar{G}$

---

- 1: **Input:** A random tree  $\bar{G}$  rooted at  $v$ .
  - 2: **Initialize:**  $L\text{-nodes} = \emptyset$ ,  $H\text{-nodes} = \emptyset$
  - 3: **repeat**
  - 4:     Add to  $L\text{-nodes}$  those nodes all of whose children are in  $H\text{-nodes}$ , including when this condition is vacuously satisfied.
  - 5:     Add to  $H\text{-nodes}$  those nodes having at least one child in  $L\text{-nodes}$ .
  - 6: **until** No new nodes are added to either set
- 

The *L-nodes* and the *H-nodes* are crucial for our study because they determine whether a node  $v$  is a target, a loser, or both, as demonstrated in Lemma 5.

**LEMMA 5 (Lemma 3 in Karp and Sipser (1981)).** *Let  $\bar{G}$  be a random tree rooted at  $v$ .*

- (i)  $v$  is a target iff  $v$  is an *H-node*;
- (ii)  $v$  is a loser iff either  $v$  is an *L-node* or  $v$  has exactly 1 child which is not an *H-node*.

Given that the nodes across different tree layers exhibit heterogeneity, we define two sets of nodes: one sampled from  $Bernoulli(b_l)$  as  $S_l$  and the other from  $Bernoulli(b_r)$  as  $S_r$ . For a flexible node in  $S_l$ , we denote the probabilities of it being a *L-node* and a *H-node* as  $y_1^f(\mathbf{b})$  and  $y_2^f(\mathbf{b})$ , respectively. Similarly, for a regular node in  $S_l$ , we denote the

probabilities as  $y_1^{nf}(\mathbf{b})$  and  $y_2^{nf}(\mathbf{b})$ . For  $S_r$ , we use an additional hat symbol to distinguish the probabilities, a notation consistently applied throughout this paper to differentiate quantities associated with  $S_r$  from those associated with  $S_l$ . In the following lemma, denoted as Lemma 6, we establish that the vector

$$\mathbf{y} = \left( y_1^f(\mathbf{b}), y_1^{nf}(\mathbf{b}), y_2^f(\mathbf{b}), y_2^{nf}(\mathbf{b}), \hat{y}_1^f(\mathbf{b}), \hat{y}_1^{nf}(\mathbf{b}), \hat{y}_2^f(\mathbf{b}), \hat{y}_2^{nf}(\mathbf{b}) \right)$$

can be computed as the smallest set of solutions to the equation characterized in (9).

**LEMMA 6.**  *$\mathbf{y}$  is given by the smallest solution to (9) as  $n \rightarrow \infty$ .*

Now, combining Lemma 5 with Lemma 6, we find the probability for nodes in  $\bar{G}$  to be a target or a loser.

**LEMMA 7.** *Let  $\bar{G}$  be a random tree rooted at  $v$ . Then, as  $n \rightarrow \infty$ ,*

(i) *if  $v$  is a flexible node in  $S_l$ ,  $v$  is a target with probability  $y_2^f(\mathbf{b})$  and a loser with probability*

$$y_1^f(\mathbf{b}) + y_1^f(\mathbf{b}) \left( (1+b_r)\alpha^f + (1-b_r)\alpha - b_r 2\alpha^f \hat{y}_2^f(\mathbf{b}) - (1-b_r)(\alpha^f + \alpha) \hat{y}_2^{nf}(\mathbf{b}) \right).$$

(ii) *if  $v$  is a regular node in  $S_l$ ,  $v$  is a target with probability  $y_2^{nf}(\mathbf{b})$  and a loser with probability*

$$y_1^{nf}(\mathbf{b}) + y_1^{nf}(\mathbf{b}) \left( b_r \alpha^f + (2-b_r)\alpha - b_r (\alpha^f + \alpha) \hat{y}_2^f(\mathbf{b}) - (1-b_r) 2\alpha \hat{y}_2^{nf}(\mathbf{b}) \right).$$

(iii) *if  $v$  is a flexible node in  $S_r$ ,  $v$  is a target with probability  $\hat{y}_1^f(\mathbf{b})$  and a loser with probability*

$$\hat{y}_1^f(\mathbf{b}) + \hat{y}_2^f(\mathbf{b}) \left( (1+b_l)\alpha^f + (1-b_l)\alpha - b_l 2\alpha^f y_2^f(\mathbf{b}) - (1-b_l)(\alpha^f + \alpha) y_2^{nf}(\mathbf{b}) \right).$$

(iv) *if  $v$  is a regular node in  $S_r$ ,  $v$  is a target with probability  $\hat{y}_1^{nf}(\mathbf{b})$  and a loser with probability*

$$\hat{y}_2^{nf}(\mathbf{b}) + \hat{y}_1^{nf}(\mathbf{b}) \left( b_l \alpha^f + (2-b_l)\alpha - b_l (\alpha^f + \alpha) y_2^f(\mathbf{b}) - (1-b_l) 2\alpha y_2^{nf}(\mathbf{b}) \right).$$

Equipped with Lemma 7, we are ready to compute the probability that  $v$  occurs in a derivation as  $n \rightarrow \infty$ .

**PROPOSITION 2 (Extension of Theorem 9 (4) in Karp and Sipser (1981)).** *Let  $v$  be a random node in  $G$ . Then, as  $n \rightarrow \infty$ :*

$$\begin{aligned} & \lim_{n \rightarrow \infty} \mathbb{P}[v \text{ in a derivation} \mid v \text{ is a flexible node in } V_l] \\ &= y_2^f(\mathbf{b}) + y_1^f(\mathbf{b}) + y_1^f(\mathbf{b}) \left[ (1+b_r)\alpha^f + (1-b_r)\alpha \right] \cdot \\ & \quad \left[ 1 - \frac{b_r 2\alpha^f}{(1+b_r)\alpha^f + (1-b_r)\alpha} \left( \hat{y}_1^f(\mathbf{b}) + \hat{y}_2^f(\mathbf{b}) \right) - \frac{(1-b_r)(\alpha^f + \alpha)}{(1+b_r)\alpha^f + (1-b_r)\alpha} \left( \hat{y}_1^{nf}(\mathbf{b}) + \hat{y}_2^{nf}(\mathbf{b}) \right) \right], \\ & \lim_{n \rightarrow \infty} \mathbb{P}[v \text{ in a derivation} \mid v \text{ is a regular node in } V_l] \\ &= y_2^{nf}(\mathbf{b}) + y_1^{nf}(\mathbf{b}) + y_1^{nf}(\mathbf{b}) \left[ b_r \alpha^f + (2-b_r)\alpha \right] \cdot \\ & \quad \left[ 1 - \frac{b_r (\alpha^f + \alpha)}{b_r \alpha^f + (2-b_r)\alpha} \left( \hat{y}_1^f(\mathbf{b}) + \hat{y}_2^f(\mathbf{b}) \right) - \frac{(1-b_r) 2\alpha}{b_r \alpha^f + (2-b_r)\alpha} \left( \hat{y}_1^{nf}(\mathbf{b}) + \hat{y}_2^{nf}(\mathbf{b}) \right) \right], \\ & \lim_{n \rightarrow \infty} \mathbb{P}[v \text{ in a derivation} \mid v \text{ is a flexible node in } V_r] \\ &= \hat{y}_2^f(\mathbf{b}) + \hat{y}_1^f(\mathbf{b}) + \hat{y}_1^f(\mathbf{b}) \left[ (1+b_l)\alpha^f + (1-b_l)\alpha \right] \cdot \\ & \quad \left[ 1 - \frac{b_l 2\alpha^f}{(1+b_l)\alpha^f + (1-b_l)\alpha} \left( y_1^f(\mathbf{b}) + y_2^f(\mathbf{b}) \right) - \frac{(1-b_l)(\alpha^f + \alpha)}{(1+b_l)\alpha^f + (1-b_l)\alpha} \left( y_1^{nf}(\mathbf{b}) + y_2^{nf}(\mathbf{b}) \right) \right], \end{aligned}$$

$$\begin{aligned} & \lim_{n \rightarrow \infty} \mathbb{P}[v \text{ in a derivation} \mid v \text{ is a regular node in } V_r] \\ &= \hat{y}_2^{nf}(\mathbf{b}) + \hat{y}_1^{nf}(\mathbf{b}) + \hat{y}_1^{nf}(\mathbf{b}) [b_l \alpha^f + (2 - b_l) \alpha] \cdot \\ & \quad \left[ 1 - \frac{b_l (\alpha^f + \alpha)}{b_l \alpha^f + (2 - b_l) \alpha} (y_1^f(\mathbf{b}) + y_2^f(\mathbf{b})) - \frac{(1 - b_l) 2 \alpha}{b_l \alpha^f + (2 - b_l) \alpha} (y_1^{nf}(\mathbf{b}) + y_2^{nf}(\mathbf{b})) \right]. \end{aligned}$$

One key property of the KS algorithm is that it is optimal in its handling of degree 1 vertices. Given any edge  $e$  that is incident to a degree-1 vertex, there is always some maximum matching containing the edge  $e$  (Bohman and Frieze 2011, Balister and Gerke 2015). This result implies that the KS algorithm is optimal until the end of phase 1. Equipped with the auxiliary results, we are ready to prove Theorem 9, Lemma 4 and Theorem 8.

*Proof of Theorem 9* Since the KS algorithm trivially provides a lower bound for  $\mu(b_l, b_r)$ , here we continue to show that under Condition 1 the algorithm is provably optimal. By Condition 1,  $\mathbb{E}[\psi_2] \in o(n)$  and the algorithm is optimal (up to an error of  $o(n)$ ) in phase 2. Since we also know that the algorithm is provably optimal until the end of phase 1, the KS algorithm is optimal under Condition 1. Specifically, by Condition 1 we find

$$\begin{aligned} \mu(b_l, b_r) &= \lim_{n \rightarrow \infty} \frac{\mathbb{E}[\mathcal{M}_n(b_l, b_r)]}{n} = \lim_{n \rightarrow \infty} \frac{\mathbb{E}[|M_1^l| + |M_2^l|]}{n} = \lim_{n \rightarrow \infty} \frac{\mathbb{E}[n - \psi_1 - \psi_2]}{n} \\ &= 1 - \lim_{n \rightarrow \infty} \frac{\mathbb{E}[\psi_1]}{n} - \lim_{n \rightarrow \infty} \frac{\mathbb{E}[\psi_2]}{n} = 1 - \lim_{n \rightarrow \infty} \frac{\mathbb{E}[\psi_1]}{n} \end{aligned}$$

provided that these limits exist.

From Proposition 1 (v), we know

$$\begin{aligned} \mu(b_l, b_r) &= 1 - \lim_{n \rightarrow \infty} \frac{\mathbb{E}[\psi_1]}{n} = 1 - \lim_{n \rightarrow \infty} \max \left\{ \mathbb{P}[v \in \Psi_1^l \mid v \in V_l], \mathbb{P}[v \in \Psi_1^r \mid v \in V_r] \right\} \\ &= 1 - \max \left\{ \lim_{n \rightarrow \infty} \mathbb{P}[v \text{ is a loser} \mid v \in V_l] - \lim_{n \rightarrow \infty} \mathbb{P}[v \text{ is a target} \mid v \in V_r], \right. \\ &\quad \left. \lim_{n \rightarrow \infty} \mathbb{P}[v \text{ is a loser} \mid v \in V_r] - \lim_{n \rightarrow \infty} \mathbb{P}[v \text{ is a target} \mid v \in V_l] \right\} \end{aligned}$$

provided that these limits exist.

By the law of iterated expectations, we have

$$\begin{aligned} & \lim_{n \rightarrow \infty} \mathbb{P}[v \text{ is a loser} \mid v \in V_l] - \lim_{n \rightarrow \infty} \mathbb{P}[v \text{ is a target} \mid v \in V_r] \\ &= \lim_{n \rightarrow \infty} \mathbb{P}[v \text{ is a loser} \mid v \text{ is a flexible node in } V_l] \cdot \mathbb{P}[v \in v_l \text{ is a flexible node}] \\ &\quad + \lim_{n \rightarrow \infty} \mathbb{P}[v \text{ is a loser} \mid v \text{ is a regular node in } V_l] \cdot \mathbb{P}[v \in v_l \text{ is a regular node}] \\ &\quad - \lim_{n \rightarrow \infty} \mathbb{P}[v \text{ is a target} \mid v \text{ is a flexible node in } V_r] \cdot \mathbb{P}[v \in v_r \text{ is a flexible node}] \\ &\quad - \lim_{n \rightarrow \infty} \mathbb{P}[v \text{ is a target} \mid v \text{ is a regular node in } V_r] \cdot \mathbb{P}[v \in v_r \text{ is a regular node}] \end{aligned}$$

provided that these limits exist.

Now we can plug in probabilities derived in Lemma 7, which we have shown in Claim 5 to be equal to the corresponding probabilities in random graphs:

$$\begin{aligned} & \lim_{n \rightarrow \infty} \mathbb{P}[v \text{ is a loser} \mid v \in V_l] - \lim_{n \rightarrow \infty} \mathbb{P}[v \text{ is a target} \mid v \in V_r] \\ &= b_l \left( y_1^f(\mathbf{b}) + y_1^f(\mathbf{b}) \left( (1 + b_r) \alpha^f + (1 - b_r) \alpha - b_r 2 \alpha^f \hat{y}_2^f(\mathbf{b}) - (1 - b_r) (\alpha^f + \alpha) \hat{y}_2^{nf}(\mathbf{b}) \right) \right) - b_r \hat{y}_2^f(\mathbf{b}) \end{aligned}$$

$$\begin{aligned}
& + (1 - b_l) \left( y_1^{nf}(\mathbf{b}) + y_1^{nf}(\mathbf{b}) \left( b_r \alpha^f + (2 - b_r) \alpha - b_r (\alpha^f + \alpha) \hat{y}_2^f(\mathbf{b}) - (1 - b_r) 2\alpha \hat{y}_2^{nf}(\mathbf{b}) \right) \right) - (1 - b_r) \hat{y}_2^{nf}(\mathbf{b}) \\
& = b_l \left( y_1^f(\mathbf{b}) + y_1^f(\mathbf{b}) \left( b_r 2\alpha^f \left( 1 - \hat{y}_2^f(\mathbf{b}) \right) + (1 - b_r) (\alpha^f + \alpha) \left( 1 - \hat{y}_2^{nf}(\mathbf{b}) \right) \right) \right) - 1 + b_r \left( 1 - \hat{y}_2^f(\mathbf{b}) \right) \\
& + (1 - b_l) \left( y_1^{nf}(\mathbf{b}) + y_1^{nf}(\mathbf{b}) \left( b_r (\alpha^f + \alpha) \left( 1 - \hat{y}_2^f(\mathbf{b}) \right) + (1 - b_r) 2\alpha \left( 1 - \hat{y}_2^{nf}(\mathbf{b}) \right) \right) \right) + (1 - b_r) \left( 1 - \hat{y}_2^{nf}(\mathbf{b}) \right) \\
& = b_l y_1^f(\mathbf{b}) + b_r \left( 1 - \hat{y}_2^f(\mathbf{b}) \right) \left( 2b_l \alpha^f y_1^f(\mathbf{b}) + (1 - b_l)(\alpha^f + \alpha) y_1^{nf}(\mathbf{b}) \right) - 1 + b_r \left( 1 - \hat{y}_2^f(\mathbf{b}) \right) \\
& + (1 - b_l) y_1^{nf}(\mathbf{b}) + (1 - b_r) \left( 1 - \hat{y}_2^{nf}(\mathbf{b}) \right) \left( b_l (\alpha^f + \alpha) y_1^f(\mathbf{b}) + 2(1 - b_l) \alpha y_1^{nf}(\mathbf{b}) \right) + (1 - b_r) \left( 1 - \hat{y}_2^{nf}(\mathbf{b}) \right) \\
& =: 1 - \xi(b_l, b_r).
\end{aligned}$$

Similarly, we find that

$$\begin{aligned}
& \lim_{n \rightarrow \infty} \mathbb{P}[v \text{ is a loser} | v \in V_r] - \lim_{n \rightarrow \infty} \mathbb{P}[v \text{ is a target} | v \in V_l] \\
& = b_r \hat{y}_1^f(\mathbf{b}) + b_l \left( 1 - \hat{y}_2^f(\mathbf{b}) \right) \left( 2b_r \alpha^f \hat{y}_1^f(\mathbf{b}) + (1 - b_r)(\alpha^f + \alpha) \hat{y}_1^{nf}(\mathbf{b}) \right) - 1 + b_l \left( 1 - \hat{y}_2^f(\mathbf{b}) \right) \\
& + (1 - b_r) \hat{y}_1^{nf}(\mathbf{b}) + (1 - b_l) \left( 1 - \hat{y}_2^{nf}(\mathbf{b}) \right) \left( b_r (\alpha^f + \alpha) \hat{y}_1^f(\mathbf{b}) + 2(1 - b_r) \alpha \hat{y}_1^{nf}(\mathbf{b}) \right) + (1 - b_l) \left( 1 - \hat{y}_2^{nf}(\mathbf{b}) \right) \\
& =: 1 - \hat{\xi}(b_l, b_r).
\end{aligned}$$

Now, taking

$$\begin{aligned}
\mu^{\text{KS}}(b_l, b_r) &= \min \left( \xi(b_l, b_r), \hat{\xi}(b_l, b_r) \right) \\
&= 1 - \max \left\{ \lim_{n \rightarrow \infty} \mathbb{P}[v \text{ is a loser} | v \in V_l] - \lim_{n \rightarrow \infty} \mathbb{P}[v \text{ is a target} | v \in V_r], \right. \\
&\quad \left. \lim_{n \rightarrow \infty} \mathbb{P}[v \text{ is a loser} | v \in V_r] - \lim_{n \rightarrow \infty} \mathbb{P}[v \text{ is a target} | v \in V_l] \right\},
\end{aligned}$$

we have that  $\mu(b_l, b_r) = \mu^{\text{KS}}(b_l, b_r)$  under Condition 1. □

*Proof of Lemma 4* From Proposition 1 (i), it is known that

$$\lim_{n \rightarrow \infty} \frac{\mathbb{E}[m_1 + \psi_1]}{n} = \max \left\{ \lim_{n \rightarrow \infty} \mathbb{P}[v \text{ in a derivation} | v \in V_l], \lim_{n \rightarrow \infty} \mathbb{P}[v \text{ in a derivation} | v \in V_r] \right\}.$$

We aim to demonstrate that if the solution to (9) is unique, then

$$\lim_{n \rightarrow \infty} \mathbb{P}[v \text{ in a derivation} | v \in V_l] = \lim_{n \rightarrow \infty} \mathbb{P}[v \text{ in a derivation} | v \in V_r] = 1. \tag{12}$$

Consequently, we have

$$\lim_{n \rightarrow \infty} \frac{\mathbb{E}[\psi_2]}{n} \leq 1 - \lim_{n \rightarrow \infty} \frac{\mathbb{E}[m_1 + \psi_1]}{n} = 0,$$

thereby verifying Condition 1.

To establish (12) when the solution to (9) is unique, we leverage Proposition 2. under the condition of a unique solution to (9), we utilize Proposition 2. We proceed by considering each possible condition of  $v$ : whether  $v$  is a flexible node in  $V_l$ , a regular node in  $V_l$ , a flexible node in  $V_r$ , or a regular node in  $V_r$ . Under each of these conditions, we shall demonstrate that  $\lim_{n \rightarrow \infty} \mathbb{P}[v \text{ in a derivation}] = 1$  provided that the solution to (9) is unique.

Note that for any solution vector  $\mathbf{w}$  to (9), it is always feasible to construct

$$\begin{aligned} x_1^f(b_l, b_r) &= w_1^f(\mathbf{b}), x_2^f(b_l, b_r) = 1 - w_1^f(\mathbf{b}), \\ x_1^{nf}(b_l, b_r) &= w_1^{nf}(\mathbf{b}), x_2^{nf}(b_l, b_r) = 1 - w_1^{nf}(\mathbf{b}), \\ \hat{x}_1^f(b_l, b_r) &= \hat{w}_1^f(\mathbf{b}), \hat{x}_2^f(b_l, b_r) = 1 - \hat{w}_1^f(\mathbf{b}), \\ \hat{x}_1^{nf}(b_l, b_r) &= \hat{w}_1^{nf}(\mathbf{b}), \hat{x}_2^{nf}(b_l, b_r) = 1 - \hat{w}_1^{nf}(\mathbf{b}), \end{aligned} \quad (13)$$

and  $\mathbf{x}$  is provably also a solution to (9). Consequently, when (9) admits a unique solution, the smallest set of solutions  $\mathbf{y}$  is known to satisfy (13). Substituting (13) into the expressions derived in Proposition 2, we find that

$$\begin{aligned} &\lim_{n \rightarrow \infty} \mathbb{P}[v \text{ in a derivation} \mid v \text{ is a flexible node in } V_l] \\ &= y_2^f(\mathbf{b}) + y_1^f(\mathbf{b}) + y_1^f(\mathbf{b}) [(1+b_r)\alpha^f + (1-b_r)\alpha] \cdot \\ &\quad \left[ 1 - \frac{b_r 2\alpha^f}{(1+b_r)\alpha^f + (1-b_r)\alpha} (\hat{y}_1^f(\mathbf{b}) + \hat{y}_2^f(\mathbf{b})) - \frac{(1-b_r)(\alpha^f + \alpha)}{(1+b_r)\alpha^f + (1-b_r)\alpha} (\hat{y}_1^{nf}(\mathbf{b}) + \hat{y}_2^{nf}(\mathbf{b})) \right] \\ &= 1 + y_1^f(\mathbf{b}) [(1+b_r)\alpha^f + (1-b_r)\alpha] \cdot \left[ 1 - \frac{b_r 2\alpha^f}{(1+b_r)\alpha^f + (1-b_r)\alpha} - \frac{(1-b_r)(\alpha^f + \alpha)}{(1+b_r)\alpha^f + (1-b_r)\alpha} \right] \\ &= 1 + y_1^f(\mathbf{b}) [(1+b_r)\alpha^f + (1-b_r)\alpha] \cdot 0 \\ &= 1. \end{aligned}$$

The probability expressions under other conditions of  $v$  can be derived analogously. This completes the proof of Lemma 4.  $\square$

*Proof of Theorem 8* By Theorem 9 and Lemma 4, to establish Theorem 8 it is sufficient to demonstrate that when  $10^{-4} < \alpha < \alpha^f$  and  $\alpha^f + \alpha < e$  the solution to (9) is unique at the points  $\mathbf{b} = (1, 0)$ ,  $(0, 1)$  and  $(1/2, 1/2)$ .

When  $\mathbf{b} = (1, 0)$ , all nodes in  $V_l$  are flexible nodes, while those in  $V_r$  are regular nodes. Thus, it suffices to analyze  $w_1^f(\mathbf{b})$ ,  $w_2^f(\mathbf{b})$ ,  $\hat{w}_1^{nf}(\mathbf{b})$  and  $\hat{w}_2^{nf}(\mathbf{b})$ . Then, (9) reduces to

$$w_1^f(\mathbf{b}) = e^{-(\alpha^f + \alpha)(1 - \hat{w}_2^{nf}(\mathbf{b}))}, \hat{w}_2^{nf}(\mathbf{b}) = 1 - e^{-(\alpha^f + \alpha)w_1^f(\mathbf{b})}, \quad (14)$$

$$\hat{w}_1^{nf}(\mathbf{b}) = e^{-(\alpha^f + \alpha)(1 - w_2^f(\mathbf{b}))}, w_2^f(\mathbf{b}) = 1 - e^{-(\alpha^f + \alpha)\hat{w}_1^{nf}(\mathbf{b})}. \quad (15)$$

Since (14) and (15) are equivalent, it suffices to show that solution to the pair  $(w_1^f(\mathbf{b}), \hat{w}_2^{nf}(\mathbf{b}))$  in (14) is unique. This is a direct application of the following result from Karp and Sipser (1981), by taking  $L = w_1^f(\mathbf{b})$ ,  $W = \hat{w}_2^{nf}(\mathbf{b})$  and  $\lambda = \alpha^f + \alpha$ :

**CLAIM 1 (Lemma 1 in Karp and Sipser (1981)).** Define  $L = e^{-\lambda(1-W)}$ ,  $W = 1 - e^{-\lambda L}$ . Then,  $L + W \leq 1$ , with equality if and only if  $\lambda \leq e$ .

The case for  $\mathbf{b} = (0, 1)$  is symmetric.

For the case of  $\mathbf{b} = (1/2, 1/2)$ , symmetry implies that

$$w_1^f(\mathbf{b}) = \hat{w}_1^f(\mathbf{b}), w_1^{nf}(\mathbf{b}) = \hat{w}_1^{nf}(\mathbf{b}), w_2^f(\mathbf{b}) = \hat{w}_2^f(\mathbf{b}), w_2^{nf}(\mathbf{b}) = \hat{w}_2^{nf}(\mathbf{b}).$$

Substituting  $\mathbf{b} = (1/2, 1/2)$  into (9), we obtain the following equations:

$$w_1^f(\mathbf{b}) = e^{-\frac{1}{2}2\alpha^f(1 - \hat{w}_2^f(\mathbf{b})) - \frac{1}{2}(\alpha^f + \alpha)(1 - \hat{w}_2^{nf}(\mathbf{b}))},$$

$$\begin{aligned} w_1^{nf}(\mathbf{b}) &= e^{-\frac{1}{2}(\alpha^f + \alpha)(1 - \hat{w}_2^f(\mathbf{b})) - \frac{1}{2}2\alpha(1 - \hat{w}_2^{nf}(\mathbf{b}))}, \\ \hat{w}_2^f(\mathbf{b}) &= 1 - e^{-\frac{1}{2}2\alpha^f w_1^f(\mathbf{b}) - \frac{1}{2}(\alpha^f + \alpha)w_1^{nf}(\mathbf{b})}, \\ \hat{w}_2^{nf}(\mathbf{b}) &= 1 - e^{-\frac{1}{2}(\alpha^f + \alpha)w_1^f(\mathbf{b}) - \frac{1}{2}2\alpha w_1^{nf}(\mathbf{b})}. \end{aligned}$$

For any  $\vec{\mathbf{x}} \in \mathbb{R}^2$ , define

$$F(\vec{\mathbf{x}}) = \begin{pmatrix} e^{-\frac{1}{2}2\alpha^f x_1 - \frac{1}{2}(\alpha^f + \alpha)x_2} \\ e^{-\frac{1}{2}(\alpha^f + \alpha)x_1 - \frac{1}{2}2\alpha x_2} \end{pmatrix}.$$

Then, the smallest solution to  $\begin{pmatrix} w_1^f(\mathbf{b}) \\ w_1^{nf}(\mathbf{b}) \end{pmatrix}$  and  $\vec{1} - \begin{pmatrix} \hat{w}_2^f(\mathbf{b}) \\ \hat{w}_2^{nf}(\mathbf{b}) \end{pmatrix}$  are respectively the values that the even and odd members of the following sequences converge to:

$$\vec{1}, F(\vec{1}), F(F(\vec{1})), F(F(F(\vec{1}))), \dots$$

In particular,  $\begin{pmatrix} w_1^f(\mathbf{b}) \\ w_1^{nf}(\mathbf{b}) \end{pmatrix} = \vec{1} - \begin{pmatrix} \hat{w}_2^f(\mathbf{b}) \\ \hat{w}_2^{nf}(\mathbf{b}) \end{pmatrix}$  and the solution is unique if  $F(\vec{\mathbf{x}})$  has a unique fixed point, i.e., there exists a unique  $\vec{\mathbf{x}}^*$  such that  $F(\vec{\mathbf{x}}^*) = \vec{\mathbf{x}}^*$ . Notice that in  $F(\vec{\mathbf{x}}) = \vec{\mathbf{x}}$  we have  $x_1 = e^{-\alpha^f x_1 - \frac{1}{2}(\alpha^f + \alpha)x_2}$ , so  $x_2 = -2\frac{\log(x_1) + \alpha^f x_1}{\alpha^f + \alpha}$ . Plugging this into  $x_2 = e^{-\frac{1}{2}(\alpha^f + \alpha)x_1 - \frac{1}{2}2\alpha x_2}$ , we find that

$$-2\frac{\log(x_1) + \alpha^f x_1}{\alpha^f + \alpha} = e^{-\frac{1}{2}(\alpha^f + \alpha)x_1 + 2\frac{\alpha}{\alpha^f + \alpha}(\log(x_1) + \alpha^f x_1)}, \quad (16)$$

so it suffices to show that (16) has a unique solution when  $\alpha^f + \alpha < e$ .

Let

$$f_1(x_1) := e^{-\frac{1}{2}(\alpha^f + \alpha)x_1 + 2\frac{\alpha}{\alpha^f + \alpha}(\log(x_1) + \alpha^f x_1)} + 2\frac{\log(x_1) + \alpha^f x_1}{\alpha^f + \alpha}.$$

The next result establishes a monotonicity property of this function:

**CLAIM 2.** *When  $10^{-4} < \alpha < \alpha^f$  and  $\alpha^f + \alpha < e$ ,  $f'_1(x_1) > 1$  for any  $x_1 \in (0, 1]$ .*

Since  $f_1(0) = -\infty$  and  $f_1(1) \geq 0$ , by continuity of  $f_1(x_1)$  with respect to  $x_1$  we know that  $f_1(x_1) = 0$  has at least one solution in  $(0, 1]$ . Since we also know from Claim 2 that  $f_1(x_1)$  is strictly monotonically increasing with respect to  $x_1$  in  $(0, 1]$  when  $10^{-4} < \alpha < \alpha^f$  and  $\alpha^f + \alpha < e$ , such solution for  $x_1$  is unique. This completes the proof of Theorem 8.  $\square$

#### A.3.4. Proof of Theorem 3 (ii)

*Proof.* Recall from Theorem 8 that, in the stated parameter regimes,  $\mu(b_l, b_r) = \mu^{\text{KS}}(b_l, b_r)$  at  $\mathbf{b} = (1, 0)$  and  $(1/2, 1/2)$ . Since the solution to (9) is unique at these points, (13) is satisfied by the smallest set of solutions  $\mathbf{y}$ . Plugging

$$y_1^f(\mathbf{b}) = 1 - y_2^f(\mathbf{b}), y_1^{nf}(\mathbf{b}) = y_2^{nf}(\mathbf{b})$$

into (10) and (11), we find that at these values of  $\mathbf{b}$

$$\begin{aligned} \mu(b_l, b_r) &= \xi(b_l, b_r) = \hat{\xi}(b_l, b_r) \\ &= 2 - b_l y_1^f(\mathbf{b}) - b_r e^{-b_1(b_l, b_r)} (1 + b_1(b_l, b_r)) - (1 - b_l) y_1^{nf}(\mathbf{b}) - (1 - b_r) e^{-b_2(b_l, b_r)} (1 + b_2(b_l, b_r)), \end{aligned}$$

where

$$\begin{aligned} b_1(b_l, b_r) &= b_l 2\alpha^f y_1^f(\mathbf{b}) + (1 - b_l) (\alpha^f + \alpha) y_1^{nf}(\mathbf{b}), \\ b_2(b_l, b_r) &= b_l (\alpha^f + \alpha) y_1^f(\mathbf{b}) + (1 - b_l) 2\alpha y_1^{nf}(\mathbf{b}). \end{aligned}$$

When  $\mathbf{b} = (1, 0)$ ,  $\mu(b_l, b_r)$  depends only on  $y_1^f(\mathbf{b})$ , which can be solved as the unique solution  $x^*$  to

$$x = e^{-(\alpha^f + \alpha)e^{-(\alpha^f + \alpha)x}}. \quad (17)$$

When  $\mathbf{b} = (1/2, 1/2)$ ,  $\mu(b_l, b_r)$  depends only on  $(y_1^f(\mathbf{b}), y_1^{nf}(\mathbf{b}))$ , which can be solved as the unique set of solution  $(x_1^*, x_2^*)$  to

$$\begin{aligned} x_1 &= e^{-\frac{1}{2}2\alpha^f x_1 - \frac{1}{2}(\alpha^f + \alpha)x_2}, \\ x_2 &= e^{-\frac{1}{2}(\alpha^f + \alpha)x_1 - \frac{1}{2}2\alpha x_2}. \end{aligned} \quad (18)$$

Our objective is to substantiate the inequality for any  $\alpha^f$  and  $\alpha$  satisfying  $10^{-4} < \alpha < \alpha^f$  and  $\alpha^f + \alpha < e$ . To do so, we derive a lower bound for the expression  $\mu(1, 0) - \mu(1/2, 1/2)$  for any  $(\bar{\alpha}^f, \bar{\alpha})$  within grid  $[\alpha^f, \alpha^f + \delta] \times [\alpha, \alpha + \delta]$ . We then employ a computer-aided proof to iterate over all grids in the claimed region and verify if this lower bound is positive for the respective grid. To do so, we need to bound  $\bar{\alpha}^f, \bar{\alpha}$  and the resulting  $\bar{x}, \bar{x}_1$  and  $\bar{x}_2$  in each grid. For a given grid  $[\alpha^f, \alpha^f + \delta] \times [\alpha, \alpha + \delta]$ , if we know the respective lower and upper bounds of  $\bar{x}, \bar{x}_1$  and  $\bar{x}_2$ , which we denote by  $x^{lb}, x^{ub}, x_1^{lb}, x_1^{ub}, x_2^{lb}$  and  $x_2^{ub}$ , then we can lower bound

$$\begin{aligned} \mu(1, 0) &= 2 - \bar{x} - e^{-(\bar{\alpha}^f + \bar{\alpha})\bar{x}} \left[ 1 + (\bar{\alpha}^f + \bar{\alpha}) \bar{x} \right] \\ &\geq 2 - x^{ub} - e^{-(\alpha^f + \alpha)x^{lb}} \left[ 1 + (\alpha^f + \alpha + 2\delta) x^{ub} \right], \forall (\bar{\alpha}^f, \bar{\alpha}) \in [\alpha^f, \alpha^f + \delta] \times [\alpha, \alpha + \delta]. \end{aligned} \quad (19)$$

Similarly, we can upper bound

$$\begin{aligned} \mu(1/2, 1/2) &= 2 - \frac{1}{2}\bar{x}_1 - \frac{1}{2}\bar{x}_2 - \frac{1}{2}e^{-(\bar{\alpha}^f)\bar{x}_1 - \frac{1}{2}(\bar{\alpha}^f + \bar{\alpha})\bar{x}_2} \left[ 1 + \bar{\alpha}^f \bar{x}_1 + \frac{1}{2}(\bar{\alpha}^f + \bar{\alpha}) \bar{x}_2 \right] \\ &\quad - \frac{1}{2}e^{-\frac{1}{2}(\bar{\alpha}^f + \bar{\alpha})\bar{x}_1 - (\bar{\alpha})\bar{x}_2} \left[ 1 + \frac{1}{2}(\bar{\alpha}^f + \bar{\alpha}) \bar{x}_1 + \bar{\alpha} \bar{x}_2 \right] \\ &\leq 2 - \frac{1}{2}x_1^{lb} - \frac{1}{2}x_2^{lb} \\ &\quad - \frac{1}{2}e^{-(\alpha^f + \delta)x_1^{ub} - \frac{1}{2}(\alpha^f + \alpha + 2\delta)x_2^{ub}} \left[ 1 + \alpha^f x_1^{lb} + \frac{1}{2}(\alpha^f + \alpha) x_2^{lb} \right] \\ &\quad - \frac{1}{2}e^{-\frac{1}{2}(\alpha^f + \alpha + 2\delta)x_1^{ub} - (\alpha + \delta)x_2^{ub}} \left[ 1 + \frac{1}{2}(\alpha^f + \alpha) x_1^{lb} + \alpha x_2^{lb} \right], \forall (\bar{\alpha}^f, \bar{\alpha}) \in [\alpha^f, \alpha^f + \delta] \times [\alpha, \alpha + \delta]. \end{aligned} \quad (20)$$

Thus, it suffices to find  $x^{lb}, x^{ub}, x_1^{lb}, x_1^{ub}, x_2^{lb}$  and  $x_2^{ub}$  in the corresponding grid. To do this, we start by showing that, for given  $\alpha^f$  and  $\alpha$ , the solution returned by `nlsolve` package in Julia programming language is provably close to the true solution  $x^*, x_1^*$  and  $x_2^*$ , and then provide a continuity argument to bound the solution  $\bar{x}, \bar{x}_1$  and  $\bar{x}_2$  for any  $(\bar{\alpha}^f, \bar{\alpha}) \in [\alpha^f, \alpha^f + \delta] \times [\alpha, \alpha + \delta]$ .

We start by bounding the value of  $x^*, x_1^*$  and  $x_2^*$  based on the numerical solutions  $x^{sol}, x_1^{sol}$  and  $x_2^{sol}$  returned by Julia `nlsolve`. Let  $f(x) := x - e^{-(\alpha^f + \alpha)x}$ , we find that  $f(x)$  is monotonically increasing and  $f'(x) > 1$ . Similarly, we know from Claim 2 that  $f'_1(x_1) = e^{-\frac{1}{2}(\alpha^f + \alpha)x_1 + 2\frac{\alpha}{\alpha^f + \alpha}(\log(x_1) + \alpha^f x_1)} + 2\frac{\log(x_1) + \alpha^f x_1}{\alpha^f + \alpha} > 1$ . For  $f(x)$ , notice that

by specifying the tolerance level  $ftol$  at  $\epsilon = 10^{-8}$ , `nlsolve` returns a solution  $x^{sol}$  such that  $|f(x^{sol})| < \epsilon$ . Since  $f'(x) > 1 \forall x$ , if  $x^* > x^{sol} + \epsilon$  then

$$f(x^*) > f(x^{sol} + \epsilon) > f(x^{sol}) + \epsilon > 0,$$

which contradicts the fact that  $f(x^*) = 0$ . Similarly, we must have  $x^* > x^{sol} - \epsilon$  and thus  $x^* \in [x^{sol} - \epsilon, x^{sol} + \epsilon]$ . Through the same argument on  $f_1(x_1)$  we find that  $x_1^* \in [x_1^{sol} - \epsilon, x_1^{sol} + \epsilon]$ . Since  $x_2^* = -2\frac{\log(x_1^*) + \alpha^f x_1^*}{\alpha^f + \alpha}$ , we can then lower bound  $x_2^*$  with  $-2\frac{\log(x_1^{sol} - \epsilon) + \alpha^f(x_1^{sol} - \epsilon)}{\alpha^f + \alpha}$  and upper bound  $x_2$  with  $-2\frac{\log(x_1^{sol} + \epsilon) + \alpha^f(x_1^{sol} + \epsilon)}{\alpha^f + \alpha}$ .

Having established closeness of  $x^{sol}, x_1^{sol}$  and  $x_2^{sol}$  to  $x^*, x_1^*$  and  $x_2^*$ , we continue to bound  $\bar{x}, \bar{x}_1$  and  $\bar{x}_2$  for  $(\bar{\alpha}^f, \bar{\alpha}) \in [\alpha^f, \alpha^f + \delta] \times [\alpha, \alpha + \delta]$ . Specifically, we leverage the following result on the continuity of  $x^*, x_1^*$  and  $x_2^*$  with respect to  $\alpha^f$  and  $\alpha$ .

**CLAIM 3.** *Let  $x^*, x_1^*$  and  $x_2^*$  be the solution to (17) and (18) given  $\alpha^f$  and  $\alpha$ . Moreover, let  $\bar{x}, \bar{x}_1$  and  $\bar{x}_2$  be the solution to (17) and (18) given  $\bar{\alpha}^f$  and  $\bar{\alpha}$ . Then, given any  $\delta \in (0, 1/2)$ , we know that for any  $\bar{\alpha}^f \in [\alpha^f, \alpha^f + \delta]$  and  $\bar{\alpha} \in [\alpha, \alpha + \delta]$  such that  $10^{-4} < \alpha < \alpha^f$  and  $\bar{\alpha}^f + \bar{\alpha} < e$ :*

- (i)  $\bar{x} \in [x^*(1 - \delta), x^*]$ ;
- (ii)  $\bar{x}_1 \in [x_1^*(1 - 2\delta), x_1^*]$  and  $\bar{x}_2 \in [x_2^*(1 - 2\delta), x_2^*]$ .

Based on the continuity result, we can lower and upper bound the solution of  $\bar{x}, \bar{x}_1$  and  $\bar{x}_2$  for  $(\bar{\alpha}^f, \bar{\alpha}) \in [\alpha^f, \alpha^f + \delta] \times [\alpha, \alpha + \delta]$  where  $\alpha^f + \alpha < e$ . In particular, for given  $\delta > 0$ , we take

$$\begin{aligned} x^{lb} &= (x^{sol} - \epsilon)(1 - \delta), x^{ub} = (x^{sol} + \epsilon), \\ x_1^{lb} &= (x_1^{sol} - \epsilon)(1 - 2\delta), x_1^{ub} = (x_1^{sol} + \epsilon), \\ x_2^{lb} &= -2\frac{\log(x_1^{sol} - \epsilon) + \alpha^f(x_1^{sol} - \epsilon)}{\alpha^f + \alpha}(1 - 2\delta), x_2^{ub} = -2\frac{\log(x_1^{sol} + \epsilon) + \alpha^f(x_1^{sol} + \epsilon)}{\alpha^f + \alpha}. \end{aligned} \tag{21}$$

Plugging these values into (19) - (20), we obtain a lower bound of  $\mu(1, 0) - \mu(1/2, 1/2)$  in each set of  $[\alpha^f, \alpha^f + \delta] \times [\alpha, \alpha + \delta]$ . If this lower bound exceeds 0, we verify that  $\mu(1, 0) > \mu(1/2, 1/2)$  for any  $(\bar{\alpha}^f, \bar{\alpha})$  in this set. In `Theorem3.ipynb`,<sup>19</sup> we compute the value of this lower bound for  $\alpha^f, \alpha = \delta, 2\delta, \dots, e$  where  $\alpha^f + \alpha < e$ . We find that by taking  $\delta = 0.01, 0.005, 0.0025$  and  $0.001$  we are able to verify  $\mu(1, 0) > \mu(1/2, 1/2)$  in the respective red regions in Fig. 17.

□

*Proof of Claim 3* We start by proving Claim 3 (i). We have shown in the proof of Theorem 8 that the solution to (17) is unique in the stated parameter regimes. Thus, we know that  $x^* = e^{-(\alpha^f + \alpha)x^*}$  because this construction trivially satisfies (17). Similarly,  $\bar{x} = e^{-(\bar{\alpha}^f + \bar{\alpha})\bar{x}}$ . Now, given that  $e^{-(\bar{\alpha}^f + \bar{\alpha})x^*} \leq e^{-(\alpha^f + \alpha)x^*} = x^*$  for any  $\bar{\alpha}^f \in \{\alpha^f, \alpha^f + \delta\}$  and  $\bar{\alpha} \in \{\alpha, \alpha + \delta\}$ , we know that  $\bar{x} \leq x^*$ . Moreover, from the uniqueness of solution we know that it suffices to show that

$$x^*(1 - \delta) \leq e^{-(\alpha^f + \alpha + 2\delta)x^*(1 - \delta)} \leq e^{-(\bar{\alpha}^f + \bar{\alpha})x^*(1 - \delta)}$$

so then the unique solution  $\bar{x} \geq x^*(1 - \delta)$ . To do so, we observe that  $e^{-(\alpha^f + \alpha)x^* - \delta x^*(1 - \delta)} \leq e^{-(\alpha^f + \alpha + 2\delta)x^*(1 - \delta)}$ , so it suffices to show that

$$x^*(1 - \delta) \leq e^{-(\alpha^f + \alpha)x^* - \delta x^*(1 - \delta)} = x^* e^{-\delta x^*(1 - \delta)}. \tag{22}$$

<sup>19</sup>The computer-aided proof can be found at <https://bit.ly/3OpQrth>.

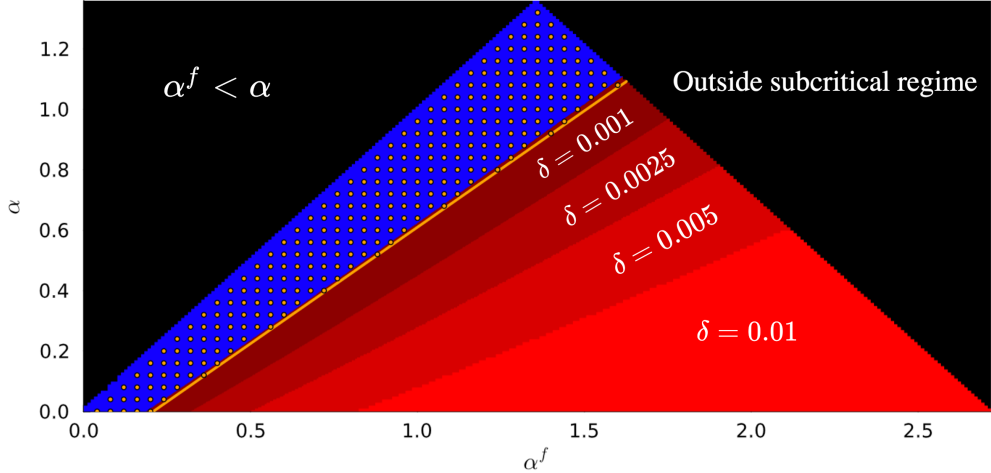


**Figure 17** In the figure we denote the boundary where  $\alpha = 0.77\alpha^f - 0.16$  by the orange line, and the area of subcritical regime where one-sided allocation dominates the balanced allocation is displayed in varying shades of red to the right of this boundary. This growth in the validation area with respect to  $\delta$  is depicted through different red gradients. The black zone denotes parameters outside the feasible or subcritical regime. Although the inequality cannot be confirmed in the blue region when  $\delta = 0.001$ , by taking  $\delta = 0$  we verify the inequality for a wide range of  $(\alpha^f, \alpha)$  values highlighted as orange dots.

Since we trivially have  $x^* \in (0, 1]$ , we can cancel out  $x^*$  and take logarithm on both sides. We find that (22) is equivalent to  $-\log(1 - \delta) \geq x^* \delta(1 - \delta)$ . Since  $x^* \in (0, 1]$ , it is then sufficient to show that  $\frac{-\log(1 - \delta)}{\delta(1 - \delta)} \geq 1$ , which holds for all  $\delta \in (0, 1)$ .

We next prove Claim 3 (ii). Given that in the claimed region

$$\begin{aligned} x_1^* &= e^{-\frac{1}{2}2\alpha^f x_1^* - \frac{1}{2}(\alpha^f + \alpha)x_2^*} \geq e^{-\frac{1}{2}2\bar{\alpha}^f x_1^* - \frac{1}{2}(\bar{\alpha}^f + \bar{\alpha})x_2^*}, \\ x_2^* &= e^{-\frac{1}{2}(\alpha^f + \alpha)x_1^* - \frac{1}{2}2\alpha x_2^*} \geq e^{-\frac{1}{2}(\bar{\alpha}^f + \bar{\alpha})x_1^* - \frac{1}{2}2\bar{\alpha} x_2^*} \end{aligned}$$

for any  $\bar{\alpha}^f \in \{\alpha^f, \alpha^f + \delta\}$  and  $\bar{\alpha} \in \{\alpha, \alpha + \delta\}$ , we know that  $\bar{x}_1 \leq x_1^*$  and  $\bar{x}_2 \leq x_2^*$ .

To prove the claimed lower bound on  $\bar{x}_1$  and  $\bar{x}_2$ , we show that

$$\begin{aligned} x_1^*(1 - 2\delta) &\leq e^{-\frac{1}{2}2\bar{\alpha}^f x_1^*(1 - 2\delta) - \frac{1}{2}(\bar{\alpha}^f + \bar{\alpha})x_2^*(1 - 2\delta)}, \\ x_2^*(1 - 2\delta) &\leq e^{-\frac{1}{2}(\bar{\alpha}^f + \bar{\alpha})x_1^*(1 - 2\delta) - \frac{1}{2}2\bar{\alpha} x_2^*(1 - 2\delta)}. \end{aligned} \tag{23}$$

In particular, (23) is implied by

$$x_1^*(1 - 2\delta) \leq e^{-\frac{1}{2}2\alpha^f x_1^* - \delta x_1^*(1 - 2\delta) - \frac{1}{2}(\alpha^f + \alpha)x_2^* - \delta x_2^*(1 - 2\delta)} = x_1^* \cdot e^{-\delta x_1^*(1 - 2\delta) - \delta x_2^*(1 - 2\delta)}.$$

Since we trivially have  $x_1^* \in (0, 1]$ , we can cancel out  $x_1^*$  and take logarithm on both sides. We find that (23) is equivalent to  $-\log(1 - 2\delta) \geq (x_1^* + x_2^*)\delta(1 - 2\delta)$ . Since  $x_1^* + x_2^* \in [0, 2]$ , it is then sufficient to show that  $\frac{-\log(1 - 2\delta)}{2\delta(1 - 2\delta)} \geq 1$ , which holds for all  $\delta \in (0, 1/2)$ . The proof of  $\bar{x}_2 \geq x_2^*(1 - 2\delta)$  is symmetric.  $\square$

### A.3.5. Proof of Theorem 7

*Proof.* We start by proving the convexity result in Theorem 7 (ii). Recall from (10) that

$$\begin{aligned}\xi(b_l, b_r) = & 2 - b_l y_1^f(\mathbf{b}) - b_r \left(1 - \hat{y}_2^f(\mathbf{b})\right) \\ & - b_r \left(1 - \hat{y}_2^f(\mathbf{b})\right) \left(2b_l \alpha^f y_1^f(\mathbf{b}) + (1 - b_l)(\alpha^f + \alpha) y_1^{nf}(\mathbf{b})\right) \\ & - (1 - b_l) y_1^{nf}(\mathbf{b}) - (1 - b_r) \left(1 - \hat{y}_2^{nf}(\mathbf{b})\right) \\ & - (1 - b_r) \left(1 - \hat{y}_2^{nf}(\mathbf{b})\right) \left(b_l (\alpha^f + \alpha) y_1^f(\mathbf{b}) + 2(1 - b_l) \alpha y_1^{nf}(\mathbf{b})\right),\end{aligned}$$

Since we are interested in the direction  $(1, -1)$ , for ease of notation we denote the sum of flexibility by  $B$  and replace  $b_r$  with  $B - b_l$ . Then, we can re-write  $\xi(b_l, b_r) = \xi(b_l, B - b_l)$  as

$$\begin{aligned}2 - b_l y_1^f(\mathbf{b}) - (B - b_l) \left(1 - \hat{y}_2^f(\mathbf{b})\right) \\ - (B - b_l) \left(1 - \hat{y}_2^f(\mathbf{b})\right) \left(2b_l \alpha^f y_1^f(\mathbf{b}) + (1 - b_l)(\alpha^f + \alpha) y_1^{nf}(\mathbf{b})\right) \\ - (1 - b_l) y_1^{nf}(\mathbf{b}) - (1 - B + b_l) \left(1 - \hat{y}_2^{nf}(\mathbf{b})\right) \\ - (1 - B + b_l) \left(1 - \hat{y}_2^{nf}(\mathbf{b})\right) \left(b_l (\alpha^f + \alpha) y_1^f(\mathbf{b}) + 2(1 - b_l) \alpha y_1^{nf}(\mathbf{b})\right).\end{aligned}\tag{24}$$

Then, the second-order derivative of  $\xi(b_l, B - b_l)$  in the direction  $(1, -1)$  is equal to  $\frac{\partial^2 \xi(b_l, B - b_l)}{\partial b_l^2}$ . We observe that

$$\xi(b_l, B - b_l) = 2 - b_l y_1^f(\mathbf{b}) - (B - b_l) e^{-b_1(b_l)} (1 + b_1(b_l)) - (1 - b_l) y_1^{nf}(\mathbf{b}) - (1 - B + b_l) e^{-b_2(b_l)} (1 + b_2(b_l)),$$

where

$$\begin{aligned}b_1(b_l) &= b_l \cdot 2\alpha^f \cdot y_1^f(\mathbf{b}) + (1 - b_l)(\alpha^f + \alpha) y_1^{nf}(\mathbf{b}), \\ b_2(b_l) &= b_l (\alpha^f + \alpha) y_1^f(\mathbf{b}) + (1 - b_l) \cdot 2\alpha \cdot y_1^{nf}(\mathbf{b}).\end{aligned}$$

Let

$$x_1(b_l, b_r) = e^{-b_l 2\alpha^f y_1^f(\mathbf{b}) - (1 - b_l)(\alpha^f + \alpha) y_1^{nf}(\mathbf{b})} \text{ and } x_2(b_l, b_r) = e^{-b_l (\alpha^f + \alpha) y_1^f(\mathbf{b}) - (1 - b_l) 2\alpha y_1^{nf}(\mathbf{b})}\tag{25}$$

For ease of notation we drop the dependency of  $x_1$  and  $x_2$  on  $\mathbf{b}$ . Then we simplify  $\xi(b_l, B - b_l)$  into

$$\begin{aligned}\xi(b_l, B - b_l) = & 2 - b_l e^{-(B - b_l) 2\alpha^f x_1 - (1 - B + b_l)(\alpha^f + \alpha) x_2} - (B - b_l) x_1 (1 - \log(x_1)) \\ & - (1 - b_l) e^{-(B - b_l)(\alpha^f + \alpha) x_1 - (1 - B + b_l) 2\alpha x_2} - (1 - B + b_l) x_2 (1 - \log(x_2)).\end{aligned}$$

By construction of  $x_1, x_2$  and the definition of  $y_1^f(q), y_1^{nf}(q)$ , we have

$$\begin{aligned}x_1 &= e^{-b_l 2\alpha^f e^{-(B - b_l) 2\alpha^f x_1 - (1 - B + b_l)(\alpha^f + \alpha) x_2} - (1 - b_l)(\alpha^f + \alpha) e^{-(B - b_l)(\alpha^f + \alpha) x_1 - (1 - B + b_l) 2\alpha x_2}} \\ x_2 &= e^{-b_l (\alpha^f + \alpha) e^{-(B - b_l) 2\alpha^f x_1 - (1 - B + b_l)(\alpha^f + \alpha) x_2} - (1 - b_l) 2\alpha e^{-(B - b_l)(\alpha^f + \alpha) x_1 - (1 - B + b_l) 2\alpha x_2}}.\end{aligned}$$

For convenience we write

$$y_1 := e^{-(B - b_l) 2\alpha^f x_1 - (1 - B + b_l)(\alpha^f + \alpha) x_2} \text{ and } y_2 := e^{-(B - b_l)(\alpha^f + \alpha) x_1 - (1 - B + b_l) 2\alpha x_2},\tag{26}$$

so that

$$x_1 = e^{-b_l 2\alpha^f y_1 - (1 - b_l)(\alpha^f + \alpha) y_2}, x_2 = e^{-b_l (\alpha^f + \alpha) y_1 - (1 - b_l) 2\alpha y_2}.$$

Now, taking second order derivative of  $\xi(b_l, B - b_l)$  with respect to  $b_l$ , we obtain

$$\begin{aligned} \frac{\partial^2 \xi(b_l, B - b_l)}{\partial b_l^2} = & -b_l \left( -2\alpha^f x_1 + (\alpha^f + \alpha) x_2 + (B - b_l) 2\alpha^f \frac{\partial x_1}{\partial b_l} + (1 - B + b_l) (\alpha^f + \alpha) \frac{\partial x_2}{\partial b_l} \right)^2 y_1 \\ & - (1 - b_l) \left( -(\alpha^f + \alpha) x_1 + 2\alpha x_2 + (B - b_l) (\alpha^f + \alpha) \frac{\partial x_1}{\partial b_l} + (1 - B + b_l) 2\alpha \frac{\partial x_2}{\partial b_l} \right)^2 y_2 \\ & + 2 \left( -2\alpha^f y_1 + (\alpha^f + \alpha) y_2 \right) x_1 + 2 \left( (\alpha^f + \alpha) y_1 - 2\alpha y_2 \right) x_2 \\ & + (B - b_l) 2 \left( 2\alpha^f y_1 - (\alpha^f + \alpha) y_2 \right) \left( \frac{\partial x_1}{\partial b_l} \right) + (1 - B + b_l) 2 \left( (\alpha^f + \alpha) y_1 - 2\alpha y_2 \right) \left( \frac{\partial x_2}{\partial b_l} \right) \\ & + (B - b_l) \left( \frac{\partial x_1}{\partial b_l} \right)^2 / x_1 + (1 - B + b_l) \left( \frac{\partial x_2}{\partial b_l} \right)^2 / x_2. \end{aligned} \quad (27)$$

Moreover, by taking derivative of  $x_1$  and  $x_2$  with respect to  $b_l$ , we find that

$$\begin{aligned} \frac{\frac{\partial x_1}{\partial b_l}}{x_1} = & y_1 2\alpha^f b_l 2\alpha^f (B - b_l) \frac{\partial x_1}{\partial b_l} + y_2 (1 - b_l) (\alpha^f + \alpha) (B - b_l) (\alpha^f + \alpha) \frac{\partial x_1}{\partial b_l} + \\ & y_1 2\alpha^f b_l (\alpha^f + \alpha) (1 - B + b_l) \frac{\partial x_2}{\partial b_l} + y_2 (1 - b_l) (\alpha^f + \alpha) (1 - B + b_l) 2\alpha \frac{\partial x_2}{\partial b_l} + \\ & y_1 2\alpha^f b_l \left[ (\alpha^f + \alpha) x_2 - 2\alpha^f x_1 \right] + y_2 (\alpha^f + \alpha) (1 - b_l) \left[ 2\alpha x_2 - (\alpha^f + \alpha) x_1 \right] - \\ & y_1 2\alpha^f + y_2 (\alpha^f + \alpha), \end{aligned} \quad (28)$$

and

$$\begin{aligned} \frac{\frac{\partial x_2}{\partial b_l}}{x_2} = & y_1 (\alpha^f + \alpha) b_l 2\alpha^f (B - b_l) \frac{\partial x_1}{\partial b_l} + y_2 (1 - b_l) 2\alpha (B - b_l) (\alpha^f + \alpha) \frac{\partial x_1}{\partial b_l} + \\ & y_1 (\alpha^f + \alpha) b_l (\alpha^f + \alpha) (1 - B + b_l) \frac{\partial x_2}{\partial b_l} + y_2 (1 - b_l) 2\alpha (1 - B + b_l) 2\alpha \frac{\partial x_2}{\partial b_l} + \\ & y_1 (\alpha^f + \alpha) b_l \left[ (\alpha^f + \alpha) x_2 - 2\alpha^f x_1 \right] + y_2 2\alpha (1 - b_l) \left[ 2\alpha x_2 - (\alpha^f + \alpha) x_1 \right] - \\ & y_1 (\alpha^f + \alpha) + y_2 2\alpha. \end{aligned} \quad (29)$$

When  $\mathbf{b} = (1/2, 1/2)$ ,  $B = 1$  and  $b_l = 1/2$ . We find that  $x_1 = y_1, x_2 = y_2$ , which allows us to simplify (28) and (29) as:

$$\frac{\partial x_1}{\partial b_l} = \frac{2x_1 \left( \alpha^2 x_1 x_2 - 2\alpha^f \alpha x_1 x_2 - 2\alpha x_2 + (\alpha^f)^2 x_1 x_2 + 4\alpha^f x_1 - 2\alpha^f x_2 \right)}{\alpha^2 x_1 x_2 - 2\alpha \alpha^f x_1 x_2 + 4\alpha x_2 + (\alpha^f)^2 x_1 x_2 + 4\alpha^f x_1 - 4}, \quad (30)$$

$$\frac{\partial x_2}{\partial b_l} = -\frac{2x_2 \left( \alpha^2 x_1 x_2 - 2\alpha^f \alpha x_1 x_2 - 2\alpha x_1 + (\alpha^f)^2 x_1 x_2 + 4\alpha x_2 - 2\alpha^f x_1 \right)}{\alpha^2 x_1 x_2 - 2\alpha \alpha^f x_1 x_2 + 4\alpha x_2 + (\alpha^f)^2 x_1 x_2 + 4\alpha^f x_1 - 4}. \quad (31)$$

Then, plugging  $x_1 = y_1, x_2 = y_2, B = 1$  and  $b_l = 1/2$  into (27), we obtain

$$\begin{aligned} \left. \frac{\partial^2 \xi(b_l, B - b_l)}{\partial b_l^2} \right|_{B=1, b_l=\frac{1}{2}} = & -\frac{1}{2} \left( -2\alpha^f x_1 + (\alpha^f + \alpha) x_2 + \frac{1}{2} 2\alpha^f \frac{\partial x_1}{\partial b_l} + \frac{1}{2} (\alpha^f + \alpha) \frac{\partial x_2}{\partial b_l} \right)^2 x_1 \\ & - \frac{1}{2} \left( -(\alpha^f + \alpha) x_1 + 2\alpha x_2 + \frac{1}{2} (\alpha^f + \alpha) \frac{\partial x_1}{\partial b_l} + \frac{1}{2} 2\alpha \frac{\partial x_2}{\partial b_l} \right)^2 x_2 \\ & + 2 \left( -2\alpha^f x_1 + (\alpha^f + \alpha) x_2 \right) x_1 + 2 \left( (\alpha^f + \alpha) x_1 - 2\alpha x_2 \right) x_2 \\ & + \left( 2\alpha^f x_1 - (\alpha^f + \alpha) x_2 \right) \left( \frac{\partial x_1}{\partial b_l} \right) + \left( (\alpha^f + \alpha) x_1 - 2\alpha x_2 \right) \left( \frac{\partial x_2}{\partial b_l} \right) \\ & + \frac{1}{2} \left( \frac{\partial x_1}{\partial b_l} \right)^2 / x_1 + \frac{1}{2} \left( \frac{\partial x_2}{\partial b_l} \right)^2 / x_2. \end{aligned}$$

By plugging the values of  $\frac{\partial x_1}{\partial b_l}$  and  $\frac{\partial x_2}{\partial b_l}$  from (30) and (31) into the above, we find that

$$\begin{aligned} \left. \frac{\partial^2 \xi(b_l, B - b_l)}{\partial b_l^2} \right|_{B=1, b_l=\frac{1}{2}} &= \frac{1}{\alpha^2 x_1 x_2 - 2\alpha \alpha^f x_1 x_2 + 4\alpha x_2 + (\alpha^f)^2 x_1 x_2 + 4\alpha^f x_1 - 4} \\ &\quad (4\alpha^2 x_1^2 x_2 + 4\alpha^2 x_1 x_2^2 - 8\alpha \alpha^f x_1^2 x_2 - 8\alpha \alpha^f x_1 x_2^2 - 16\alpha x_1 x_2 \\ &\quad + 16\alpha x_2^2 + 4(\alpha^f)^2 x_1^2 x_2 + 4(\alpha^f)^2 x_1 x_2^2 + 16\alpha^f x_1^2 - 16\alpha^f x_1 x_2) \\ &= \frac{(\alpha^f - \alpha)^2 4x_1 x_2 (x_1 + x_2) - 16(x_2 - x_1)(\alpha^f x_1 - \alpha x_2)}{(\alpha^f - \alpha)^2 x_1 x_2 + 4(\alpha x_2 + \alpha^f x_1 - 1)}. \end{aligned} \quad (32)$$

Recall that we have

$$x_1 = e^{-\alpha^f x_1 - 1/2(\alpha^f + \alpha)x_2}, x_2 = e^{-1/2(\alpha^f + \alpha)x_1 - \alpha x_2} \quad (33)$$

when  $B = 1, b_l = 1/2$ . This allows us to solve  $x_1$  and  $x_2$  and determine the size of convexity numerically. In particular, we know from (21) that we can provide bounds  $x_1^{lb}, x_1^{ub}, x_2^{lb}, x_2^{ub}$  for any  $(\bar{\alpha}^f, \bar{\alpha}) \in [\alpha^f, \alpha^f + \delta] \times [\alpha, \alpha + \delta]$  where  $10^{-4} < \alpha < \alpha^f$  and  $\alpha^f + \alpha < e$ . Thus, we can lower bound (32) for any  $(\bar{\alpha}^f, \bar{\alpha}) \in [\alpha^f, \alpha^f + \delta] \times [\alpha, \alpha + \delta]$  as:

$$\begin{aligned} &\frac{(\bar{\alpha}^f - \bar{\alpha})^2 4\bar{x}_1 \bar{x}_2 (\bar{x}_1 + \bar{x}_2) - 16(\bar{x}_2 - \bar{x}_1)(\bar{\alpha}^f \bar{x}_1 - \bar{\alpha} \bar{x}_2)}{(\bar{\alpha}^f - \bar{\alpha})^2 \bar{x}_1 \bar{x}_2 + 4(\bar{\alpha} \bar{x}_2 + \bar{\alpha}^f \bar{x}_1 - 1)} \\ &\geq \frac{-(\alpha^f - \alpha + \delta)^2 4x_1^{ub} x_2^{ub} (x_1^{ub} + x_2^{ub}) + 16 \max(0, x_2^{lb} - x_1^{ub}) \alpha^f x_1^{lb} - 16(x_2^{ub} - x_1^{lb})(\alpha + \delta) x_2^{ub}}{-(\max(\alpha^f - \alpha - \delta, 0))^2 x_1^{lb} x_2^{lb} + 4[1 - \alpha x_2^{lb} - \alpha^f x_1^{lb}]} \end{aligned} \quad (34)$$

If this lower bound exceeds 0, we know that  $\xi(b_l, b_r)$  is strictly convex in the direction  $(1, -1)$  at  $\mathbf{b} = (1/2, 1/2)$  for any  $(\bar{\alpha}^f, \bar{\alpha}) \in [\alpha^f, \alpha^f + \delta] \times [\alpha, \alpha + \delta]$ . At  $\mathbf{b} = (1/2, 1/2)$ , we find by symmetry that  $\xi(b_l, b_r) = \hat{\xi}(b_l, b_r)$ ,

$$\left. \frac{\partial \xi(b_l, B - b_l)}{\partial b_l} \right|_{B=1, b_l=\frac{1}{2}} = \left. \frac{\partial \hat{\xi}(b_l, B - b_l)}{\partial b_l} \right|_{B=1, b_l=\frac{1}{2}} = 0 \text{ and } \left. \frac{\partial^2 \xi(b_l, B - b_l)}{\partial b_l^2} \right|_{B=1, b_l=\frac{1}{2}} = \left. \frac{\partial^2 \hat{\xi}(b_l, B - b_l)}{\partial b_l^2} \right|_{B=1, b_l=\frac{1}{2}}.$$

Thus, at  $\mathbf{b} = (1/2, 1/2)$ , by Claim 4 below we know that to show  $\nabla_{(1,-1)}^2 \mu^{\text{KS}}(b_l, b_r) > 0$  it suffices to verify strict local convexity for  $\xi(b_l, b_r)$  in the direction  $(1, -1)$ . That is, we verify  $\left. \frac{\partial^2 \xi(b_l, B - b_l)}{\partial b_l^2} \right|_{B=1, b_l=\frac{1}{2}} > 0$ .

**CLAIM 4.** *If for some  $\mathbf{b}' \in (0, 1)^2$  and direction  $v \in \mathbb{R}^2$ ,  $\hat{\xi}(\mathbf{b}') = \hat{\xi}(\mathbf{b}')$ ,  $\nabla_v \hat{\xi}(\mathbf{b}') = \nabla_v \hat{\xi}(\mathbf{b}')$  and  $\nabla_v^2 \hat{\xi}(\mathbf{b}') = \nabla_v^2 \hat{\xi}(\mathbf{b}')$ , then  $\nabla_v^2 \mu^{\text{KS}}(\mathbf{b}') = \nabla_v^2 \hat{\xi}(\mathbf{b}') = \nabla_v^2 \hat{\xi}(\mathbf{b}')$ .*

In Theorem7.ipynb,<sup>20</sup> we compute the lower bound of  $\left. \frac{\partial^2 \xi(b_l, B - b_l)}{\partial b_l^2} \right|_{B=1, b_l=\frac{1}{2}}$  in (34) for  $\alpha^f, \alpha = \delta, 2\delta, \dots, e$  where  $\alpha^f + \alpha < e$ . We find that by taking  $\delta = 0.01, 0.005, 0.0025$  and  $0.001$  we are able to verify strict local convexity of  $\mu^{\text{KS}}(1/2, 1/2)$  in the direction  $(1, -1)$  in the respective red regions in Fig. 18.

We next prove the concavity result in Theorem 7 (i). We again focus on  $\xi(b_l, b_r)$ , and the second-order derivative of  $\xi(b_l, b_r)$  in the direction  $(0, 1)$  is equal to  $\left. \frac{\partial^2 \xi(b_l, B - b_l)}{\partial B^2} \right|_{B=1}$ .

<sup>20</sup>The computer-aided proof can be found at <https://bit.ly/3OpKRqP>.

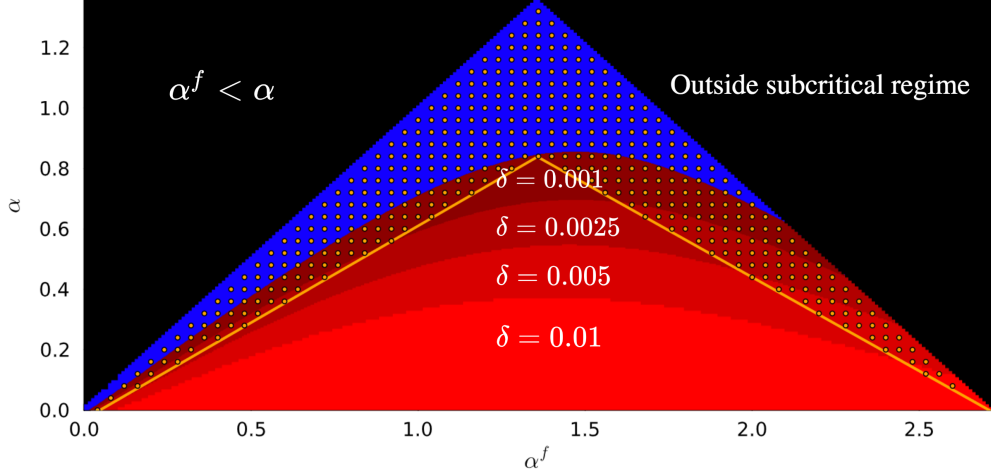


**Figure 18** In the figure we denote the boundary where  $10^{-4} < \alpha < 0.64\alpha^f - 0.03$  and  $0.62\alpha^f + \alpha < 1.68$  by the orange lines, and the area of subcritical regime where convexity and concavity properties are verified is displayed in varying shades of red below this boundary. The growth in the validation area with respect to  $\delta$  is depicted through different red gradients. The black zone denotes parameters outside the feasible or subcritical regime. Although the convexity and concavity properties cannot be confirmed in the blue region when  $\delta = 0.001$ , by taking  $\delta = 0$  we verify the properties for a wide range of  $(\alpha^f, \alpha)$  values highlighted as orange dots.

Based on  $x_1, x_2, y_1, y_2$  constructed in (25) and (26), we obtain

$$\begin{aligned} \frac{\partial^2 \xi(b_l, B - b_l)}{\partial B^2} = & -b_l \left( 2\alpha^f x_1 - (\alpha^f + \alpha) x_2 + (B - b_l) 2\alpha^f \frac{\partial x_1}{\partial B} + (1 - B + b_l) (\alpha^f + \alpha) \frac{\partial x_2}{\partial B} \right)^2 y_1 \\ & - (1 - b_l) \left( (\alpha^f + \alpha) x_1 - 2\alpha x_2 + (B - b_l) (\alpha^f + \alpha) \frac{\partial x_1}{\partial B} + (1 - B + b_l) 2\alpha \frac{\partial x_2}{\partial B} \right)^2 y_2 \quad (35) \\ & + (B - b_l) \left( \frac{\partial x_1}{\partial B} \right)^2 / x_1 + (1 - B + b_l) \left( \frac{\partial x_2}{\partial B} \right)^2 / x_2. \end{aligned}$$

Moreover, by taking derivative of  $x_1$  and  $x_2$  with respect to  $B$ , we find that

$$\begin{aligned} \frac{\frac{\partial x_1}{\partial B}}{x_1} = & y_1 2\alpha^f b_l 2\alpha^f (B - b_l) \frac{\partial x_1}{\partial B} + y_2 (1 - b_l) (\alpha^f + \alpha) (B - b_l) (\alpha^f + \alpha) \frac{\partial x_1}{\partial B} + \\ & y_1 2\alpha^f b_l (\alpha^f + \alpha) (1 - B + b_l) \frac{\partial x_2}{\partial B} + y_2 (1 - b_l) (\alpha^f + \alpha) (1 - B + b_l) 2\alpha \frac{\partial x_2}{\partial B} - \\ & y_1 2\alpha^f b_l [(\alpha^f + \alpha) x_2 - 2\alpha^f x_1] - y_2 (\alpha^f + \alpha) (1 - b_l) [2\alpha x_2 - (\alpha^f + \alpha) x_1], \end{aligned}$$

and

$$\begin{aligned} \frac{\frac{\partial x_2}{\partial B}}{x_2} = & y_1 (\alpha^f + \alpha) b_l 2\alpha^f (B - b_l) \frac{\partial x_1}{\partial B} + y_2 (1 - b_l) 2\alpha (B - b_l) (\alpha^f + \alpha) \frac{\partial x_1}{\partial B} + \\ & y_1 (\alpha^f + \alpha) b_l (\alpha^f + \alpha) (1 - B + b_l) \frac{\partial x_2}{\partial B} + y_2 (1 - b_l) 2\alpha (1 - B + b_l) 2\alpha \frac{\partial x_2}{\partial B} - \\ & y_1 (\alpha^f + \alpha) b_l [(\alpha^f + \alpha) x_2 - 2\alpha^f x_1] - y_2 2\alpha (1 - b_l) [2\alpha x_2 - (\alpha^f + \alpha) x_1]. \end{aligned}$$

When  $B = 1$  and  $b_l = 1/2$ , we have  $x_1 = y_1, x_2 = y_2$ . Applying these observations to simplify (35), we obtain

$$\begin{aligned} \frac{\partial^2 \xi(b_l, B - b_l)}{\partial B^2} \Bigg|_{a=1, q=\frac{1}{2}} &= \frac{1}{-\left(x_1 x_2 (\alpha^f - \alpha)^2\right)^2 + 8x_1 x_2 (\alpha^f + \alpha)^2 + 16 \left(\alpha^2 x_2^2 + (\alpha^f)^2 x_1^2 - 1\right)} \\ &\quad (-2(x_1 + x_2) \left(x_1 x_2 (\alpha^f - \alpha)^2\right)^2 - 16(x_1 + x_2) x_1 x_2 \alpha^f \alpha \\ &\quad + 8(\alpha^f)^2 x_1 (x_2^2 - 3x_1 x_2 + 4x_1^2) + 8\alpha^2 x_2 (x_1^2 - 3x_1 x_2 + 4x_2^2)). \end{aligned} \quad (36)$$

Again, we know from (21) that we can provide bounds  $x_1^{lb}, x_1^{ub}, x_2^{lb}, x_2^{ub}$  for any  $(\bar{\alpha}^f, \bar{\alpha}) \in [\alpha^f, \alpha^f + \delta] \times [\alpha, \alpha + \delta]$  where  $\alpha^f + \alpha < e$ . Thus, we can upper bound (36) for any  $(\bar{\alpha}^f, \bar{\alpha}) \in [\alpha^f, \alpha^f + \delta] \times [\alpha, \alpha + \delta]$  as:

$$\begin{aligned} &\frac{1}{-\left[x_1^{ub} x_2^{ub} (\alpha^f - \alpha + \delta)^2\right]^2 + 8(\alpha^f + \alpha)^2 x_1^{lb} x_2^{lb} + 16\alpha^2 (x_2^{lb})^2 + 16(\alpha^f)^2 (x_1^{lb})^2 - 16} \\ &\cdot \left( -2(x_1^{lb} + x_2^{lb}) \left[x_1^{lb} x_2^{lb} (\max(0, \alpha^f - \alpha - \delta))^2\right]^2 - 16(x_1^{lb} + x_2^{lb}) x_1^{lb} x_2^{lb} \alpha^f \alpha \right. \\ &+ 8(\alpha^f + \delta)^2 \left(x_1^{ub} (x_2^{ub})^2 + 4(x_1^{ub})^3\right) + 8(\alpha + \delta)^2 \left(x_2^{ub} (x_1^{ub})^2 + 4(x_2^{ub})^3\right) \\ &\left. - 24(\alpha^f)^2 (x_1^{lb})^2 x_2^{lb} - 24\alpha^2 (x_2^{lb})^2 x_1^{lb} \right). \end{aligned} \quad (37)$$

If this upper bound is strictly below 0, we know that  $\xi(b_l, b_r)$  is strictly concave in the direction  $(0, 1)$  at  $\mathbf{b} = (1/2, 1/2)$  for any  $(\bar{\alpha}^f, \bar{\alpha}) \in [\alpha^f, \alpha^f + \delta] \times [\alpha, \alpha + \delta]$ . By symmetry at  $\mathbf{b} = (1/2, 1/2)$  we find that  $\xi(b_l, b_r) = \hat{\xi}(b_l, b_r)$ ,

$$\frac{\partial \xi(b_l, B - b_l)}{\partial B} \Bigg|_{B=1, b_l=\frac{1}{2}} = \frac{\partial \hat{\xi}(b_l, B - b_l)}{\partial B} \Bigg|_{B=1, b_l=\frac{1}{2}} \quad \text{and} \quad \frac{\partial^2 \xi(b_l, B - b_l)}{\partial B^2} \Bigg|_{B=1, b_l=\frac{1}{2}} = \frac{\partial^2 \hat{\xi}(b_l, B - b_l)}{\partial B^2} \Bigg|_{B=1, b_l=\frac{1}{2}}.$$

Thus, at  $\mathbf{b} = (1/2, 1/2)$ , by Claim 4 we know it suffices to verify strict local concavity for  $\xi(b_l, b_r)$  in the direction  $(0, 1)$ . That is, we verify  $\frac{\partial^2 \xi(b_l, B - b_l)}{\partial B^2} \Bigg|_{B=1, b_l=\frac{1}{2}} < 0$ .

In Theorem4.ipynb,<sup>21</sup> we compute the upper bound of  $\frac{\partial^2 \xi(b_l, B - b_l)}{\partial B^2} \Bigg|_{a=1, q=\frac{1}{2}}$  in (37) for  $\alpha^f, \alpha = 10^{-4}, \delta, 2\delta, \dots, e$  where  $\alpha^f + \alpha < e$ . We find that taking  $\delta = 0.01$  is sufficient for verifying (37)  $< 0$  for all  $\alpha^f$  and  $\alpha$  such that  $10^{-4} < \alpha < \alpha^f$  and  $\alpha^f + \alpha < e$ . The concavity in the direction  $(1, 0)$  is exactly symmetric.

□

*Proof of Claim 4* By definition, we need to show that

$$\nabla_{\mathbf{v}}^2 \mu^{\text{KS}}(\mathbf{b}') = \lim_{h \rightarrow 0} \frac{\mu^{\text{KS}}(\mathbf{b}' + \mathbf{v}h) - 2\mu^{\text{KS}}(\mathbf{b}') + \mu^{\text{KS}}(\mathbf{b}' - \mathbf{v}h)}{h^2}$$

exists and is equal to the claimed value. By Taylor series expansion, we know that for  $h \in \mathbb{R}$ ,

$$\begin{aligned} \xi(\mathbf{b}' + \mathbf{v}h) &= \xi(\mathbf{b}') + h \cdot \nabla_{\mathbf{v}} \xi(\mathbf{b}') + h^2 \cdot \nabla_{\mathbf{v}}^2 \xi(\mathbf{b}') + o(h^2), \\ \hat{\xi}(\mathbf{b}' + \mathbf{v}h) &= \hat{\xi}(\mathbf{b}') + h \cdot \nabla_{\mathbf{v}} \hat{\xi}(\mathbf{b}') + h^2 \cdot \nabla_{\mathbf{v}}^2 \hat{\xi}(\mathbf{b}') + o(h^2), \\ \xi(\mathbf{b}' - \mathbf{v}h) &= \xi(\mathbf{b}') - h \cdot \nabla_{\mathbf{v}} \xi(\mathbf{b}') - h^2 \cdot \nabla_{\mathbf{v}}^2 \xi(\mathbf{b}') - o(h^2), \\ \hat{\xi}(\mathbf{b}' - \mathbf{v}h) &= \hat{\xi}(\mathbf{b}') - h \cdot \nabla_{\mathbf{v}} \hat{\xi}(\mathbf{b}') - h^2 \cdot \nabla_{\mathbf{v}}^2 \hat{\xi}(\mathbf{b}') - o(h^2). \end{aligned}$$

<sup>21</sup>The computer-aided proof can be found at <https://bit.ly/3HMJL13>.

In particular, since  $\hat{\xi}(\mathbf{b}') = \hat{\xi}(\mathbf{b}')$ ,  $\nabla_v \hat{\xi}(\mathbf{b}') = \nabla_v \hat{\xi}(\mathbf{b}')$  and  $\nabla_v^2 \hat{\xi}(\mathbf{b}') = \nabla_v^2 \hat{\xi}(\mathbf{b}')$ , from the above we know that

$$\xi(\mathbf{b}' + \mathbf{v}h) - \hat{\xi}(\mathbf{b}' + \mathbf{v}h) = o(h^2) \text{ and } \xi(\mathbf{b}' - \mathbf{v}h) - \hat{\xi}(\mathbf{b}' - \mathbf{v}h) = o(h^2).$$

Thus,

$$\begin{aligned} \nabla_v^2 \mu^{\text{KS}}(\mathbf{b}') &= \lim_{h \rightarrow 0} \frac{\mu^{\text{KS}}(\mathbf{b}' + \mathbf{v}h) - 2\mu^{\text{KS}}(\mathbf{b}') + \mu^{\text{KS}}(\mathbf{b}' - \mathbf{v}h)}{h^2} \\ &= \lim_{h \rightarrow 0} \frac{\min(\xi(\mathbf{b}' + \mathbf{v}h), \hat{\xi}(\mathbf{b}' + \mathbf{v}h)) - 2\min(\xi(\mathbf{b}'), \hat{\xi}(\mathbf{b}')) + \min(\xi(\mathbf{b}' - \mathbf{v}h), \hat{\xi}(\mathbf{b}' - \mathbf{v}h))}{h^2} \\ &= \lim_{h \rightarrow 0} \frac{\xi(\mathbf{b}' + \mathbf{v}h) - 2\xi(\mathbf{b}') + \xi(\mathbf{b}' - \mathbf{v}h) + o(h^2)}{h^2} \\ &= \nabla_v^2 \xi(\mathbf{b}') = \nabla_v^2 \hat{\xi}(\mathbf{b}'). \end{aligned}$$

□

### A.3.6. Proofs of the Auxiliary Results in Appendix A.3.3

*Proof of Proposition 1* Theorem 8 in Karp and Sipser (1981) (1) - (4) establishes the validity of the statements in Proposition 1 (i) - (iv) for a general graph  $G = (V, E)$ . Since bipartite graphs are a subset of such general graphs, these results immediately extend.

For Proposition 1 (v), to determine  $|\Psi_1^l|$  and  $|\Psi_1^r|$ , we start by finding  $m_1$ . By (iii), every edge in  $M_1$  is connected to at least one target. By (ii), if an edge in  $M_1$  is connected to two targets  $u$  and  $v$ , then  $v \otimes u$  and  $u \otimes v$ . Hence,

$$m_1 = |M_1| \leq \left| \{v \in V_l \mid v \text{ is a target}\} \right| + \left| \{v \in V_r \mid v \text{ is a target}\} \right| - \left| \{(v, u) \mid v \otimes u \text{ and } u \otimes v\} \right|.$$

The equality follows from (ii) because every target is connected to an edge in  $M_1$ .

By Theorem 9 (4) in Karp and Sipser (1981), a node  $v$  appears in a derivation if and only if it is a target or a loser or both. Furthermore,  $v$  is both a target and a loser if and only if there exists a unique  $u$  such that  $v \otimes u$  and  $u \otimes v$ . Hence, the number of nodes in  $V_l$  that appear in a derivation is given by

$$\left| \{v \in V_l \mid v \text{ is a target}\} \right| + \left| \{v \in V_l \mid v \text{ is a loser}\} \right| - \left| \{(v, u) \mid v \otimes u \text{ and } u \otimes v\} \right|.$$

Then, we can find  $\Psi_1^l$  as the set of nodes in  $V_l$  that appear in a derivation but do not belong to  $M_1^l$ . Specifically,

$$\begin{aligned} |\Psi_1^l| &= \left| \{v \in V_l \mid v \text{ is a target}\} \right| + \left| \{v \in V_l \mid v \text{ is a loser}\} \right| - \left| \{(v, u) \mid v \otimes u \text{ and } u \otimes v\} \right| \\ &\quad - \left( \left| \{v \in V_l \mid v \text{ is a target}\} \right| + \left| \{v \in V_r \mid v \text{ is a target}\} \right| - \left| \{(v, u) \mid v \otimes u \text{ and } u \otimes v\} \right| \right) \\ &= \left| \{v \in V_l \mid v \text{ is a loser}\} \right| - \left| \{v \in V_r \mid v \text{ is a target}\} \right|. \end{aligned}$$

The computation of  $|\Psi_1^r|$  is symmetric. Since  $\psi_1 = \max \{|\Psi_1^l|, |\Psi_1^r|\}$  by definition, we obtain Proposition 1 (v).

□

*Proof of Lemma 6* We start from the leaf of a random tree, i.e.,  $d = 1$ , and iteratively trace back to the root of the tree as  $d$  scales large. For a flexible node  $u \in S_l$ , the number of its children follows a Binomial distribution  $\text{Binom}(n, (1 + b_r)p_n^f + (1 - b_r)p_n)$ . Thus, the probability for it to have  $k$  children is given by

$$z_k^f(\mathbf{b}) := \binom{n}{k} ((1 + b_r)p_n^f + (1 - b_r)p_n)^k (1 - (1 + b_r)p_n^f - (1 - b_r)p_n)^{n-k} \quad \forall k.$$

Moreover, since the probability that  $u$  connects with a flexible node is  $2p^f$  and the probability that it connects with a regular node is  $p^f + p$ , by Bayes' Theorem we have

$$\begin{aligned}\mathbb{P}[u' \text{ is flex} | u \text{ is flex}, u' \text{ is a child of } u] &= \frac{b_r \cdot 2p_n^f}{b_r \cdot 2p_n^f + (1 - b_r) \cdot (p_n^f + p_n)} \\ &= \frac{b_r \cdot 2p_n^f}{(1 + b_r)p_n^f + (1 - b_r)p_n}\end{aligned}$$

and similarly

$$\mathbb{P}[u' \text{ is non-flex} | u \text{ is flex}, u' \text{ is a child of } u] = \frac{(1 - b_r) \cdot (p_n^f + p_n)}{(1 + b_r)p_n^f + (1 - b_r)p_n}.$$

By definition,  $u$  is an  $L$ -node if all of its children are  $H$ -nodes, including when it has no children. Thus,

$$\begin{aligned}y_1^f(\mathbf{b}, d) &= \sum_{k=0}^n z_k^f(\mathbf{b}) \cdot \left( \frac{2b_r p_n^f}{(1 + b_r)p_n^f + (1 - b_r)p_n} \hat{y}_2^f(\mathbf{b}, d-1) + \frac{(1 - b_r) \cdot (p_n^f + p_n)}{(1 + b_r)p_n^f + (1 - b_r)p_n} \hat{y}_2^{nf}(\mathbf{b}, d-1) \right)^k \\ &= \sum_{k=0}^n \binom{n}{k} ((1 + b_r)p_n^f + (1 - b_r)p_n)^k (1 - (1 + b_r)p_n^f - (1 - b_r)p_n)^{n-k} \\ &\quad \cdot \left( \frac{2b_r p_n^f}{(1 + b_r)p_n^f + (1 - b_r)p_n} \hat{y}_2^f(\mathbf{b}, d-1) + \frac{(1 - b_r) \cdot (p_n^f + p_n)}{(1 + b_r)p_n^f + (1 - b_r)p_n} \hat{y}_2^{nf}(\mathbf{b}, d-1) \right)^k \\ &= \sum_{k=1}^n \binom{n}{k} (1 - (1 + b_r)p_n^f - (1 - b_r)p_n)^{n-k} \cdot \left( 2b_r p_n^f \hat{y}_2^f(\mathbf{b}, d-1) + (1 - b_r) \cdot (p_n^f + p_n) \hat{y}_2^{nf}(\mathbf{b}, d-1) \right)^k \\ &= \left[ 2b_r p_n^f \hat{y}_2^f(\mathbf{b}, d-1) + (1 - b_r) \cdot (p_n^f + p_n) \hat{y}_2^{nf}(\mathbf{b}, d-1) + 1 - (1 + b_r)p_n^f - (1 - b_r)p_n \right]^n \\ &= \left[ 1 - 2b_r p_n^f \left( 1 - \hat{y}_2^f(\mathbf{b}, d-1) \right) - (1 - b_r) \cdot (p_n^f + p_n) \left( 1 - \hat{y}_2^{nf}(\mathbf{b}, d-1) \right) \right]^n \\ &= \left[ 1 - \frac{2b_r \alpha^f \left( 1 - \hat{y}_2^f(\mathbf{b}, d-1) \right) - (1 - b_r) \cdot (\alpha^f + \alpha) \left( 1 - \hat{y}_2^{nf}(\mathbf{b}, d-1) \right)}{n} \right]^n \\ &= e^{-2b_r \alpha^f \left( 1 - \hat{y}_2^f(\mathbf{b}, d-1) \right) - (1 - b_r) \cdot (\alpha^f + \alpha) \left( 1 - \hat{y}_2^{nf}(\mathbf{b}, d-1) \right)} \text{ as } n \rightarrow \infty.\end{aligned}$$

Notice that the fourth equality is an application of the Binomial Theorem, and the last equality follows from

$$\lim_{n \rightarrow \infty} \left( 1 - \frac{x}{n} \right)^n = e^{-x}, \forall x.$$

The expressions for  $y_1^{nf}(\mathbf{b}, d)$ ,  $\hat{y}_1^f(\mathbf{b}, d)$  and  $\hat{y}_1^{nf}(\mathbf{b}, d)$  can be derived in a similar fashion.

Next, by definition,  $u$  is an  $H$ -node if it has at least one child in  $L$ -nodes. Thus,

$$\begin{aligned}y_2^f(\mathbf{b}, d) &= 1 - \sum_{k=0}^n z_k^f(\mathbf{b}) \cdot \left( \frac{2b_r p_n^f}{(1 + b_r)p_n^f + (1 - b_r)p_n} \left( 1 - \hat{y}_1^f(\mathbf{b}, d-1) \right) + \frac{(1 - b_r) \cdot (p_n^f + p_n)}{(1 + b_r)p_n^f + (1 - b_r)p_n} \left( 1 - \hat{y}_1^{nf}(\mathbf{b}, d-1) \right) \right)^k \\ &= 1 - \sum_{k=0}^n \binom{n}{k} ((1 + b_r)p_n^f + (1 - b_r)p_n)^k (1 - (1 + b_r)p_n^f - (1 - b_r)p_n)^{n-k} \\ &\quad \cdot \left( \frac{2b_r p_n^f}{(1 + b_r)p_n^f + (1 - b_r)p_n} \left( 1 - \hat{y}_1^f(\mathbf{b}, d-1) \right) + \frac{(1 - b_r) \cdot (p_n^f + p_n)}{(1 + b_r)p_n^f + (1 - b_r)p_n} \left( 1 - \hat{y}_1^{nf}(\mathbf{b}, d-1) \right) \right)^k \\ &= 1 - \sum_{k=1}^n \binom{n}{k} (1 - (1 + b_r)p_n^f - (1 - b_r)p_n)^{n-k} \cdot \left( 2b_r p_n^f \left( 1 - \hat{y}_1^f(\mathbf{b}, d-1) \right) + (1 - b_r) \cdot (p_n^f + p_n) \left( 1 - \hat{y}_1^{nf}(\mathbf{b}, d-1) \right) \right)^k \\ &= 1 - \left[ 1 - 2b_r p_n^f \left( 1 - \hat{y}_1^f(\mathbf{b}, d-1) \right) - (1 - b_r) \cdot (p_n^f + p_n) \left( 1 - \hat{y}_1^{nf}(\mathbf{b}, d-1) \right) \right]^n\end{aligned}$$

$$\begin{aligned}
& \cdot \left( 2b_r p_n^f \left( 1 - \hat{y}_1^f(\mathbf{b}, d-1) \right) + (1-b_r) \cdot (p_n^f + p_n) \left( 1 - \hat{y}_1^{nf}(\mathbf{b}, d-1) \right) \right)^k \\
&= 1 - \left[ 2b_r p_n^f \left( 1 - \hat{y}_1^f(\mathbf{b}, d-1) \right) + (1-b_r) \cdot (p_n^f + p_n) \left( 1 - \hat{y}_1^{nf}(\mathbf{b}, d-1) \right) + 1 - (1+b_r)p_n^f - (1-b_r)p_n \right]^n \\
&= 1 - \left[ 1 - 2b_r p_n^f \hat{y}_1^f(\mathbf{b}, d-1) - (1-b_r) \cdot (p_n^f + p_n) \hat{y}_1^{nf}(\mathbf{b}, d-1) \right]^n \\
&= 1 - \left[ 1 - \frac{2b_r \alpha^f \hat{y}_1^f(\mathbf{b}, d-1) - (1-b_r) \cdot (\alpha^f + \alpha) \hat{y}_1^{nf}(\mathbf{b}, d-1)}{n} \right]^n \\
&= 1 - e^{-2b_r \alpha^f \hat{y}_1^f(\mathbf{b}, d-1) - (1-b_r) \cdot (\alpha^f + \alpha) \hat{y}_1^{nf}(\mathbf{b}, d-1)} \text{ as } n \rightarrow \infty.
\end{aligned}$$

The expressions for  $y_2^{nf}(\mathbf{b}, d)$ ,  $\hat{y}_2^f(\mathbf{b}, d)$  and  $\hat{y}_2^{nf}(\mathbf{b}, d)$  can be derived in a similar fashion. Since all leaf nodes are lonely, we have

$$y_2^f(\mathbf{b}, 1) = y_2^{nf}(\mathbf{b}, 1) = \hat{y}_2^f(\mathbf{b}, 1) = \hat{y}_2^{nf}(\mathbf{b}, 1) = 0.$$

Moreover, since  $y_1^f(\mathbf{b}, d), y_1^{nf}(\mathbf{b}, d), y_2^f(\mathbf{b}, d), y_2^{nf}(\mathbf{b}, d), \hat{y}_1^f(\mathbf{b}, d), \hat{y}_1^{nf}(\mathbf{b}, d), \hat{y}_2^f(\mathbf{b}, d), \hat{y}_2^{nf}(\mathbf{b}, d)$  are all bounded increasing sequences with respect to  $d$ , these sequences converge as  $d \rightarrow \infty$  and  $\mathbf{y}$  is given by the smallest solution to (9).  $\square$

*Proof of Lemma 5* Theorems 3 (1) and 3 (2) in Karp and Sipser (1981) respectively establish the statements in Lemma 5(i) and (ii) for a general tree rooted at vertex  $v$ . As  $\bar{G}$  under consideration is also rooted at vertex  $v$ , these results immediately extend.  $\square$

*Proof of Lemma 7* By Lemma 5 (i), we have

$$\mathbb{P}[v \text{ is a target} | v \text{ is a flexible node in } S_l] = \mathbb{P}[v \text{ is an } H\text{-node} | v \text{ is a flexible node in } S_l] = y_2^f(\mathbf{b}).$$

To find the probability for a flexible node  $v$  in  $S_l$  to be a loser, we need to sum the probability that  $v$  is an  $L$ -node and that  $v$  has exactly 1 child which is not an  $H$ -node. The former is simply given by  $y_1^f(\mathbf{b})$ , while the latter can be computed as

$$\begin{aligned}
& \mathbb{P}[v \text{ has exactly 1 child that is not an } H\text{-node} | v \text{ is a flexible node in } S_l] \\
&= \sum_{k=0}^n z_k^f(\mathbf{b}) \cdot k \cdot \left( \frac{2b_r p_n^f}{(1+b_r)p_n^f + (1-b_r)p_n} \hat{y}_2^f(\mathbf{b}) + \frac{(1-b_r) \cdot (p_n^f + p_n)}{(1+b_r)p_n^f + (1-b_r)p_n} \hat{y}_2^{nf}(\mathbf{b}) \right)^{k-1} \\
&\quad \cdot \left( 1 - \frac{2b_r p_n^f}{(1+b_r)p_n^f + (1-b_r)p_n} \hat{y}_2^f(\mathbf{b}) - \frac{(1-b_r) \cdot (p_n^f + p_n)}{(1+b_r)p_n^f + (1-b_r)p_n} \hat{y}_2^{nf}(\mathbf{b}) \right) \\
&= \sum_{k=0}^n \binom{n}{k} ((1+b_r)p_n^f + (1-b_r)p_n)^k (1 - (1+b_r)p_n^f - (1-b_r)p_n)^{n-k} \\
&\quad \cdot k \cdot \left( \frac{2b_r p_n^f}{(1+b_r)p_n^f + (1-b_r)p_n} \hat{y}_2^f(\mathbf{b}) + \frac{(1-b_r) \cdot (p_n^f + p_n)}{(1+b_r)p_n^f + (1-b_r)p_n} \hat{y}_2^{nf}(\mathbf{b}) \right)^{k-1} \\
&\quad \cdot \left( 1 - \frac{2b_r p_n^f}{(1+b_r)p_n^f + (1-b_r)p_n} \hat{y}_2^f(\mathbf{b}) - \frac{(1-b_r) \cdot (p_n^f + p_n)}{(1+b_r)p_n^f + (1-b_r)p_n} \hat{y}_2^{nf}(\mathbf{b}) \right) \\
&= \sum_{k=1}^n n \binom{n-1}{k-1} ((1+b_r)p_n^f + (1-b_r)p_n)^{k-1} (1 - (1+b_r)p_n^f - (1-b_r)p_n)^{n-k} \\
&\quad \cdot \left( \frac{2b_r p_n^f}{(1+b_r)p_n^f + (1-b_r)p_n} \hat{y}_2^f(\mathbf{b}) + \frac{(1-b_r) \cdot (p_n^f + p_n)}{(1+b_r)p_n^f + (1-b_r)p_n} \cdot \hat{y}_2^{nf}(\mathbf{b}) \right)^{k-1}
\end{aligned}$$

$$\begin{aligned}
& \cdot \left( (1+b_r)p_n^f + (1-b_r)p_n - 2b_r p_n^f \hat{y}_2^f(\mathbf{b}) - (1-b_r) \cdot (p_n^f + p_n) \hat{y}_2^{nf}(\mathbf{b}) \right) \\
&= \sum_{k=0}^n \binom{n-1}{k} \left( (1+b_r)p_n^f + (1-b_r)p_n \right)^k \left( 1 - (1+b_r)p_n^f - (1-b_r)p_n \right)^{n-1-k} \\
&\quad \cdot \left( \frac{2b_r p_n^f}{(1+b_r)p_n^f + (1-b_r)p_n} \hat{y}_2^f(\mathbf{b}) + \frac{(1-b_r) \cdot (p_n^f + p_n)}{(1+b_r)p_n^f + (1-b_r)p_n} \cdot \hat{y}_2^{nf}(\mathbf{b}) \right)^k \\
&\quad \cdot n \cdot \left( (1+b_r)p_n^f + (1-b_r)p_n - 2b_r p_n^f \hat{y}_2^f(\mathbf{b}) - (1-b_r) \cdot (p_n^f + p_n) \hat{y}_2^{nf}(\mathbf{b}) \right) \\
&= \sum_{k=0}^n \binom{n-1}{k} \left( 1 - (1+b_r)p_n^f - (1-b_r)p_n \right)^{n-1-k} \cdot \left( 2b_r p_n^f \hat{y}_2^f(\mathbf{b}) + (1-b_r) \cdot (p_n^f + p_n) \hat{y}_2^{nf}(\mathbf{b}) \right)^k \\
&\quad \cdot \left( (1+b_r)\alpha^f + (1-b_r)\alpha - 2b_r \alpha^f \hat{y}_2^f(\mathbf{b}) - (1-b_r) \cdot (\alpha^f + \alpha) \hat{y}_2^{nf}(\mathbf{b}) \right) \\
&= \left( 1 - (1+b_r)p_n^f - (1-b_r)p_n + 2b_r p_n^f \hat{y}_2^f(\mathbf{b}) + (1-b_r) \cdot (p_n^f + p_n) \hat{y}_2^{nf}(\mathbf{b}) \right)^{n-1} \\
&\quad \cdot \left( (1+b_r)\alpha^f + (1-b_r)\alpha - 2b_r \alpha^f \hat{y}_2^f(\mathbf{b}) - (1-b_r) \cdot (\alpha^f + \alpha) \hat{y}_2^{nf}(\mathbf{b}) \right) \\
&= \left[ 1 - \frac{2b_r \alpha^f \left( 1 - \hat{y}_2^f(\mathbf{b}) \right) - (1-b_r) \cdot (\alpha^f + \alpha) \left( 1 - \hat{y}_2^{nf}(\mathbf{b}) \right)}{n} \right]^{n-1} \\
&\quad \cdot \left( (1+b_r)\alpha^f + (1-b_r)\alpha - 2b_r \alpha^f \hat{y}_2^f(\mathbf{b}) - (1-b_r) \cdot (\alpha^f + \alpha) \hat{y}_2^{nf}(\mathbf{b}) \right) \\
&= e^{-2b_r \alpha^f \left( 1 - \hat{y}_2^f(\mathbf{b}) \right) - (1-b_r) \cdot (\alpha^f + \alpha) \left( 1 - \hat{y}_2^{nf}(\mathbf{b}) \right)} \\
&\quad \cdot \left( (1+b_r)\alpha^f + (1-b_r)\alpha - 2b_r \alpha^f \hat{y}_2^f(\mathbf{b}) - (1-b_r) \cdot (\alpha^f + \alpha) \hat{y}_2^{nf}(\mathbf{b}) \right) \text{ as } n \rightarrow \infty \\
&= y_1^f(\mathbf{b}) \left( (1+b_r)\alpha^f + (1-b_r)\alpha - b_r 2\alpha^f \hat{y}_2^f(\mathbf{b}) - (1-b_r) (\alpha^f + \alpha) \hat{y}_2^{nf}(\mathbf{b}) \right) \text{ as } n \rightarrow \infty.
\end{aligned}$$

Notice that the third equality above follows from  $k \binom{n}{k} = n \binom{n-1}{k-1}$ , the fourth equality substitutes  $k$  with  $k-1$  everywhere and starts summation from  $k=0$ , and the sixth equality is an application of the Binomial Theorem.

Thus,  $\mathbb{P}[v \text{ is a target} | v \text{ is a flexible node in } S_l]$  is given by

$$y_1^f(\mathbf{b}) + y_1^f(\mathbf{b}) \left( (1+b_r)\alpha^f + (1-b_r)\alpha - b_r 2\alpha^f \hat{y}_2^f(\mathbf{b}) - (1-b_r) (\alpha^f + \alpha) \hat{y}_2^{nf}(\mathbf{b}) \right).$$

The probabilities conditional on  $v$  being a regular node or being from  $S_r$  can be derived analogously.  $\square$

*Proof of Proposition 2* Following closely the proof of Theorem 9 in Karp and Sipser (1981), we start by showing that a random tree is a good approximation to the structure obtained by conducting a breadth-first search from  $v$ . Denote the sub-graph of  $G$  induced by vertices at most distance  $d$  from  $v$  as the  $d$ -neighborhood of  $v$ . A vertex  $v$  is referred to as a  $d$ -target if there exists a derivation proving  $v$  to be a target within the  $d$ -neighborhood of  $v$ . Note that if  $d$ -neighborhood proves that  $v$  is a target then  $v$  is a target in any other graph that yields the same  $d$ -neighborhood.

Let

$$Y_n := \mathbb{P}[v \text{ is a target in } G_n | v \text{ is a flexible node in } V_l],$$

$$Y_n^d := \mathbb{P}[v \text{ is a } d\text{-target in } G_n | v \text{ is a flexible node in } V_l],$$

$$Y^d := \mathbb{P}[v \text{ is a } d\text{-target root in } \bar{G} | v \text{ is a flexible node in } S_l].$$

Claim 5 shows that, for large  $n$ , the probability that a  $d$ -neighborhood occurs in a random graph approaches the probability of that  $d$ -neighborhood occurring in a random tree.

CLAIM 5.

$$\lim_{n \rightarrow \infty} Y_n = \lim_{n \rightarrow \infty} \lim_{d \rightarrow \infty} Y_n^d = \lim_{d \rightarrow \infty} \lim_{n \rightarrow \infty} Y_n^d = \lim_{d \rightarrow \infty} Y^d = y_2^f(\mathbf{b}).$$

That is,  $\mathbb{P}[v \text{ is a target} | v \text{ is a flexible node in } V_l] = y_2^f(\mathbf{b})$  as  $n \rightarrow \infty$ . Similarly, the probabilities for  $v$  to be a target or a loser, when  $v \in V_l$  or  $V_r$ , and when  $v$  is a flexible or regular node, follow those derived for random trees in Lemma 7.

Since all members of derivations are targets or losers or both, we next find the probability for a random edge  $(v, u)$  in  $G$  to satisfy both  $v \otimes u$  and  $u \otimes v$  i.e.,  $v$  is both a target and a loser. By Theorem 9 (3) in Karp and Sipser (1981), in  $\bar{G}$  this occurs if and only if both  $u$  and  $v$  are  $L$ -nodes. We compute this probability conditional on the types of root nodes  $v$ , and the extension from  $\bar{G}$  to  $G$  follows from Claim 5.

$$\begin{aligned} & \lim_{n \rightarrow \infty} \mathbb{P}[v \otimes u \text{ and } u \otimes v | v \text{ is a flexible node in } V_l] \\ &= \mathbb{P}[v, u \text{ are both } L\text{-nodes} | v \text{ is a flexible node in } V_l] \\ &= y_1^f(\mathbf{b}) \mathbb{P}[u \text{ is a flexible node} | (v, u) \in E] \hat{y}_1^f(\mathbf{b}) + y_1^f(\mathbf{b}) \mathbb{P}[u \text{ is a regular node} | (v, u) \in E] \hat{y}_1^{nf}(\mathbf{b}) \\ &= y_1^f(\mathbf{b}) \frac{b_r 2\alpha^f}{(1+b_r)\alpha^f + (1-b_r)\alpha} \hat{y}_1^f(\mathbf{b}) + y_1^f(\mathbf{b}) \frac{(1-b_r)(\alpha^f + \alpha)}{(1+b_r)\alpha^f + (1-b_r)\alpha} \hat{y}_1^{nf}(\mathbf{b}). \end{aligned}$$

Similarly, we find

$$\begin{aligned} & \lim_{n \rightarrow \infty} \mathbb{P}[v \otimes u \text{ and } u \otimes v | v \text{ is a regular node in } V_l] \\ &= y_1^{nf}(\mathbf{b}) \frac{b_r(\alpha^f + \alpha)}{b_r\alpha^f + (2-b_r)\alpha} \hat{y}_1^f(\mathbf{b}) + y_1^{nf}(\mathbf{b}) \frac{(1-b_r)2\alpha}{b_r\alpha^f + (2-b_r)\alpha} \hat{y}_1^{nf}(\mathbf{b}), \\ & \lim_{n \rightarrow \infty} \mathbb{P}[v \otimes u \text{ and } u \otimes v | v \text{ is a flexible node in } V_r] \\ &= \hat{y}_1^f(\mathbf{b}) \frac{b_l 2\alpha^f}{(1+b_l)\alpha^f + (1-b_l)\alpha} y_1^f(\mathbf{b}) + \hat{y}_1^f(\mathbf{b}) \frac{(1-b_l)(\alpha^f + \alpha)}{(1+b_l)\alpha^f + (1-b_l)\alpha} y_1^{nf}(\mathbf{b}), \\ & \lim_{n \rightarrow \infty} \mathbb{P}[v \otimes u \text{ and } u \otimes v | v \text{ is a regular node in } V_r] \\ &= \hat{y}_1^{nf}(\mathbf{b}) \frac{b_l(\alpha^f + \alpha)}{b_l\alpha^f + (2-b_l)\alpha} y_1^f(\mathbf{b}) + \hat{y}_1^{nf}(\mathbf{b}) \frac{(1-b_l)2\alpha}{b_l\alpha^f + (2-b_l)\alpha} y_1^{nf}(\mathbf{b}). \end{aligned}$$

Thus,

$$\begin{aligned} & \lim_{n \rightarrow \infty} \mathbb{P}[v \text{ in a derivation} | v \text{ is a flexible node in } V_l] \\ &= \lim_{n \rightarrow \infty} \mathbb{P}[v \text{ is a target} | v \text{ is a flexible node in } V_l] + \lim_{n \rightarrow \infty} \mathbb{P}[v \text{ is a loser} | v \text{ is a flexible node in } V_l] \\ &\quad - \lim_{n \rightarrow \infty} \mathbb{P}[v \otimes u \text{ and } u \otimes v | v \text{ is a regular node in } V_l] \cdot \mathbb{E}\left[\left|u \text{ s.t. } (v, u) \in E\right| \middle| v \text{ is a regular node in } V_l\right] \\ &= y_2^f(\mathbf{b}) + y_1^f(\mathbf{b}) + y_1^f(\mathbf{b}) \left( (1+b_r)\alpha^f + (1-b_r)\alpha - b_r 2\alpha^f \hat{y}_2^f(\mathbf{b}) - (1-b_r)(\alpha^f + \alpha) \hat{y}_2^{nf}(\mathbf{b}) \right) \\ &\quad - \left[ y_1^f(\mathbf{b}) \frac{b_r 2\alpha^f}{(1+b_r)\alpha^f + (1-b_r)\alpha} \hat{y}_1^f(\mathbf{b}) + y_1^f(\mathbf{b}) \frac{(1-b_r)(\alpha^f + \alpha)}{(1+b_r)\alpha^f + (1-b_r)\alpha} \hat{y}_1^{nf}(\mathbf{b}) \right] \cdot ((1+b_r)\alpha^f + (1-b_r)\alpha) \\ &= y_2^f(\mathbf{b}) + y_1^f(\mathbf{b}) + y_1^f(\mathbf{b}) [(1+b_r)\alpha^f + (1-b_r)\alpha] \cdot \\ &\quad \left[ 1 - \frac{b_r 2\alpha^f}{(1+b_r)\alpha^f + (1-b_r)\alpha} (\hat{y}_1^f(\mathbf{b}) + \hat{y}_2^f(\mathbf{b})) - \frac{(1-b_r)(\alpha^f + \alpha)}{(1+b_r)\alpha^f + (1-b_r)\alpha} (\hat{y}_1^{nf}(\mathbf{b}) + \hat{y}_2^{nf}(\mathbf{b})) \right]. \end{aligned}$$

The probabilities conditional on other types of nodes are computed similarly.  $\square$

*Proof of Claim 5* The proof of this claim follows the proof of Theorem 9 (1) in Karp and Sipser (1981). The first and last equalities in the claim arise directly from our definitions and Lemma 7. To justify the limit exchange, we sketch a proof that for every positive  $\epsilon$ , there exists a  $d$  such that for all sufficiently large  $n$ ,  $\mathbb{P}[v \text{ is a target but not a } d\text{-target}] < \epsilon$ . This implies that for all sufficiently large  $n$ ,  $n'd, d', Y_n^d$  is close to  $Y_{n'}^{d'}$  and thus we may exchange limit.

We start by computing the expected rate at which degree-1 vertices are removed during Phase 1 of the KS algorithm, following the method in Section 3.5 of Balister and Gerke (2015). Define  $n_{d_1, d_2}^f$  as the number of flexible nodes in  $V_l$  connected to  $d_1$  flexible and  $d_2$  regular nodes in  $V_r$ . Similarly, define  $n_{d_1, d_2}^{nf}$  the number of regular nodes in  $V_l$  connected to  $d_1$  flexible and  $d_2$  regular nodes in  $V_r$ . Let  $\hat{n}_{d_1, d_2}^f$  and  $\hat{n}_{d_1, d_2}^{nf}$  be the corresponding counts in  $V_r$ . We then define the fraction of nodes of each degree type as:

$$\zeta = (\zeta_{d_1, d_2}^f, \zeta_{d_1, d_2}^{nf}, \hat{\zeta}_{d_1, d_2}^f, \hat{\zeta}_{d_1, d_2}^{nf}) := \left( n_{d_1, d_2}^f/n, n_{d_1, d_2}^{nf}/n, \hat{n}_{d_1, d_2}^f/n, \hat{n}_{d_1, d_2}^{nf}/n \right).$$

As the number of flexible nodes on the right-hand side follows  $\text{Binom}(n, b_r)$ , we can apply the Chernoff bound to conclude that the number of flexible nodes on the right-hand side is  $b_r n + o(n)$  with high probability (*w.p.*  $1 - e^{-\Omega(n^{1/4})}$ ). Consider a flexible node  $v_i$  in  $V_l$ ;  $v_i$  connects to each flexible node  $v_j \in V_r$  with a probability of  $2p_n^f$ . Then, the number of flexible nodes that  $v_i$  connects to follows  $\text{Binom}(b_r n + o(n), 2p_n^f)$  with high probability. Applying the Poisson Limit Theorem, we deduce that as  $n \rightarrow \infty$ , the number of flexible nodes that  $v_i$  connects to converges in distribution to  $\text{Poisson}(b_r 2\alpha^f)$  with high probability. A similar argument can be applied to all other node types. Thus, in the initialized random graph  $G$ , for any  $d_1$  and  $d_2$ , with high probability we have:

$$\begin{aligned} \zeta_{d_1, d_2}^f &= b_l \mathbb{P} [\text{Poisson}(b_r 2\alpha^f) = d_1] \cdot \mathbb{P} [\text{Poisson}((1 - b_r)(\alpha^f + \alpha)) = d_2], \\ \zeta_{d_1, d_2}^{nf} &= (1 - b_l) \mathbb{P} [\text{Poisson}(b_r(\alpha^f + \alpha)) = d_1] \cdot \mathbb{P} [\text{Poisson}((1 - b_r)2\alpha) = d_2], \\ \hat{\zeta}_{d_1, d_2}^f &= b_r \mathbb{P} [\text{Poisson}(b_l 2\alpha^f) = d_1] \cdot \mathbb{P} [\text{Poisson}((1 - b_l)(\alpha^f + \alpha)) = d_2], \\ \hat{\zeta}_{d_1, d_2}^{nf} &= (1 - b_r) \mathbb{P} [\text{Poisson}(b_l(\alpha^f + \alpha)) = d_1] \cdot \mathbb{P} [\text{Poisson}((1 - b_l)2\alpha) = d_2]. \end{aligned} \tag{38}$$

We shall employ the differential equation method of Wormald et al. (1999). However, to directly apply this method in the form proved in Wormald et al. (1999), we shall modify the KS algorithm slightly to ensure that the differential equation method is Lipschitz: fix a  $\delta > 0$ ; at each step of the KS algorithm, if the total number of degree 1 vertices, denoted by  $N_1$ , is less than  $\delta n$  but more than 0, then with probability  $N_1/(\delta n)$  we run the original KS algorithm, and with probability  $1 - N_1/(\delta n)$  we instead pick an edge uniformly from the graph. Thus, the probability for the modified KS algorithm to next pick a flexible node from  $V_r$  that has degree 1 and connects to a flexible node in  $V_l$  is given by:

$$\eta_1^f = \frac{\zeta_{1,0}^f}{\max(\delta, \zeta_{1,0}^f, \zeta_{0,1}^f, \zeta_{1,0}^{nf}, \zeta_{0,1}^{nf}, \hat{\zeta}_{1,0}^f, \hat{\zeta}_{0,1}^f, \hat{\zeta}_{1,0}^{nf}, \hat{\zeta}_{0,1}^{nf})}.$$

Similarly, the probability to next pick a regular node from  $V_r$  that has degree 1 and connects to a regular node in  $V_l$  is given by:

$$\eta_2^f = \frac{\zeta_{0,1}^f}{\max(\delta, \zeta_{1,0}^f, \zeta_{0,1}^f, \zeta_{1,0}^{nf}, \zeta_{0,1}^{nf}, \hat{\zeta}_{1,0}^f, \hat{\zeta}_{0,1}^f, \hat{\zeta}_{1,0}^{nf}, \hat{\zeta}_{0,1}^{nf})}.$$

$\eta_1^{nf}, \eta_2^{nf}, \hat{\eta}_1^f, \hat{\eta}_2^f, \hat{\eta}_1^{nf}, \hat{\eta}_2^{nf}$  are defined analogously. Finally, the probability to next pick a random edge is given by:

$$\eta_0 = 1 - (\eta_1^f + \eta_2^f + \eta_1^{nf} + \eta_2^{nf} + \hat{\eta}_1^f + \hat{\eta}_2^f + \hat{\eta}_1^{nf} + \hat{\eta}_2^{nf}).$$

We next analyze the expected change in  $\zeta_{d_1, d_2}^f$  for  $d_1$  and  $d_2$ , denoted by  $h_{d_1, d_2}^f \in \mathbb{R}^2$ . Notice that the fraction of flexible nodes in  $v_l$  that connect to  $d_1$  flexible nodes in  $V_r$  drops if and only if (1)  $d_1 = 1$  and such a flexible node is deleted as a degree 1 node, (2) such a flexible node is connected to a deleted flexible node of degree 1 in  $V_r$ , or (3) such a flexible node is incident to the selected random edge and thus deleted. On the other hand, the fraction of such nodes increases if and only if some node that connects to  $d_1 + 1$  flexible nodes in  $V_r$  loses one edge. This happens if and only if such a flexible node is connected to a flexible node in  $V_r$  that is incident to a deleted edge. A similar argument applies to  $d_2$ . This allows us to derive

$$h_{d_1, d_2}^f(\zeta) = \left( -\mathbb{1}_{d_1=1} \eta_1^f - \hat{\eta}_1^f \frac{\zeta_{d_1, d_2}^f d_1}{\sum_{d'_1, d'_2} \zeta_{d'_1, d'_2}^f \cdot d'_1} - \eta_0 \frac{\zeta_{d_1, d_2}^f (d_1 + d_2)}{\sum_{d'_1, d'_2} (\zeta_{d'_1, d'_2}^f + \zeta_{d'_1, d'_2}^{nf}) \cdot (d'_1 + d'_2)} + \frac{\zeta_{d_1+1, d_2}^f (d_1 + 1) - \zeta_{d_1, d_2}^f d_1}{\sum_{d'_1, d'_2} \zeta_{d'_1, d'_2}^f \cdot d'_1} \right. \\ \left. \cdot \left[ \eta_1^f \frac{\sum_{d'_1, d'_2} (\hat{\zeta}_{d'_1, d'_2}^f d'_1 (d'_1 - 1))}{\sum_{d'_1, d'_2} \hat{\zeta}_{d'_1, d'_2}^f \cdot d'_1} + \eta_1^{nf} \frac{\sum_{d'_1, d'_2} (\hat{\zeta}_{d'_1, d'_2}^f d'_2 d'_1)}{\sum_{d'_1, d'_2} \hat{\zeta}_{d'_1, d'_2}^f \cdot d'_2} + \eta_0 \frac{\sum_{d'_1, d'_2} (\hat{\zeta}_{d'_1, d'_2}^f (d'_1 (d'_1 - 1) + d'_2 d'_1))}{\sum_{d'_1, d'_2} (\hat{\zeta}_{d'_1, d'_2}^f + \hat{\zeta}_{d'_1, d'_2}^{nf}) \cdot (d'_1 + d'_2)} \right], \right. \\ \left. - \mathbb{1}_{d_2=1} \eta_2^f - \hat{\eta}_1^{nf} \frac{\zeta_{d_1, d_2}^f d_2}{\sum_{d'_1, d'_2} \zeta_{d'_1, d'_2}^f \cdot d'_2} - \eta_0 \frac{\zeta_{d_1, d_2}^f (d_1 + d_2)}{\sum_{d'_1, d'_2} (\zeta_{d'_1, d'_2}^f + \zeta_{d'_1, d'_2}^{nf}) \cdot (d'_1 + d'_2)} + \frac{\zeta_{d_1, d_2+1}^f (d_2 + 1) - \zeta_{d_1, d_2}^f d_2}{\sum_{d'_1, d'_2} \zeta_{d'_1, d'_2}^f \cdot d'_2} \right. \\ \left. \cdot \left[ \eta_2^f \frac{\sum_{d'_1, d'_2} (\hat{\zeta}_{d'_1, d'_2}^{nf} d'_1 (d'_1 - 1))}{\sum_{d'_1, d'_2} \hat{\zeta}_{d'_1, d'_2}^{nf} \cdot d'_1} + \eta_2^{nf} \frac{\sum_{d'_1, d'_2} (\hat{\zeta}_{d'_1, d'_2}^{nf} d'_2 d'_1)}{\sum_{d'_1, d'_2} \hat{\zeta}_{d'_1, d'_2}^{nf} \cdot d'_2} + \eta_0 \frac{\sum_{d'_1, d'_2} (\hat{\zeta}_{d'_1, d'_2}^{nf} (d'_1 (d'_1 - 1) + d'_2 d'_1))}{\sum_{d'_1, d'_2} (\hat{\zeta}_{d'_1, d'_2}^f + \hat{\zeta}_{d'_1, d'_2}^{nf}) \cdot (d'_1 + d'_2)} \right] \right).$$

Similarly,

$$h_{d_1, d_2}^{nf}(\zeta) = \left( -\mathbb{1}_{d_1=1} \eta_1^{nf} - \hat{\eta}_2^f \frac{\zeta_{d_1, d_2}^{nf} d_1}{\sum_{d'_1, d'_2} \zeta_{d'_1, d'_2}^{nf} \cdot d'_1} - \eta_0 \frac{\zeta_{d_1, d_2}^{nf} (d_1 + d_2)}{\sum_{d'_1, d'_2} (\zeta_{d'_1, d'_2}^f + \zeta_{d'_1, d'_2}^{nf}) \cdot (d'_1 + d'_2)} + \frac{\zeta_{d_1+1, d_2}^{nf} (d_1 + 1) - \zeta_{d_1, d_2}^{nf} d_1}{\sum_{d'_1, d'_2} \zeta_{d'_1, d'_2}^{nf} \cdot d'_1} \right. \\ \left. \cdot \left[ \eta_1^f \frac{\sum_{d'_1, d'_2} (\hat{\zeta}_{d'_1, d'_2}^f d'_1 d'_2)}{\sum_{d'_1, d'_2} \hat{\zeta}_{d'_1, d'_2}^f \cdot d'_1} + \eta_1^{nf} \frac{\sum_{d'_1, d'_2} (\hat{\zeta}_{d'_1, d'_2}^f d'_2 (d'_2 - 1))}{\sum_{d'_1, d'_2} \hat{\zeta}_{d'_1, d'_2}^f \cdot d'_2} + \eta_0 \frac{\sum_{d'_1, d'_2} (\hat{\zeta}_{d'_1, d'_2}^f (d'_2 (d'_2 - 1) + d'_2 d'_1))}{\sum_{d'_1, d'_2} (\hat{\zeta}_{d'_1, d'_2}^f + \hat{\zeta}_{d'_1, d'_2}^{nf}) \cdot (d'_1 + d'_2)} \right], \right. \\ \left. - \mathbb{1}_{d_2=1} \eta_2^{nf} - \hat{\eta}_2^{nf} \frac{\zeta_{d_1, d_2}^{nf} d_2}{\sum_{d'_1, d'_2} \zeta_{d'_1, d'_2}^{nf} \cdot d'_2} - \eta_0 \frac{\zeta_{d_1, d_2}^{nf} (d_1 + d_2)}{\sum_{d'_1, d'_2} (\zeta_{d'_1, d'_2}^f + \zeta_{d'_1, d'_2}^{nf}) \cdot (d'_1 + d'_2)} + \frac{\zeta_{d_1, d_2+1}^{nf} (d_2 + 1) - \zeta_{d_1, d_2}^{nf} d_2}{\sum_{d'_1, d'_2} \zeta_{d'_1, d'_2}^{nf} \cdot d'_2} \right. \\ \left. \cdot \left[ \eta_2^f \frac{\sum_{d'_1, d'_2} (\hat{\zeta}_{d'_1, d'_2}^{nf} d'_1 d'_2)}{\sum_{d'_1, d'_2} \hat{\zeta}_{d'_1, d'_2}^{nf} \cdot d'_1} + \eta_2^{nf} \frac{\sum_{d'_1, d'_2} (\hat{\zeta}_{d'_1, d'_2}^{nf} d'_2 (d'_2 - 1))}{\sum_{d'_1, d'_2} \hat{\zeta}_{d'_1, d'_2}^{nf} \cdot d'_2} + \eta_0 \frac{\sum_{d'_1, d'_2} (\hat{\zeta}_{d'_1, d'_2}^{nf} (d'_2 (d'_2 - 1) + d'_2 d'_1))}{\sum_{d'_1, d'_2} (\hat{\zeta}_{d'_1, d'_2}^f + \hat{\zeta}_{d'_1, d'_2}^{nf}) \cdot (d'_1 + d'_2)} \right] \right).$$

The expressions for  $\hat{h}_{d_1, d_2}^f(\zeta)$  and  $\hat{h}_{d_1, d_2}^{nf}(\zeta)$  can be derived analogously. Now we can apply Theorem 5.1 of Wormald et al. (1999) and deduce that, with probability  $1 - e^{-\Omega(n^{1/4})}$ ,  $\zeta$  evolves according to the system of differential equations

$$\frac{d}{dt} \zeta_{d_1, d_2}^f(t) = h_{d_1, d_2}^f(\zeta(t)), \frac{d}{dt} \zeta_{d_1, d_2}^{nf}(t) = h_{d_1, d_2}^{nf}(\zeta(t)), \frac{d}{dt} \hat{\zeta}_{d_1, d_2}^f(t) = \hat{h}_{d_1, d_2}^f(\zeta(t)), \frac{d}{dt} \hat{\zeta}_{d_1, d_2}^{nf}(t) = \hat{h}_{d_1, d_2}^{nf}(\zeta(t)), \forall d_1, d_2, \quad (39)$$

with initial conditions provided in (38) until  $\sum_{d_1, d_2} (\zeta_{d_1, d_2}^f(t) + \zeta_{d_1, d_2}^{nf}(t)) \cdot (d_1 + d_2) < \sqrt{\delta}$ .

Now we can continue with the analyses of Phase 1 of KS algorithm. Specifically, we modify Phase 1 so that it operates in stages. In the first stage, instead of randomly choosing any degree-1 node for removal, it randomly chooses one that was present in the original graph. When there are none left, stage 1 ends and stage 2 begins. In stage  $i$ , the algorithm chooses a random degree-1 node that was created during stage  $i - 1$ . Note that this does not change the expected performance of the algorithm. Let  $T_n^i$  be the expected time of completion of stage  $i$ . By the results above we

know that the expected rate of removal of degree-1 nodes during Phase 1 is calculable from (39). Hence, there is a series of times  $T^1, T^2, \dots$  such that  $\lim_{n \rightarrow \infty} T_n^i = T^i$ . This sequence is monotonically increasing and upper bounded by  $n$ , and thus  $T^* := \lim_{i \rightarrow \infty} \lim_{n \rightarrow \infty} T_n^i$  is well-defined and is the expected completion time of Phase 1 as  $n \rightarrow \infty$ .

Given  $\epsilon$ , let time  $t_\epsilon = T^* - \epsilon$ . Since each step of the algorithm eliminates at most 2 targets, there is some  $\epsilon' < \epsilon$  such that as  $n \rightarrow \infty$ , the expected number of unmatched targets at time  $t_\epsilon \rightarrow \epsilon'n$ . Since  $t_\epsilon < T^*$  and  $\lim_{i \rightarrow \infty} T^i = T^*$ , there is a maximum  $i$  such that  $T_i \leq t_\epsilon$ . Thus, letting  $d = i + 1$ , for sufficiently large  $n$ , the expected number of unmatched targets at the end of stage  $d$  is upper bounded by  $\epsilon n$ . However, all targets matched within stage  $d$  are  $d$ -targets. Thus, the probability that a node is a target but not a  $d$ -target is upper bounded by  $\epsilon$ . This completes the proof that  $\lim_{n \rightarrow \infty} \lim_{d \rightarrow \infty} Y_n^d = \lim_{d \rightarrow \infty} \lim_{n \rightarrow \infty} Y_n^d$ .

Then, the only equality left to show is  $\lim_{d \rightarrow \infty} \lim_{n \rightarrow \infty} Y_n^d = \lim_{d \rightarrow \infty} Y^d$ . By the Poisson Limit Theorem, for any flexible node  $v \in V_l$ , the distribution of its degrees follows Poisson  $(b_r 2\alpha^f + (1 - b_r)(\alpha^f + \alpha))$  as  $n \rightarrow \infty$ . Thus, for any  $\epsilon > 0$  there is a constant  $k$  such that  $\lim_{n \rightarrow \infty} \mathbb{P}[\text{there is a node of degree } > k \text{ in the } d\text{-neighborhood of } v] < \epsilon$ . The rest of the analyses exactly follow the proof of Theorem 9 (1) in Karp and Sipser (1981).  $\square$

*Proof of Claim 2* Firstly, we calculate the derivative of  $f_1(x_1)$ :

$$\begin{aligned} f'_1(x_1) &= \frac{\partial e^{-\frac{1}{2}(\alpha^f+\alpha)x_1+2\frac{\alpha}{\alpha^f+\alpha}(\log(x_1)+\alpha^fx_1)} + 2\frac{\log(x_1)+\alpha^fx_1}{\alpha^f+\alpha}}{\partial x_1} \\ &= e^{-\frac{1}{2}(\alpha^f+\alpha)x_1+2\frac{\alpha}{\alpha^f+\alpha}(\log(x_1)+\alpha^fx_1)} \left( -\frac{1}{2}(\alpha^f+\alpha) + 2\frac{\alpha}{\alpha^f+\alpha}(\alpha^f+1/x_1) \right) + \frac{2}{\alpha^f+\alpha}(\alpha^f+1/x_1). \end{aligned}$$

We next employ a computer-aided proof to verify that  $f'_1(x_1) > 1$  for any  $x_1 \in (0, 1]$  when  $10^{-4} < \alpha < \alpha^f$  and  $\alpha^f + \alpha < e$ . Fixing  $\delta_1, \delta_2 > 0$ , we establish a lower bound on the value of  $f'_1(x_1)$  for any  $(\bar{\alpha}^f, \bar{\alpha}, \bar{x}_1)$  in the set  $[\alpha^f, \alpha^f + \delta_1] \times [\alpha, \alpha + \delta_1] \times [x_1, x_1 + \delta_2]$ , where  $10^{-4} < \alpha < \alpha^f$  and  $\alpha^f + \alpha < e$ . We find that:

$$\begin{aligned} f'_1(x_1) &\geq e^{-\frac{1}{2}(\alpha^f+\alpha)x_1+2\frac{2(\alpha^f+\delta_1)(\alpha+\delta_1)(x_1+\delta_2)}{\alpha^f+\alpha}+\frac{2\alpha\log(x_1+\delta_2)}{\alpha^f+\alpha+2\delta_1}} \left( -\frac{1}{2}(\alpha^f+\alpha+2\delta_1) \right) \\ &\quad + e^{-\frac{1}{2}(\alpha^f+\alpha+2\delta_1)(x_1+\delta_2)+2\frac{2\alpha^f\alpha x_1}{\alpha^f+\alpha+2\delta_1}+\frac{2(\alpha+\delta_1)\log(x_1)}{\alpha^f+\alpha}} \left( \frac{2\alpha\left(\alpha^f+\frac{1}{x_1+\delta_2}\right)}{\alpha^f+\alpha+2\delta_1} \right) \\ &\quad + \frac{2\left(\alpha^f+\frac{1}{x_1+\delta_2}\right)}{\alpha^f+\alpha+2\delta_1} \text{ when } x_1 > 0, \\ f'_1(x_1) &\geq e^{-\frac{1}{2}(\alpha^f+\alpha)x_1+2\frac{2(\alpha^f+\delta_1)(\alpha+\delta_1)(x_1+\delta_2)}{\alpha^f+\alpha}+\frac{2\alpha\log(x_1+\delta_2)}{\alpha^f+\alpha+2\delta_1}} \left( -\frac{1}{2}(\alpha^f+\alpha+2\delta_1) \right) \\ &\quad + \frac{2\left(\alpha^f+\frac{1}{x_1+\delta_2}\right)}{\alpha^f+\alpha+2\delta_1} \text{ when } x_1 = 0. \end{aligned} \tag{40}$$

For given  $\delta_1, \delta_2 > 0$ , if the lower bound in (40) is greater than 1, then  $f'_1(x_1) > 1$  for any  $(\bar{\alpha}^f, \bar{\alpha}, \bar{x}_1)$  in the corresponding set  $[\alpha^f, \alpha^f + \delta_1] \times [\alpha, \alpha + \delta_1] \times [x_1, x_1 + \delta_2]$ . In the computational notebook titled `Claim3.ipynb`,<sup>22</sup> we compute the value of (40) for  $x_1 = 0, \delta_2, 2\delta_2, \dots, 1$  and  $\alpha^f, \alpha = 10^{-4}, \delta_1, 2\delta_1, \dots, e$ , under the constraint  $\alpha^f + \alpha < e$ . Through this computation, we find that taking  $\delta_1 = \delta_2 = 0.01$  is sufficient for verifying (40)  $> 1$  for all  $x_1 \in (0, 1], 10^{-4} < \alpha < \alpha^f$  and  $\alpha^f + \alpha < e$ .

$\square$

<sup>22</sup>The computer-aided proof can be found at <https://bit.ly/3ShNSL3>.

## Appendix B: Proofs of the $2 \times 2$ Model

In this section we prove Theorem 1 and Theorem 5. In the  $2 \times 2$  model, the function  $\mu(b_l, b_r)$  can be expressed as an eighth-order polynomial with respect to  $b_l$ ,  $b_r$ ,  $p^f$ , and  $p$ . This closed-form solution facilitates the comparison between one-sided and balanced allocation, and the analysis of the convexity and concavity properties of  $\mu(b_l, b_r)$ .

### B.1. Proof of Theorem 1

*Proof.* In the  $2 \times 2$  model, we begin by proving the following closed-form solution for  $\mu(b_l, b_r)$ .

$$\begin{aligned} \mu(b_l, b_r) = & -p^4 \left( (4 - 3b_r)^2 + b_l^2 (9 - 10b_r + 2b_r^2) - 2b_l (12 - 16b_r + 5b_r^2) \right) \\ & - p^f \left( b_r (-2 + p^f + p^f b_r - 2(p^f)^2 b_r + (p^f)^3 b_r) \right. \\ & + b_l (-2 + p^f + 4p^f b_r + 6(p^f)^3 b_r^2 - 4(p^f)^2 b_r (1 + b_r)) \\ & \left. + p^f b_l^2 (1 - 2p^f (1 + 2b_r) + (p^f)^2 (1 + 6b_r + 2b_r^2)) \right) \\ & + 2p^3 \left( (-4 + 3b_r) (-2 + b_r + 2p^f b_r) + b_l^2 (3 - 2b_r + 2p^f (3 - 6b_r + 2b_r^2)) \right. \\ & \left. - 2b_l (5 - 5b_r + b_r^2 + 2p^f (2 - 6b_r + 3b_r^2)) \right) \\ & + 2p \left( 2 + (-1 - 3p^f + 2(p^f)^2) b_r + (p^f + (p^f)^2 - 2(p^f)^3) b_r^2 \right. \\ & + b_l \left( -1 + 4(p^f)^3 (-2 + b_r) b_r + p^f (-3 + 4b_r) + (p^f)^2 (2 + 6b_r - 6b_r^2) \right) \\ & \left. + p^f b_l^2 (1 + p^f - 6p^f b_r + (p^f)^2 (-2 + 4b_r + 4b_r^2)) \right) \\ & - p^2 \left( 8 + (-7 - 16p^f + 8(p^f)^2) b_r + (1 + 10p^f - 2(p^f)^2) b_r^2 \right. \\ & + b_l \left( -7 + 4b_r + (p^f)^2 (8 - 12b_r^2) - 4p^f (4 - 9b_r + 3b_r^2) \right) \\ & \left. + b_l^2 (1 - 2p^f (-5 + 6b_r) + 2(p^f)^2 (-1 - 6b_r + 6b_r^2)) \right). \end{aligned} \quad (41)$$

To derive the expected fraction of matched nodes, we analyze each possible realization of the number of flexible nodes in  $V_l$  and  $V_r$ , denoted by  $k_l$  and  $k_r$ , respectively.

$k_l = 0, k_r = 0$ : This scenario occurs with probability (w.p.)  $(1 - b_l)^2 (1 - b_r)^2$ . Given this realization of nodes, the resulting number of matches is zero if the graph contains no edges, which occurs w.p.  $(1 - 2p)^4$ . The number of matches is one if there is only one edge or if two edges connect to the same node, occurring w.p.  $4(1 - 2p)^3 2p + 4(1 - 2p)^2 (2p)^2$ . The number of matches is two if there are two edges that do not share common nodes or if there are more than two edges in the graph, occurring w.p.  $2(1 - 2p)^2 (2p)^2 + 4(1 - 2p)(2p)^3 + (2p)^4$ . Thus, the expected number of matched nodes conditional on  $k_l = 0, k_r = 0$  is

$$4(1 - 2p)^3 2p + 4(1 - 2p)^2 (2p)^2 + 2 [2(1 - 2p)^2 (2p)^2 + 4(1 - 2p)(2p)^3 + (2p)^4]. \quad (42)$$

$k_l = 1, k_r = 0$ : This scenario occurs w.p.  $2b_l(1 - b_l)(1 - b_r)^2 + 2b_r(1 - b_r)(1 - b_l)^2$ . Given this realization of nodes, the analyses of different edge realizations and resulting matches follow from the above. The expected number of matched nodes conditional on  $k_l = 1, k_r = 0$  is

$$\begin{aligned} & 2(p^f + p)(1 - p^f - p)(1 - p)^2 + 2(1 - p^f - p)^2 2p(1 - 2p) + ((p^f + p)(1 - 2p) + (1 - p^f - p)2p)^2 \\ & + 2 \cdot [2(p^f + p)2p(1 - p^f - p)(1 - 2p) + 2(p^f + p)^2 2p(1 - 2p) + 2(p^f + p)(1 - p^f - p)(2p)^2 + (p^f + p)^2 (2p)^2]. \end{aligned} \quad (43)$$

$k_l = 1, k_r = 1$  : This scenario occurs w.p.  $4b_l(1 - b_l)b_r(1 - b_r)$ . Given this realization of nodes, the expected number of matched nodes is

$$\begin{aligned} & (2p^f)(1 - p^f - p)^2(1 - 2p) + (1 - 2p^f)2p(1 - p^f - p)^2 + 2(p^f + p)(1 - p^f - p)(1 - 2p^f)(1 - 2p) \\ & + 2(2p^f)(p^f + p)(1 - p^f - p)(1 - 2p) + 2(2p)(p^f + p)(1 - p^f - p)(1 - 2p^f) \\ & + 2 \cdot \left( (p^f + p)^2(1 - 2p^f)(1 - 2p) + (2p^f)(2p)(1 - p^f - p)^2 + 2(2p^f)(2p)(p^f + p)(1 - p^f - p) \right. \\ & \left. + (2p^f)(p^f + p)^2(1 - 2p) + (1 - 2p^f)(p^f + p)^2(2p) + (2p^f)(p^f + p)^2(2p) \right). \end{aligned} \quad (44)$$

$k_l = 2, k_r = 0$  : This scenario occurs w.p.  $b_l^2(1 - b_r)^2 + b_r^2(1 - b_l)^2$ . Given this realization of nodes, the expected number of matched nodes is

$$\begin{aligned} & 4(1 - p^f - p)^3(p^f + p) + 4(1 - p^f - p)^2(p^f + p)^2 \\ & + 2 \cdot [2(1 - p^f - p)^2(p^f + p)^2 + 4(1 - p^f - p)(p^f + p)^3 + (p^f + p)^4]. \end{aligned} \quad (45)$$

$k_l = 2, k_r = 1$  : This scenario occurs w.p.  $2b_l^2b_r(1 - b_r) + 2b_r^2b_l(1 - b_l)$ . Given this realization of nodes, the expected number of matched nodes is

$$\begin{aligned} & 2(2p^f)(1 - p^f - p)^2(1 - 2p^f) + 2(1 - 2p^f)^2(p^f + p)(1 - p^f - p) + ((2p^f)(1 - p^f - p) + (1 - 2p^f)(p^f + p))^2 \\ & + 2 \cdot \left( 2(2p^f)(p^f + p)(1 - p^f - p)(1 - 2p^f) + 2(2p^f)^2(p^f + p)(1 - p^f - p) \right. \\ & \left. + 2(2p^f)(1 - 2p^f)(p^f + p)^2 + (2p^f)^2(p^f + p)^2 \right). \end{aligned} \quad (46)$$

$k_l = 2, k_r = 2$  : This scenario occurs w.p.  $b_l^2b_r^2$ . Given this realization of nodes, the expected number of matched nodes is

$$4(1 - 2p^f)^32p^f + 4(1 - 2p^f)^2(2p^f)^2 + 2[2(1 - 2p^f)^2(2p^f)^2 + 4(1 - 2p^f)(2p^f)^3 + (2p^f)^4]. \quad (47)$$

Multiplying equations (42) through (47) by the respective probabilities of node realizations and dividing the sum by  $n = 2$ , we obtain (41).

Given the closed-form expression for  $\mu(b_l, b_r)$  in (41), to prove Theorem 1 it suffices to compute  $\mu(B, 0) - \mu(B/2, B/2)$  and verify that the difference is strictly positive. Using Wolfram Mathematica, as documented in Theorem1.nb,<sup>23</sup> we verify that  $\mu(B, 0) - \mu(B/2, B/2) > 0$  holds true for all  $B \in (0, 1)$  and  $0 \leq p < p^f \leq 1/2$ .

□

## B.2. Proof of Theorem 5

*Proof.* For the proof of Theorem 5 (i), we calculate  $\nabla_{(0,1)}^2\mu(b_l, b_r)$ , which is equivalently expressed as  $\frac{\partial^2\mu(b_l, b_r)}{\partial b_r^2}$ . This calculation is verified in Theorem5.nb,<sup>24</sup> using Wolfram Mathematica, establishing that  $\frac{\partial^2\mu(b_l, b_r)}{\partial b_r^2} < 0$  for all  $\mathbf{b} \in (0, 1)^2$  and  $0 \leq p < p^f \leq 1/2$ . The case for  $\nabla_{(1,0)}^2\mu(b_l, b_r)$  is symmetric. Furthermore, for  $\nabla_{(1,1)}^2\mu(b_l, b_r)$ , we compute  $\frac{\partial^2\mu(b_l+h, b_r+h)}{\partial h^2}\Big|_{h=0}$  and verify that it is negative under the same conditions.

Next, to prove Theorem 5 (ii), we observe that  $\nabla_{(1,-1)}^2\mu(b_l, b_r)$  is equivalent to  $\frac{\partial^2\mu(b_l, B-b_l)}{\partial b_l^2}$ . Verification in Wolfram Mathematica, as documented in Theorem5.nb,<sup>25</sup> shows that  $\frac{\partial^2\mu(b_l, B-b_l)}{\partial b_l^2} > 0$  for all  $b_l \in (0, 1)$ ,  $B \in (b_l, b_l + 1)$  and  $0 \leq p < p^f \leq 1/2$ . This result implies that  $\nabla_{(1,-1)}^2\mu(b_l, b_r) > 0$  for all  $\mathbf{b} \in (0, 1)^2$  and  $0 \leq p < p^f \leq 1/2$ .

□

<sup>23</sup>The codes can be found at <https://bit.ly/3HHIETU>.

<sup>24</sup>The codes can be found at <https://bit.ly/48WdIvd>.

<sup>25</sup>The codes can be found at <https://bit.ly/48WdIvd>.

## Appendix C: Proofs of the Local Model

In this section we prove all results for the local model. We demonstrate that a greedy matching scheme that iteratively matches any node of degree 1 in lexicographical order is asymptotically optimal in the local model as the graph size  $n$  becomes large. This scheme allows us to recursively establish a system of equations to determine the matching probability for each node. The resulting  $\mu(b_l, b_r)$  is a rational function, with both the denominator and numerator being eighth-order polynomials in terms of  $b_l$ ,  $b_r$ ,  $p^f$ , and  $p$ . This expression facilitates the comparison between one-sided and balanced allocation, as well as the analysis of the convexity and concavity properties of  $\mu(b_l, b_r)$  along specific diagonals where analyses of directional second-order derivatives are tractable.

### C.1. Proof of Theorem 2

*Proof.* We begin by characterizing the asymptotic fraction of nodes that are matched in the local model. Let  $E$  denote the set of all edges. We propose Algorithm 3 to construct a matching  $M$ , which we argue asymptotically yields a maximum matching.

---

#### Algorithm 3 Maximum Matching Construction in Local Model

---

```

1: Initialize the matching set  $M \leftarrow \emptyset$ 
2: if  $(v_1^l, v_1^r) \in E$  then
3:   Add  $(v_1^l, v_1^r)$  to  $M$ 
4: for each subsequent node  $v_i^r$  with  $i > 1$  do
5:   if  $(v_{i-1}^l, v_i^r) \in E$  and  $v_{i-1}^l$  is not already matched in  $M$  then
6:     Add  $(v_{i-1}^l, v_i^r)$  to  $M$ 
7:   else if  $(v_i^l, v_i^r) \in E$  then
8:     Add  $(v_i^l, v_i^r)$  to  $M$ 
9: return  $M$ 

```

---

To prove the asymptotic optimality of this algorithm, observe that each node  $v_i^l$  in  $V_l$  can only connect to its two neighbors in  $V_r$ . If  $(v_i^l, v_i^r) \notin E$  and  $(v_i^l, v_{i+1}^r) \in E$ , there exists a maximum matching containing  $(v_i^l, v_{i+1}^r)$ . This is because node  $v_i^l$  cannot be matched otherwise, and not using  $(v_i^l, v_{i+1}^r)$  in the matching would at most save  $v_{i+1}^r$  for one additional matching. Hence, this algorithm is provably optimal for all nodes except  $v_1^r$ , which is myopically matched to  $v_1^l$  if an edge exists. As we are interested in computing  $\mu(b_l, b_r) = \lim_{n \rightarrow \infty} \mathbb{E} \left[ \frac{\mathcal{M}_n(b_l, b_r)}{n} \right]$ , the resulting error in  $\mu(b_l, b_r)$  approaches 0 in the asymptotic setting where  $n \rightarrow \infty$ .

Therefore, to find  $\mu(b_l, b_r)$  it is sufficient to compute the asymptotic fraction of nodes matched through this algorithm. Notably, in this algorithm, whether a node  $v_i^r \in V_r$  is matched to  $v_{i-1}^l \in V_l$  depends only on edges incident to  $v_{i-1}^l$  and is independent of  $v_i^l$ . We show that there exist the following stationary probabilities as  $n \rightarrow \infty$ :

$$x^f := \mathbb{P} \left[ (v_{i-1}^l, v_i^r) \in M \mid v_i^r \text{ is flex} \right] = \mathbb{P} \left[ (v_i^l, v_{i+1}^r) \in M \mid v_{i+1}^r \text{ is flex} \right],$$

$$x^n := \mathbb{P} \left[ (v_{i-1}^l, v_i^r) \in M \mid v_i^r \text{ is non-flex} \right] = \mathbb{P} \left[ (v_i^l, v_{i+1}^r) \in M \mid v_{i+1}^r \text{ is non-flex} \right].$$

We derive a system of recursion equations that the local model must satisfy to solve for stationary  $x^f$  and  $x^n$ . Assume that  $v_i^l$  and  $v_i^r$  are both flexible nodes. A flexible node  $v_{i+1}^r$  will only be matched with  $v_i^l$  if (1)  $(v_{i-1}^l, v_i^r) \in M$  and  $(v_i^l, v_{i+1}^r) \in E$ , which occurs with probability  $x^f 2p^f$ , or (2)  $(v_i^l, v_i^r) \notin E$  and  $(v_i^l, v_{i+1}^r) \in E$ , which occurs with probability  $(1 - x^f)(1 - p^f - p)(p^f + p)$ . Thus, conditional on  $v_i^l$ ,  $v_i^r$ , and  $v_{i+1}^r$  all being flexible nodes,  $(v_i^l, v_{i+1}^r) \in M$  with probability

$$x^f 2p^f + (1 - x^f)(1 - 2p^f)2p^f.$$

Similar probabilities can be computed conditionally on other node types, yielding:

$$\begin{aligned} x^f &= b_l b_r [x^f 2p^f + (1 - x^f)(1 - 2p^f)2p^f] + (1 - b_l) b_r [x^f (p^f + p) + (1 - x^f)(1 - p^f - p)(p^f + p)] \\ &\quad + b_l (1 - b_r) [x^n 2p^f + (1 - x^n)(1 - p^f - p)2p^f] + (1 - b_l)(1 - b_r) [x^n (p^f + p) + (1 - x^n)(1 - 2p)(p^f + p)]. \\ x^n &= b_l b_r [x^f (p^f + p) + (1 - x^f)(1 - 2p^f)(p^f + p)] + (1 - b_l) b_r [x^f 2p + (1 - x^f)(1 - p^f - p)2p] \\ &\quad + b_l (1 - b_r) [x^n (p^f + p) + (1 - x^n)(1 - p^f - p)(p^f + p)] + (1 - b_l)(1 - b_r) [x^n 2p + (1 - x^n)(1 - 2p)2p]. \end{aligned} \quad (48)$$

The asymptotic fraction of matched nodes is equal to the probability that a random node  $v_i^r \in V_r$  is matched. If  $v_i^r$  is a flexible node, it is matched with  $v_{i-1}^l$  with probability  $x^f$  and matched with  $v_i^l$  with probability  $(1 - x^f)[(1 + b_l)p^f + (1 - b_l)p]$ . If it is a regular node, it is matched with  $v_{i-1}^l$  with probability  $x^n$  and matched with  $v_i^l$  with probability  $(1 - x^n)[b_l p^f + (2 - b_l)p]$ . Thus,

$$\begin{aligned} \mu(b_l, b_r) &= b_r x^f + b_r (1 - x^f) [(1 + b_l)p^f + (1 - b_l)p] \\ &\quad + (1 - b_r)x^n + (1 - b_r)(1 - x^n) [b_l p^f + (2 - b_l)p]. \end{aligned} \quad (49)$$

Solving  $x^f$  and  $x^n$  from (48) and plugging into (49), we obtain

$$\begin{aligned} \mu(b_l, b_r) &= \left( 2(b_l + b_r)^2 p^4 b_l^2 - 2(b_l + b_r)^2 p^4 b_l - 8(b_l + b_r)^2 p^3 p^f b_l^2 + 8(b_l + b_r)^2 p^3 p^f b_l + 12(b_l + b_r)^2 p^2 (p^f)^2 b_l^2 \right. \\ &\quad - 12(b_l + b_r)^2 p^2 (p^f)^2 b_l - (b_l + b_r)^2 p^2 - 8(b_l + b_r)^2 p (p^f)^3 b_l^2 + 8(b_l + b_r)^2 p (p^f)^3 b_l + 2(b_l + b_r)^2 p p^f \\ &\quad + 2(b_l + b_r)^2 (p^f)^4 b_l^2 - 2(b_l + b_r)^2 (p^f)^4 b_l - (b_l + b_r)^2 (p^f)^2 - 4(b_l + b_r)p^4 b_l^3 + 2(b_l + b_r)p^4 b_l^2 \\ &\quad + 2(b_l + b_r)p^4 b_l + 16(b_l + b_r)p^3 p^f b_l^3 - 8(b_l + b_r)p^3 p^f b_l^2 - 8(b_l + b_r)p^3 p^f b_l - 24(b_l + b_r)p^2 (p^f)^2 b_l^3 \\ &\quad + 12(b_l + b_r)p^2 (p^f)^2 b_l^2 + 12(b_l + b_r)p^2 (p^f)^2 b_l - 2(b_l + b_r)p^2 b_l + 7(b_l + b_r)p^2 + 16(b_l + b_r)p (p^f)^3 b_l^3 \\ &\quad - 8(b_l + b_r)p (p^f)^3 b_l^2 - 8(b_l + b_r)p (p^f)^3 b_l + 4(b_l + b_r)p p^f b_l - 6(b_l + b_r)p p^f - 2(b_l + b_r)p \\ &\quad - 4(b_l + b_r)(p^f)^4 b_l^3 + 2(b_l + b_r)(p^f)^4 b_l^2 + 2(b_l + b_r)(p^f)^4 b_l - 2(b_l + b_r)(p^f)^2 b_l - (b_l + b_r)(p^f)^2 \\ &\quad + 2(b_l + b_r)p^f + 2p^4 b_l^4 - 2p^4 b_l^2 - 8p^3 p^f b_l^4 + 8p^3 p^f b_l^2 + 12p^2 (p^f)^2 b_l^4 - 12p^2 (p^f)^2 b_l^2 \\ &\quad \left. + 2p^2 b_l^2 - 8p^2 - 8p (p^f)^3 b_l^4 + 8p (p^f)^3 b_l^2 - 4p p^f b_l^2 + 4p + 2 (p^f)^4 b_l^4 - 2 (p^f)^4 b_l^2 + 2 (p^f)^2 b_l^2 \right) / \\ &\quad \left( (b_l + b_r)^2 p^4 b_l^2 - (b_l + b_r)^2 p^4 b_l - 4(b_l + b_r)^2 p^3 p^f b_l^2 + 4(b_l + b_r)^2 p^3 p^f b_l + 6(b_l + b_r)^2 p^2 (p^f)^2 b_l^2 \right. \\ &\quad - 6(b_l + b_r)^2 p^2 (p^f)^2 b_l - 4(b_l + b_r)^2 p (p^f)^3 b_l^2 + 4(b_l + b_r)^2 p (p^f)^3 b_l + (b_l + b_r)^2 (p^f)^4 b_l^2 \\ &\quad - (b_l + b_r)^2 (p^f)^4 b_l - 2(b_l + b_r)p^4 b_l^3 + (b_l + b_r)p^4 b_l^2 + (b_l + b_r)p^4 b_l + 8(b_l + b_r)p^3 p^f b_l^3 - 4(b_l + b_r)p^3 p^f b_l^2 \\ &\quad \left. - 4(b_l + b_r)p^3 p^f b_l - 12(b_l + b_r)p^2 (p^f)^2 b_l^3 + 6(b_l + b_r)p^2 (p^f)^2 b_l^2 + 6(b_l + b_r)p^2 (p^f)^2 b_l - 2(b_l + b_r)p^2 b_l \right) \end{aligned}$$

$$\begin{aligned}
& + 3(b_l + b_r)p^2 + 8(b_l + b_r)p(p^f)^3 b_l^3 - 4(b_l + b_r)p(p^f)^3 b_l^2 - 4(b_l + b_r)p(p^f)^3 b_l + 4(b_l + b_r)pp^f b_l \\
& - 2(b_l + b_r)pp^f - 2(b_l + b_r)(p^f)^4 b_l^3 + (b_l + b_r)(p^f)^4 b_l^2 + (b_l + b_r)(p^f)^4 b_l - 2(b_l + b_r)(p^f)^2 b_l \\
& - (b_l + b_r)(p^f)^2 + p^4 b_l^4 - p^4 b_l^2 - 4p^3 p^f b_l^4 + 4p^3 p^f b_l^2 + 6p^2 (p^f)^2 b_l^4 - 6p^2 (p^f)^2 b_l^2 + 2p^2 b_l^2 - 4p^2 \\
& - 4p(p^f)^3 b_l^4 + 4p(p^f)^3 b_l^2 - 4pp^f b_l^2 + (p^f)^4 b_l^4 - (p^f)^4 b_l^2 + 2(p^f)^2 b_l^2 + 1 \Big). \tag{50}
\end{aligned}$$

Given the closed-form expression for  $\mu(b_l, b_r)$  in (50), to prove Theorem 6 (i) it suffices to compute  $\mu(B, 0) - \mu(B/2, B/2)$  and verify that the difference is strictly positive. Using Wolfram Mathematica in Theorem2.nb,<sup>26</sup> we verify that  $\mu(B, 0) - \mu(B/2, B/2) > 0$  for all  $B \in (0, 1)$  and  $0 \leq p < p^f \leq 1/2$ .  $\square$

## C.2. Proof of Theorem 6

*Proof.* For the concavity result, we evaluate  $\nabla_{(0,1)}^2 \mu(b_l, b_r)$  with  $b_l = 1/2$ , which is equivalent to  $\frac{\partial^2 \mu(1/2, b_r)}{\partial b_r^2}$ . In Theorem6.nb,<sup>27</sup> we again use Wolfram Mathematica to verify that  $\frac{\partial^2 \mu(1/2, b_r)}{\partial b_r^2} < 0$  for all  $b_r \in (0, 1)$  and  $0 \leq p < p^f \leq 1/2$ . The case for the direction  $(1, 0)$  is symmetric. The proof for  $\frac{\partial^2 \mu(0, b_r)}{\partial b_r^2} < 0$  for all  $b_r \in (0, 1)$  and  $0 \leq p < p^f \leq 1/2$  follows from the same analyses by taking  $b_l = 0$ .

To prove the convexity result, we set  $b_r = 1 - b_l$  to simplify (50) to

$$\mu(b_l, 1 - b_l) = 2 \frac{(p^f)^2 b_l^2 - (p^f)^2 b_l - 2p^f p b_l^2 + 2p^f p b_l + p^f + p^2 b_l^2 - p^2 b_l + p}{(p^f)^2 b_l^2 - (p^f)^2 b_l - 2p^f p b_l^2 + 2p^f p b_l + p^f + p^2 b_l^2 - p^2 b_l + p + 1}.$$

Taking the second-order derivative with respect to  $b_l$ , we obtain

$$\frac{\partial^2 \mu(b_l, 1 - b_l)}{\partial b_l^2} = \frac{4(p^f - p)^2 \underbrace{\left[ -(p^f)^2 - 3b_l^2 (p^f - p)^2 + 3b_l (p^f - p)^2 + 2p^f p + p^f - p^2 + p + 1 \right]}_{(I)}}{\underbrace{\left( b_l^2 (p^f - p)^2 - b_l (p^f - p)^2 + p^f + p + 1 \right)}_{II}^3}.$$

We demonstrate that both (I) and (II) are strictly positive for all  $b_l \in (0, 1)$  and  $0 \leq p < p^f \leq 1/2$ , ensuring  $\frac{\partial^2 \mu(b_l, 1 - b_l)}{\partial b_l^2} > 0$ .

For (I) we have

$$\begin{aligned}
(I) &= 3b_l(1 - b_l)(p^f - p)^2 - (p^f - p)^2 + p^f + p + 1 \\
&= (3b_l - 3b_l^2 - 1)(p^f - p)^2 + p^f + p + 1 \\
&\geq -(p^f - p)^2 + p^f + p + 1 \geq -1 + p^f + p + 1 > 0.
\end{aligned}$$

For (II) we have

$$(II) = b_l(b_l - 1)(p^f - p)^2 + p^f + p + 1 \geq -0.25 + (p^f)^2 + p + 1 > 0.$$

Since  $\nabla_{(1,-1)}^2 \mu(b_l, b_r)$  with  $b_l + b_r = 1$  is given by  $\frac{\partial^2 \mu(b_l, 1 - b_l)}{\partial b_l^2} > 0$ , we conclude the proof.  $\square$

<sup>26</sup>The codes can be found at <https://bit.ly/4bkvD03>.

<sup>27</sup>The codes can be found at <https://bit.ly/3vY8Bw1>.

## Appendix D: Implications of the Structural Properties

The convexity and concavity results exhibited in Section 3 imply that, in a wide range of settings, balanced allocation emerges as a sub-optimal (local) Nash Equilibrium (NE) and a saddle point. We start by providing the textbook definition of NE and local NE for a general function  $g(b_l, b_r)$  in Definition 6-7 and also the definition of a saddle point in Definition 8. We then verify these conditions in the contexts of  $g^{2 \times 2}(b_l, b_r)$ ,  $g^{loc}(b_l, b_r)$  and  $g^{glb}(b_l, b_r)$ .

**DEFINITION 6 (GAME  $\Gamma$ ).** A game  $\Gamma$  is defined by:

1. The set of players  $\{1, 2\}$ ;
2. For each player  $i \in \{1, 2\}$ ,  $\mathcal{B}_i \subseteq \mathbb{R}$  is the set of strategies available to player  $i$ ;
3.  $g : \mathcal{B}_l \times \mathcal{B}_r \rightarrow \mathbb{R}$  is the payoff function, with  $g(b_l, b_r)$  representing the payoff to a player for the strategy profile  $\mathbf{b} = (b_l, b_r) \in \mathcal{B}_1 \times \mathcal{B}_2 \subseteq \mathbb{R}^2$ .

**DEFINITION 7 (NASH EQUILIBRIUM).** In a game  $\Gamma$  where the function  $g(b_l, b_r)$  has its domain  $\mathcal{B} = \mathcal{B}_1 \times \mathcal{B}_2 \subseteq \mathbb{R}^2$ ,

- (i) A point  $\mathbf{b}'$  is a *Nash Equilibrium (NE)* if

$$g(b'_l, b'_r) \geq g(b_l, b'_r), \forall b_l \in \mathcal{B}_1 \text{ and } g(b'_l, b'_r) \geq g(b'_l, b_r), \forall b_r \in \mathcal{B}_2.$$

- (ii) A point  $\mathbf{b}'$  is a *local Nash Equilibrium* if there exists some  $\delta > 0$  such that

$$g(b'_l, b'_r) \geq g(b_l, b'_r), \forall b_l \in \mathcal{B}_1 \cap (b_l - \delta, b_l + \delta), \text{ and}$$

$$g(b'_l, b'_r) \geq g(b'_l, b_r), \forall b_r \in \mathcal{B}_2 \cap (b_r - \delta, b_r + \delta).$$

- (iii) A point  $\mathbf{b}'$  is a *sub-optimal (local) Nash Equilibrium* if  $\mathbf{b}'$  is an (local) NE but there exists another point  $\mathbf{b}^*$  for which  $g(b_l^*, b_r^*) > g(b'_l, b'_r)$ .

**DEFINITION 8 (SADDLE POINT).** For function  $g(b_l, b_r)$  with its domain  $\mathcal{B} = \mathcal{B}_1 \times \mathcal{B}_2 \subseteq \mathbb{R}^2$ , assume that its first and second directional derivatives exist in all directions at  $\mathbf{b}' \in \mathcal{B}$ . Then,  $\mathbf{b}'$  is said to be a saddle point of the function  $g$  if the following conditions are satisfied:

- (i) The gradient  $\nabla g(\mathbf{b}') = \mathbf{0}$ ;
- (ii) The second directional derivatives  $\nabla_{\mathbf{v}}^2 g(\mathbf{b}') < 0$  and  $\nabla_{\mathbf{u}}^2 g(\mathbf{b}') > 0$  in some directions  $\mathbf{v}$  and  $\mathbf{u} \in \mathbb{R}^2$ .

To identify sub-optimal (local) NE in the models we leverage the results that  $g(b_l, b_r)$  is concave in the directions  $(0, 1)$  and  $(1, 0)$ , and convex in the directions  $(-1, 1)$  and  $(1, -1)$ . Because the directional derivative at an NE is zero along all directions, having both concavity and convexity effectively means that the NE is also a saddle point. We formalize these conditions in Lemma 8 and Lemma 9.

**DEFINITION 9 (INTERIOR OF A SET).** Let  $(\mathcal{B}, \tau)$  be a topological space. Then

- (i) A point  $\mathbf{b} \in \mathcal{B}$  is an *interior point* of the set  $\mathcal{B}$  if there exists an open set  $U$  with  $\mathbf{b} \in U \subseteq \mathcal{B}$ .
- (ii) The *interior* of  $\mathcal{B}$ , denoted by  $\text{int}(\mathcal{B})$ , consists of all its interior points.

**LEMMA 8 (Sub-Optimal NE and Saddle Point).** In a game  $\Gamma$  where the function  $g(b_l, b_r)$  has its domain  $\mathcal{B} \subseteq \mathbb{R}^2$ , assume that its first and second directional derivatives exist in all directions for any  $\mathbf{b} \in \text{int}(\mathcal{B})$ . Then, for any NE  $\mathbf{b}' \in \text{int}(\mathcal{B})$  satisfying the following conditions:

- (i)  $g(b_l, b_r)$  is strictly concave in the direction  $(0, 1)$  at any  $\mathbf{b} \in \text{int}(\mathcal{B})$  such that  $b_l = b'_l$ ;

- (ii)  $g(b_l, b_r)$  is strictly concave in the direction  $(1, 0)$  at any  $\mathbf{b} \in \text{int}(\mathcal{B})$  such that  $b_r = b'_r$ ;
- (iii)  $g(b_l, b_r)$  is strictly convex in the direction  $(1, -1)$  for any  $\mathbf{b} \in \text{int}(\mathcal{B})$  such that  $b_l + b_r = b'_l + b'_r$ ,  $\mathbf{b}'$  is a sub-optimal NE and a saddle point.

**LEMMA 9 (Sub-Optimal Local NE and Saddle Point).** *In a game  $\Gamma$  where the function  $g(b_l, b_r)$  has its domain  $\mathcal{B} \subseteq \mathbb{R}^2$ , assume that its first and second directional derivatives exist in all directions at  $\mathbf{b}' \in \text{int}(\mathcal{B})$ . Then, under the following conditions:*

- (i)  $g(b_l, b_r)$  is strictly concave in the directions  $(0, 1)$  and  $(1, 0)$  at  $\mathbf{b}'$ ;
- (ii)  $g(b_l, b_r)$  is strictly convex in the direction  $(1, -1)$  at  $\mathbf{b}'$ ;
- (iii) The gradient of  $g(b_l, b_r)$  is the zero vector at  $\mathbf{b}'$ ,  $\mathbf{b}'$  is a sub-optimal local NE and a saddle point.

Then we demonstrate that the balanced allocation is indeed a sub-optimal NE and a saddle point for a range of graph models examined in this paper.

**PROPOSITION 3.** *In the  $2 \times 2$  model, for any  $c \in \left( \frac{\partial \mu(B/2, B/2)}{\partial B} \Big|_{B=2}, \frac{\partial \mu(B/2, B/2)}{\partial B} \Big|_{B=0} \right)$ , there exists a  $B' \in (0, 2)$  such that  $\mathbf{b}' = (B'/2, B'/2)$  is a sub-optimal NE and a saddle point for  $g(b_l, b_r)$ .*

**PROPOSITION 4.** *In the local model, there exists  $c > 0$  such that  $\mathbf{b}' = (1/2, 1/2)$  is a sub-optimal NE and a saddle point for  $g(b_l, b_r)$ .*

**PROPOSITION 5.** *In the global model, assume that  $10^{-4} < \alpha < 0.64\alpha^f - 0.03$  and  $0.62\alpha^f + \alpha < 1.68$ . Then, there exists  $c > 0$  such that  $\mathbf{b}' = (1/2, 1/2)$  is a sub-optimal local NE and a saddle point for  $\bar{g}(b_l, b_r) := \mu^{KS}(b_l, b_r) - \Gamma(b_l, b_r)$ .*

### D.1. Proofs for Nash Equilibrium and Saddle Point

*Proof of Lemma 8* Let  $\mathbf{b}'$  be a Nash Equilibrium (NE) in  $\text{int}(\mathcal{B})$  for the function  $g(b_l, b_r)$  with domain  $\mathcal{B} \subseteq \mathbb{R}^2$ . We start by showing that  $g(b_l, b_r)$  has a gradient of  $\mathbf{0}$  at  $\mathbf{b}'$ . If  $\nabla_{(0,1)}g(\mathbf{b}') > 0$ , then there exists  $\epsilon > 0$  such that  $g(b'_l, b'_r + \epsilon) > g(b'_l, b'_r)$ , contradicting the definition of NE. Similarly, if  $\nabla_{(0,1)}g(\mathbf{b}') < 0$ , then there exists  $\epsilon > 0$  such that  $g(b'_l, b'_r - \epsilon) > g(b'_l, b'_r)$ , again contradicting the definition of NE. Thus,  $\nabla_{(0,1)}g(\mathbf{b}') = \mathbf{0}$ . Applying a similar argument to the direction of  $(1, 0)$  we find that  $\nabla_{(1,0)}g(\mathbf{b}') = \mathbf{0}$ . Since  $g(b_l, b_r)$  has a directional derivative of 0 in two orthogonal directions at  $\mathbf{b}'$ , it has a gradient of  $\mathbf{0}$  at  $\mathbf{b}'$ . Since we also know that  $\nabla_{(0,1)}^2g(\mathbf{b}') < 0$  and  $\nabla_{(1,-1)}^2g(\mathbf{b}') > 0$ ,  $\mathbf{b}'$  is a saddle point.

We then show that  $\mathbf{b}'$  is a sub-optimal NE. Since  $g(b_l, b_r)$  is strictly convex in the direction of  $(1, -1)$  at any  $\mathbf{b}$  such that  $b_l + b_r = b'_l + b'_r$  and  $g(b_l, b_r)$  has a gradient of  $\mathbf{0}$  at  $\mathbf{b}'$ ,  $\mathbf{b}'$  is a global minimum in the direction of  $(1, -1)$ . That is, there exists  $\epsilon > 0$  such that  $g(b'_l + \epsilon, b'_r - \epsilon) > g(b'_l, b'_r)$ . Thus,  $g(b_l, b_r)$  is a sub-optimal NE.  $\square$

*Proof of Lemma 9* Since  $g(b_l, b_r)$  is strictly concave in the direction of  $(0, 1)$  and  $(1, 0)$  but also strictly convex in the direction of  $(1, -1)$  at  $\mathbf{b}'$ ,  $\mathbf{b}'$  is neither a local maximum nor a local minimum. Combined with the condition that  $g(b_l, b_r)$  has a gradient of  $\mathbf{0}$  at  $\mathbf{b}'$ , we conclude that  $\mathbf{b}'$  is a saddle point.

Now, since  $\nabla_{(0,1)}g(\mathbf{b}') = 0$  and  $\nabla_{(0,1)}^2g(b_l, b_r) < 0$ , we know that  $\mathbf{b}'$  is a local maximum in the direction of  $(0, 1)$  and we can find  $\epsilon_1 > 0$  such that

$$g(b'_l, b'_r) \geq g(b'_l, b_r), \forall b_r \in b_r \cap (b_r - \epsilon_1, b_r + \epsilon_1).$$

Similarly, from  $\nabla_{(1,0)}g(\mathbf{b}') = 0$  and  $\nabla_{(1,0)}^2g(b_l, b_r) < 0$  we find  $\epsilon_2 > 0$  such that

$$g(b'_l, b'_r) \geq g(b_l, b'_r), \forall b_l \in b_l \cap (b_l - \epsilon_2, b_l + \epsilon_2).$$

Taking  $\delta = \min(\epsilon_1, \epsilon_2)$ , we find that  $\mathbf{b}'$  is a local NE.

We then show that  $\mathbf{b}'$  is a sub-optimal local NE. Since  $\nabla_{(1,-1)}g(\mathbf{b}') = 0$  and  $\nabla_{(1,-1)}^2g(b_l, b_r) > 0$ ,  $\mathbf{b}'$  is a local minimum in the direction of  $(1, -1)$ . That is, there exists  $\epsilon > 0$  such that  $g(b'_l + \epsilon, b'_r - \epsilon) > g(b'_l, b'_r)$ . Thus,  $g(b_l, b_r)$  is a sub-optimal local NE.  $\square$

*Proof of Proposition 3* In Theorem 5, we have verified the local convexity of  $\mu(b_l, b_r)$  in the direction  $(1, -1)$  and local concavity in the directions  $(0, 1)$  and  $(1, 0)$  for any  $\mathbf{b} \in (0, 1)^2$ . Consequently,  $g(b_l, b_r)$  exhibits the same local convexity and concavity properties. Given that both conditions in Lemma 8 are satisfied, it suffices to demonstrate that for any  $c \in \left( \frac{\partial \mu(B/2, B/2)}{\partial B} \Big|_{B=2}, \frac{\partial \mu(B/2, B/2)}{\partial B} \Big|_{B=0} \right)$ , there exists a  $B' \in (0, 2)$  such that  $\mathbf{b}' = (B'/2, B'/2)$  is an NE.

By concavity of  $\mu(b_l, b_r)$  in the direction  $(1, 1)$  we know that  $\frac{\partial \mu(B/2, B/2)}{\partial B}$  is monotonically decreasing with respect to  $B$  and the interval  $\left( \frac{\partial \mu(B/2, B/2)}{\partial B} \Big|_{B=2}, \frac{\partial \mu(B/2, B/2)}{\partial B} \Big|_{B=0} \right)$  is non-empty. Thus, for any  $c$  in the interval, by continuity of the directional derivative we know that  $c = \frac{\partial \mu(B/2, B/2)}{\partial B} \Big|_{B=B'} = \nabla_{(1/2, 1/2)}\mu(b_l, b_r) \Big|_{\mathbf{b}=(B'/2, B'/2)}$  at some  $B' \in (0, 2)$ .

Thus, we have

$$\nabla_{(1/2, 1/2)}g(b_l, b_r) \Big|_{\mathbf{b}=(B'/2, B'/2)} = \nabla_{(1/2, 1/2)}\mu(b_l, b_r) \Big|_{\mathbf{b}=(B'/2, B'/2)} - c = 0.$$

Given that  $\nabla_{(1,-1)}^2g(b_l, b_r) \Big|_{\mathbf{b}=(B'/2, B'/2)} > 0$  and by the symmetry  $g(b_l, b_r) = \bar{g}(b_r, b_l), \forall (b_l, b_r) \in (0, 1)^2$ ,  $\nabla_{(1,-1)}g(b_l, b_r)$  is well-defined at  $(B'/2, B'/2)$ . If the directional derivative is strictly positive, there exists  $\epsilon > 0$  such that  $g(B'/2 + \epsilon, B'/2 - \epsilon) > g(B'/2 - \epsilon, B'/2 + \epsilon)$ , which contradicts the symmetry condition. By the same argument the directional derivative cannot be strictly negative, leading to  $\nabla_{(1,-1)}g(b_l, b_r) = 0$  at  $(B'/2, B'/2)$ . Since at  $\mathbf{b}' = (B'/2, B'/2)$  the derivative of  $g(b_l, b_r)$  is equal to 0 in two independent directions, the gradient of  $g(b_l, b_r)$  is  $\mathbf{0}$  at  $\mathbf{b}' = (B'/2, B'/2)$ .

Combined with the result that  $g(b_l, b_r)$  is strictly concave in the direction  $(1, 0)$  when  $b_r = B'/2$ , we conclude that the point  $\mathbf{b}' = (B'/2, B'/2)$  is a global maximum in this direction. That is,

$$g(B'/2, B'/2) \geq g(b_l, B'/2), \forall b_l \in (0, 1).$$

By symmetry, the same result holds in the direction  $(0, 1)$ . Thus, by Definition 7 (i), we establish that for the given  $c$ , the point  $\mathbf{b}' = (B'/2, B'/2)$  is an NE. This completes the proof.  $\square$

*Proof of Proposition 4* As established in Theorem 6, we have verified the local convexity of  $\mu(b_l, b_r)$  in the direction  $(1, -1)$  and local concavity in the directions  $(0, 1)$  and  $(1, 0)$  along diagonals that intersect at  $\mathbf{b}' = (1/2, 1/2)$ . Consequently, the function  $g(b_l, b_r)$  exhibits the same local convexity and concavity properties. According to Lemma 8, to demonstrate the existence of a constant  $c > 0$  such that  $\mathbf{b}' = (1/2, 1/2)$  is a sub-optimal Nash Equilibrium (NE) for  $\bar{g}(b_l, b_r)$ , it is sufficient to show that  $(1/2, 1/2)$  is indeed an NE.

We construct  $c = \nabla_{(1,0)}\mu(b_l, b_r) = \left. \frac{\partial\mu(b_l, 1/2)}{\partial b_l} \right|_{b_l=1/2}$ . Then, we have

$$\nabla_{(1,0)}g(b_l, b_r) = \nabla_{(1,0)}\mu(b_l, b_r) - c = 0.$$

Since  $g(b_l, b_r)$  is strictly concave in the direction of  $(1, 0)$  when  $b_r = 1/2$ ,  $\mathbf{b}' = (1/2, 1/2)$  is a global maximum in the direction  $(1, 0)$ . That is,

$$g(1/2, 1/2) \geq g(b_l, 1/2), \forall b_l \in (0, 1).$$

By symmetry, the same result holds in the direction  $(0, 1)$ . Thus, according to Definition 7 (i), we conclude that the point  $\mathbf{b}' = (1/2, 1/2)$  is indeed an NE for the selected constant  $c$ . This completes the proof.  $\square$

*Proof of Proposition 5* Given that Theorem 7 has established the local convexity of  $\mu^{\text{KS}}(b_l, b_r)$  in the direction  $(1, -1)$  and its local concavity in the directions  $(0, 1)$  and  $(1, 0)$  within the specified region of  $\alpha^f$  and  $\alpha$ , the same local convexity and concavity properties hold for  $\bar{g}(b_l, b_r) := \mu^{\text{KS}}(b_l, b_r) - \Gamma(b_l, b_r)$ . By Lemma 9, to show that there exists  $c > 0$  such that  $\mathbf{b}' = (1/2, 1/2)$  is a sub-optimal local NE for  $\bar{g}(b_l, b_r)$ , it suffices to show that there exists  $c > 0$  such that the gradient of  $\bar{g}(b_l, b_r)$  is the zero vector at  $\mathbf{b} = (1/2, 1/2)$ .

Since  $\nabla_{(1,-1)}^2 \bar{g}(b_l, b_r) > 0$  at  $(1/2, 1/2)$  and by symmetry we have  $\bar{g}(b_l, b_r) = \bar{g}(b_r, b_l), \forall (b_l, b_r) \in (0, 1)^2$ ,  $\nabla_{(1,-1)} \bar{g}(b_l, b_r)$  is well-defined at  $(1/2, 1/2)$ . Now, if the directional derivative is strictly positive, we know that there exists  $\epsilon > 0$  such that  $\bar{g}(1/2 + \epsilon, 1/2 - \epsilon) > \bar{g}(1/2 - \epsilon, 1/2 + \epsilon)$ , which contradicts the symmetry condition. By the same argument the directional derivative cannot be strictly negative, so we find that  $\nabla_{(1,-1)} \bar{g}(b_l, b_r) = 0$  at  $(1/2, 1/2)$ .

We then construct  $c = \left. \frac{\partial\mu^{\text{KS}}(b_l, 1/2)}{\partial b_l} \right|_{b_l=1/2}$ . Since  $\nabla_{(1,0)}^2 \mu^{\text{KS}}(b_l, b_r) < 0$  at  $(1/2, 1/2)$ ,  $\nabla_{(1,0)} \mu^{\text{KS}}(b_l, b_r)$  is well-defined and equal to  $\left. \frac{\partial\mu^{\text{KS}}(b_l, 1/2)}{\partial b_l} \right|_{b_l=1/2}$ . Now, since  $c = \left. \frac{\partial\mu^{\text{KS}}(b_l, 1/2)}{\partial b_l} \right|_{b_l=1/2}$ , we have

$$\nabla_{(1,0)} \bar{g}(b_l, b_r) = \nabla_{(1,0)} \mu^{\text{KS}}(b_l, b_r) - c = 0.$$

Since the derivative of  $\bar{g}(b_l, b_r)$  at  $\mathbf{b}' = (1/2, 1/2)$  is zero in two independent directions, it implies that the gradient of  $\bar{g}(b_l, b_r)$  is a zero vector at  $\mathbf{b}' = (1/2, 1/2)$ , thereby completing the proof.  $\square$